University of
South-Eastern Norway

www.usn.no

FMH606 Master's Thesis 2021

Electrical Power Engineering

Hydropower unit – An analysis of operational efficiencies and energy losses

Sigurd S. Berg

Faculty of Technology, Natural sciences and Maritime Sciences

Campus Porsgrunn

University of South-Eastern Norway

www.usn.no

Course: FMH606 Master's Thesis 2021

Title: Hydropower unit – An analysis of operational efficiencies and energy losses

Pages: 148

Keywords: Weighted average efficiency, hydropower, efficiency, losses

Student: *Sigurd S. Berg*

Supervisor: *Gunne J. Hegglid and Thomas Øyvang*

External partner: *Skagerak Kraft AS*

Summary:

The beginning of the "green shift" has already started in the Nordic power grid. In this context, it means extensive use of intermittent energy sources like wind and solar power. The intermittent sources impact the operational regime of conventional hydropower units (HPU) into unfavourable situations, resulting in reduced operational efficiency and increased energy losses or revenue.

One of Norway's largest power producers, Skagerak Kraft, has started a research program collaborated with the University of South-Eastern Norway (USN) to investigate the upcoming challenges related to HPUs and the "green shift". This thesis will be the beginning of this research program with the purpose of analysing Åbjøra and Sundsbarm HPU concerning operational efficiency and investigate the efficiency under extended operational regimes.

For the analyse, it has been made a static model in MATLAB that estimates and maps the efficiencies and energy losses of the HPUs. The model determines the operational efficiency based on the operational data from the generators. The data was provided by Skagerak Kraft and contained information from the period 2020 with measurements of active power, reactive power and voltage.

The results identified the best efficiency point (BEP) of 92.25 % and 92.14 % in Åbjøra and Sundsbarm, respectfully, with an estimated weighted average efficiency (WAE) of 91.6 % for Åbjøra and 91.9 % for Sundsbarm. The analysis has shown a solid correlation between reduced operational efficiency and frequent use of frequency restoration reserve (FRR), also known as grid balancing. The magnitude of the active power has shown to be the dominating factor related to efficiency, where operations at low active power attain the lowest efficiencies. However, changes in reactive power could be assumed to have only a minor effect on efficiency.

Preface

This master's thesis concludes my Master of Science (MSc) degree within Electrical Power Engineering, University of South-Eastern Norway (USN). This thesis covers a broad topic and has given me an excellent introduction to the energy process of hydropower plants, and have built a solid foundation for potential future work within the areas of hydropower.

I want to thank my supervisors Gunne J. Hegglid and Thomas Øyvang, for the support and effort put into this thesis. I would also thank my fellow student from NTNU, Yannick C. Karekezi, who has been very helpful with many great tips, in particular, regarding the generator calculations.

Porsgrunn, 19th May 2021

Sigurd S. Berg

Contents

List of Figures

List of Tables

Abbreviations

AVR	Automatic Voltage Regulator
BEP	Best Efficiency Point
CFD	Computational Fluid Dynamic
CSV	Comma-Separated Value
EAE	Expected Average Efficiency
ENTSO-E	European Network of Transmission System Operators for Electricity
FCR	Frequency Containment Reserve
FEM	Finite Element Method
FFR	Fast Frequency Reserve
FIKS	Funksjonskrav i kraftsystemet (Functional requirements in the power system)
FRR	Frequency Restoration Reserve
HPU	Hydropower Unit
IEC	International Electrotechnical Commission
IEEE	Institute of Electrical and Electronics Engineers
NC-RfG	Network Code on Requirements for Generators
NVE	Norges vassdrags- og energridirektorat (The Norwegian Water Resources and Energy Directorate)
NVF	Nasjonal veileder for funksjonskrav i kraftsystemet (National guide for functional requirements in the power system)
OCC	Open Circuit Characteristic
SCADA	Supervisory Control and Data Acquisition
TSO	Transmission System Operator
WAE	Weighted Average Efficiency

Nomenclature

Symbol	Description
V	Voltage [kV] or [Pu]
I	Current [A] or [Pu]
R	Resistance [Ω] or [Pu]
P	Active power [MW] or [Pu]
Q	Reactive power [MVAr] or [Pu]
S	Apparent power [MVA] or [Pu]
φ	Power factor angle [Rad] or [Deg]
PF	Power Factor
Q_{flow}	Volumetric flow rate [m^3/s]
H	Head [m]
v	Velocity [m/s]
K	Total head loss coefficient
k_i	Head loss coefficient of a section
E, E_p	Excitation voltage, Potier voltage [kV] or [Pu]
X_d, X_q, X'_d, X_l, X_p	Reactance d-axis, q-axis, transient, leakage and Potier [Pu]
δ	Load angle [Rad] or [Deg]
η	Efficiency [%]
T_s, T_0	Temperature [℃]
α_t	Temperature coefficient of resistance [$(℃)^{-1}$]
b_v	The slope of the air-gap line [Pu/A] or [Pu/Pu]
A_k	Weighting factor
f	Friction factor
D	Diameter [m]
g	Gravitational constant [m/s^2]
L	Length [m]
ρ	Water density [kg/m^3]
T	Total duration time [h]
Δt_k	Duration of a loading point [h]

1 Introduction

The Norwegian power grid is mainly powered by hydropower with a share of about 90 %, where 75 % of all hydropower plants are so-called impoundment or reservoir plants[1]. The operating regimes of impoundment types are usually marked based, i.e., their production is carefully scheduled to the energy market called Nord Pool to optimise profit. Some hydropower plants may also be in the so-called capacity market, a market used to balance and stabilise the grid. Hydropower has a unique feature, particularly impoundment power plants can store a significant amount of energy that can be used whenever there is a need. Thus, with the large share of hydropower, Norway or the Nordic grid can utilise energy sources with high intermittencies, such as wind and solar power plants. Although hydropower can handle excessive use of wind and solar power, it can negatively influence the operational regime and affect efficiency, which will lead to reduced revenue.

1.1 Background

In recent years, several situations have been identified where conventional power plants have had their operating regimes changed due to extensive use of renewables like solar and wind [2]. This ongoing shift exposes new operating regimes with many start/stop cycles, extended range of operation and large voltage fluctuations [2]. Earlier studies [3] have analysed the effect of greater wind power penetration in transmission constrained areas. The study showed a possible reduced revenue to hydropower producers, particularly impoundment power plants, which are forced to operate with higher variations in production. A hydropower plant consists of turbines and generators sensitive to changes in the operational regime. These are optimised to a specific operating point, usually around the rated power. Deviating far from this point may cause a steep reduction of efficiency and large energy losses, energy which could have been stored and utilised in periods with a higher market price.

Skagerak Kraft has shown interest in this topic by starting a research program collaborated with the University of South-Eastern Norway (USN) to investigate losses and efficiency in their hydropower plants to gain better insight into possible future losses.

1.2 Problem Statement

The main goal of this project is to analyse the operational efficiency and energy losses of specific hydropower units (HPU) based on today's and future operating regime. The objectives of this thesis are listed below. The task description for this thesis was formally adjusted, where the first iteration can be found in Appendix A. The corrections are covered in the minutes of meeting to the formal meeting, found in Appendix B.

1. Review the existing regulation and requirements and typical operating conditions of the Norwegian Bulk Hydropower.
2. Explore the losses (energy conversion) of a hydropower system.

3. Build a suitable mathematical model of the HPU (waterway, turbine, generator and transformer) to identify energy loss and efficiency under stationary conditions.
4. Identify the optimal operating point/pattern of the HPU regarding efficiency. This from operation statistic for specific units for one or some years.
5. Run different cases based on future predictions to identify energy loss under new operating regimes.

1.3 Report structure

The report is structured to provide the reader with a general understanding of loss, regulation, construction and the operation of a hydropower units, followed by an in-depth analysis of specific hydropower units with respect to losses and their operation. A summary of each chapter's content is as follows:

Chapter 2 will give a short overview of the operating regimes and energy production in today's hydropower units and the future challenges regarding wind and solar. In addition, a brief description of the energy market and the regulations relevant for hydropower units, concerning limits in energy production.

Chapter 3 will give the reader a basic understanding of the main components of a hydropower unit concerning function, construction and energy losses.

Chapter 4 will present general background information about the hydropower plants analysed and their specifications.

Chapter 5 will present a description of the methods used in this analysis.

Chapter 6 will present an in-depth analysis of the specific hydropower units with a focus on operational efficiencies and energy losses.

Chapter 7 will present a brief sensitivity analysis under selected operational scenarios to identify changes to the average efficiency in possible future operating regimes.

Chapter 8 will present the discussion of the methods used and for the simulation results presented in chapter 6 and 7.

Chapter 9 will present the conclusions.

Chapter 10 will present the future work.

2 Operation of the Nordic grid

This chapter gives an overview of today's and possible future operating regime of HPUs and an introduction to the energy market and national and international regulations, focusing primarily on synchronous generators and their operation in the Norwegian grid. The energy market and the regulations are vital factors that describe the operating regimes of hydropower plants and are therefore described in this thesis.

The inter-Nordic system collaborates between Norway, Sweden, Finland and eastern Denmark, creating one large synchronous power grid, depicted in Figure 2.1. The energy composition in the Nordic gird consists of mostly hydropower, nuclear, wind and thermal, where today's shares of hydropower production in Norway, Sweden and Finland consist of around 90 %, 40 % and 23 %, respectfully [1] [4]. The Nordic grid utilises HPUs with energy storage primarily, often referred to as impoundment plants. The impoundment plants are, in particular, essential for the Norwegian power grid, which allows sufficient production throughout the year. However, the HPUs are often used to balance the grid. The balance might heavily be affected by what is known as the "green shift", where intermittent energy sources, like wind and solar power, become excessively used and can cause a significant imbalance.

Although the Nordic grid, notably Norway, has large energy storage in HPU, it must be enough stored energy in periods with a limited inflow. Thus, the energy market is valuable. It maintains a balance between supply and demand and ensures cheap run-of-river plants before the energy storages essential for periods with limited inflow, like in the winter season. In addition, there are national and international standards established for having an interconnected synchronous grid collaborated between multiple nations and numerous generators, which will also affect the operational regimes of the power plants. The standards and requirements discussed in this chapter will focus primarily on synchronous generators and their operation in the Norwegian grid.

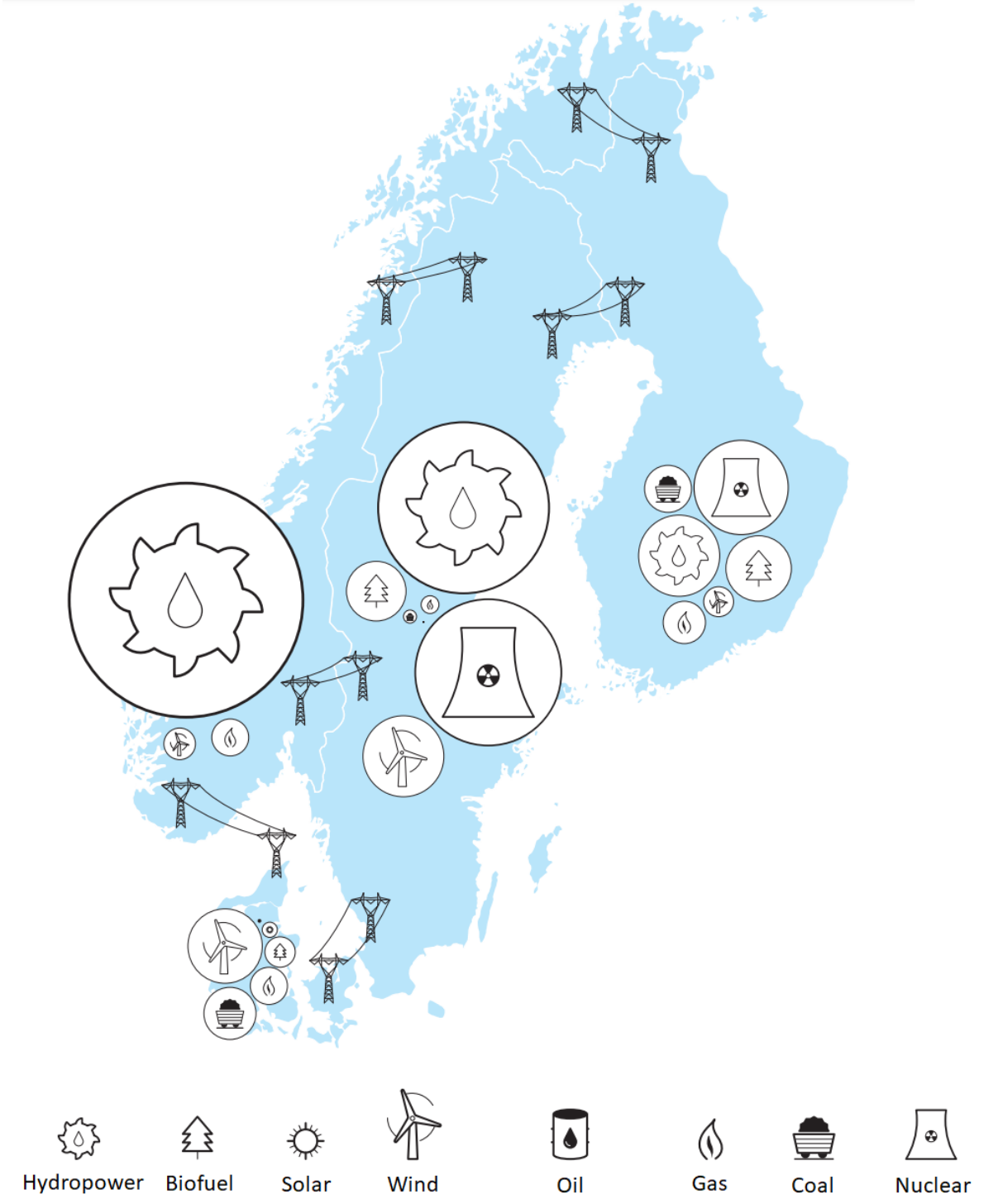

Figure 2.1: The Nordic power grid and the composition of energy sources. The size of the circles corresponds to the magnitude of the energy production. Denmark (except eastern Denmark) is not a part of the synchronous grid but connected through DC-links. Source: NVE/[5].

2.1 Operating regimes and energy production

There are two main types of hydropower units, regulated and unregulated, where in Norway, the regulated types account for about 75 % of the total hydropower production [1]. The most common type of regulated and unregulated power plants in the Nordic countries are the impoundment (reservoir) type and the run-or-river type.

Impoundments plants store water in natural or artificial lakes at high elevations and often seen with dams to increase the reservoir capacity. This feature allows the power plants to produce power whenever there is a need, assuming there is enough water in the reservoir. With the exceptional controllability of impoundment plants, production scheduling becomes possible, allowing the power plants to plan or predict their operation into the future to optimise profit.

Run-of-river plants are often located in or close to rivers, sometimes in combination with dams to increase the headwater allowing for a higher level of control to the production. The downside to this type of plants is their limited controllability, i.e., the inflow of water has to be equal or close to identical to the water discharged through the turbines at all times. Otherwise, water will overflow and get wasted.

In the context of energy production, one may divide the term power plants into:

1. Baseload power plants.
2. Load-following power plants.
3. Peak power plants.

Baseload power plants operate with constant or maximum power output and are often associated with run-of-river plants. The operation of a run-of-river plant is usually equal to the inflow as there are often little to no storage capacity and has an extended operational range, resulting in a low utilisation time of around 3000-4000 hours. Impoundment plants with a high mean annual inflow can also be considered base load power plants or load-following power plants. These impoundment plants usually operate with a close to constant power output, resulting in a high utilisation time of around 6000-7000 hours. In Norway, these type of power plants was generally used in combination with energy-dense industries like steelworks which had a high baseload with minor variations in consumption.

Peak power plants are, in comparison, power plants used to operate under high demand mainly. Some impoundment plants are considered peak power plants, with a large capacity to utilise the annual inflow within a short utilisation time, often in the range of 1000-2000 hours. The Norwegian power grid uses hydropower primarily with a quick response time and large energy reserves, which has led to limited interests in peak power plants in Norway. Peak power plants usually have high investment costs, mainly due to the increased unit cost, and are therefore located where the head is high, head losses are low, and the ability for regulation is good.
The utilisation times described in the last two paragraph’s was stated by the main supervisor Prof. Hegglid, by mail (27.04.2021).

The total energy production and water inflow of all hydropower units in Norway are shown in Figure 2.2. How reservoirs utilise and distribute the stored energy throughout the year is illustrated by the figure. When the water inflow (measured as energy) is greater than the energy production or consumption, the water fills the reservoirs. The filling process occurs during the late spring to late autumn due to severe rainfall and snow melting from the mountains.

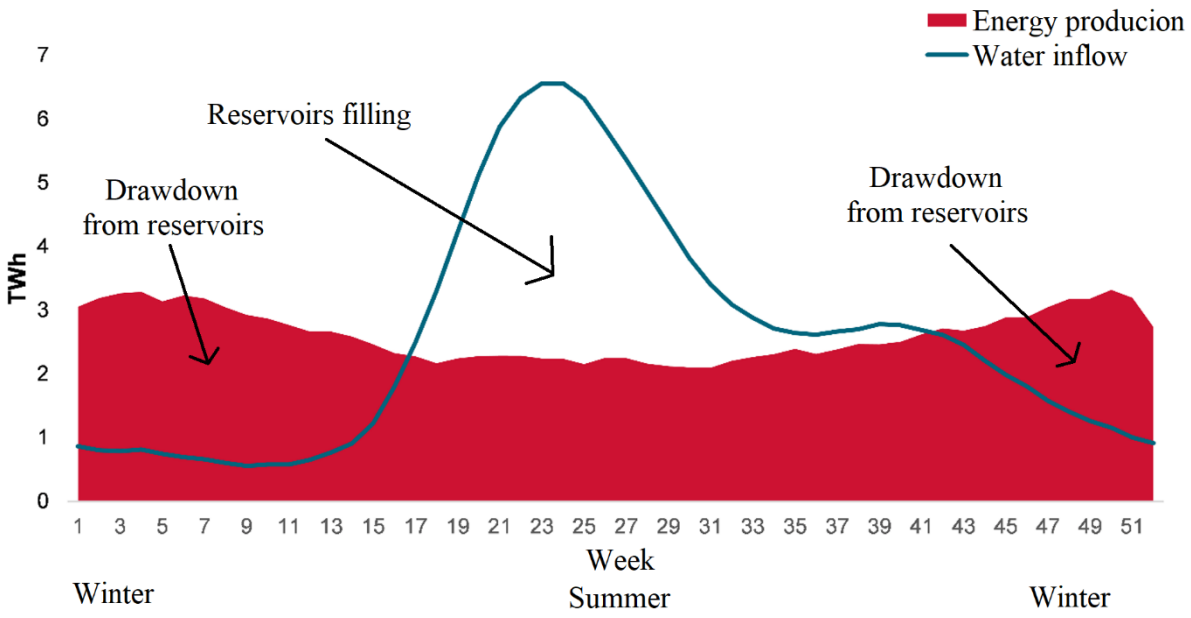

Figure 2.2: Weekly energy production and water inflow statistics of the Norwegian hydropower [6].

2.2 Complications to the future power grid

In today's "green shift", one can expect a radical transformation of the power grid in the future power grid due to the extensive use of renewable energy sources and other technologies. The change may influence the operating regimes of today's conventional hydropower units, particularly impoundment plants, which are often used to balances the grid (FRR). The energy balance and stability of the grid might be limited and reduced with excessive use of solar and wind power plants as these are considered to have ha high intermittency, i.e., irregular and unpredictable production.

A long-term power market analysis given by NVE [7] speculates that there will be a significant increase in wind and solar power for the Nordic nations, as shown in Figure 2.3. The analysis estimates wind and solar power shares in the Nordic region would increase from around 20 % in 2020 to approximately 40 % in 2040 [7].

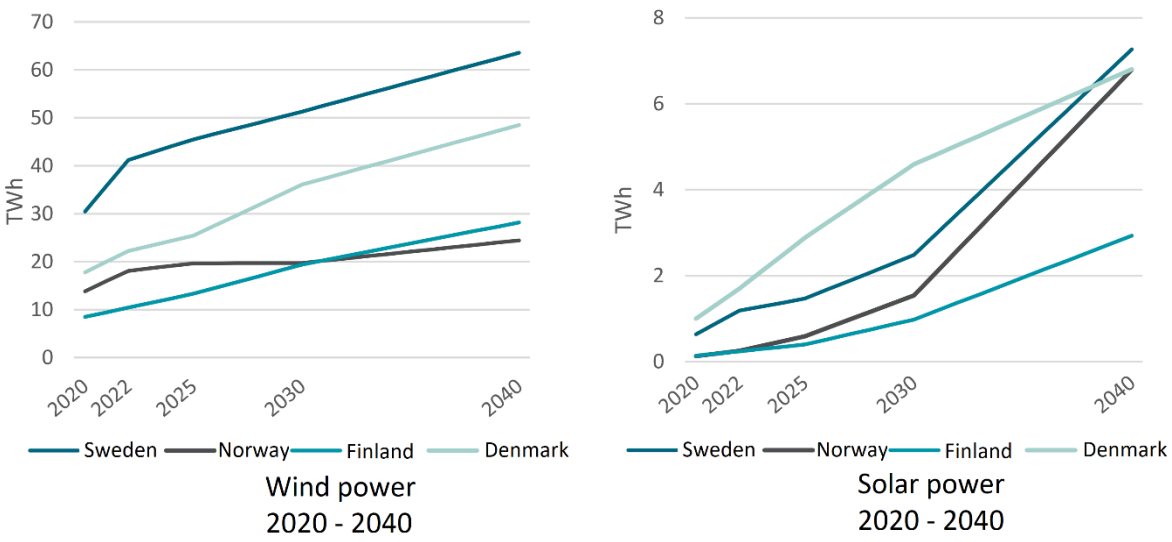

Figure 2.3: Estimated growth in wind and solar power in the Nordic [7].

2.2.1 Energy storage

Countries with excessive use of solar and wind production have difficulties regarding energy storage in the grid. The so-called "Duck curve", as depicted in Figure 2.4, describes the net load variation, i.e., the imbalance between peak demand and renewable (solar) energy production. The owner of such a grid may invest in additional peak power plants to support the high demand when renewable sources are inactive. Thus, hydropower, particularly impoundment plants, would be ideal to be combined with solar power to balance the production.

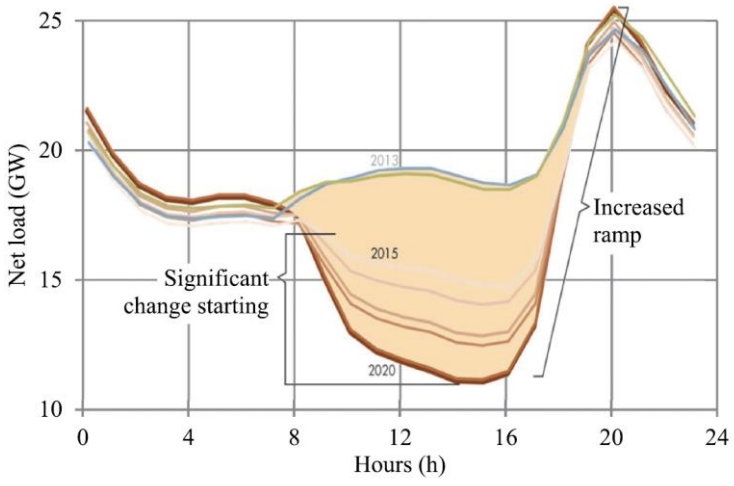

Figure 2.4: The "Duck curve", a typical representation of the net load variation in power grids with a high solar generation [8].

Excessive use of wind power may also result in challenges regarding energy storage as the wind does not always blow enough to run the wind turbines. Fortunately for Norway and Sweden, the power grid has a large energy storage capacity. The master thesis of Bødal [3] analysed how the coordination of hydro and wind power in a transmission constrained area would affect the revenue to the power producers. The thesis concludes that hydro and wind power coordination would result in lower power levels for impoundment plants as production moves to benefit run-of-river plants. The increased penetration of wind might give a small reduction in the total profit for impoundment hydropower, whereas the run-of-river would expect increased profit [3].

2.2.2 Intermittency

Another challenge associated with the excessive use of wind and solar is their intermittency. Intermittency is a common term used to describe the irregular and unpredictable production of wind and solar. There has been plenty of research on predicting both wind and solar production from weather data in recent time. Prediction of the production could help planning ahead of production coordination, but the irregular output of wind and solar will still be present, as depicted in Figure 2.5 and Figure 2.6. In both figures, one can see large intermittency as the production is highly irregular and unpredictable. In Figure 2.5, one can see that an entire wind farm will have more or less the same intermittency as a single turbine. As shown in Figure 2.6, the solar power production illustrates a predictable pattern that follows the sun but has irregular production, most likely due to clouds. Wind or solar farms with high intermittency can result in what is generally referred to as a “voltage dip” and is one of the main concerns for every TSO [9]. In most cases, the low voltage or dips are resolved by the reactive power controllers, thus increasing the fluctuations in the reactive production regime for the conventional power plants. In the worst-case scenarios, the voltage dip may lead to island operation or blackouts.

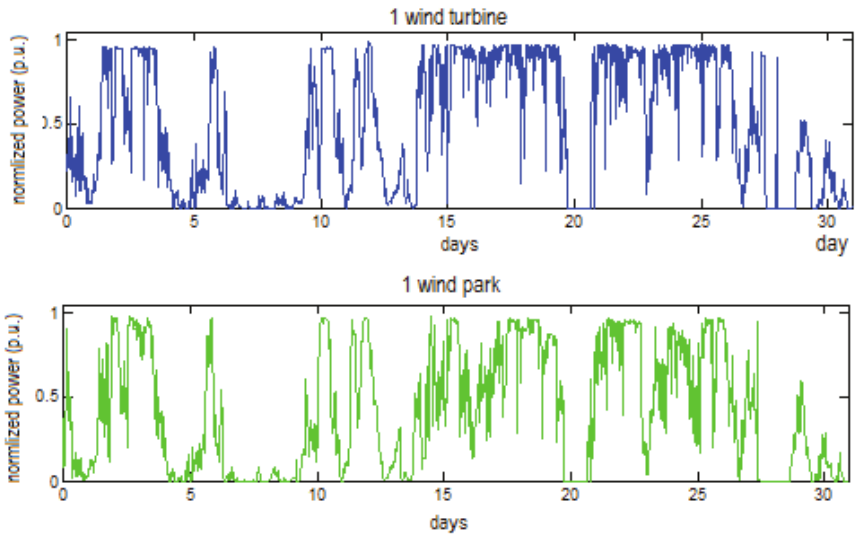

Figure 2.5: Wind power production profile for a single turbine and an entire wind park over one month [9]. The bottom figure shows production data for a find farm, whereas the upper figure shows a single turbine from the same farm and under the same period.

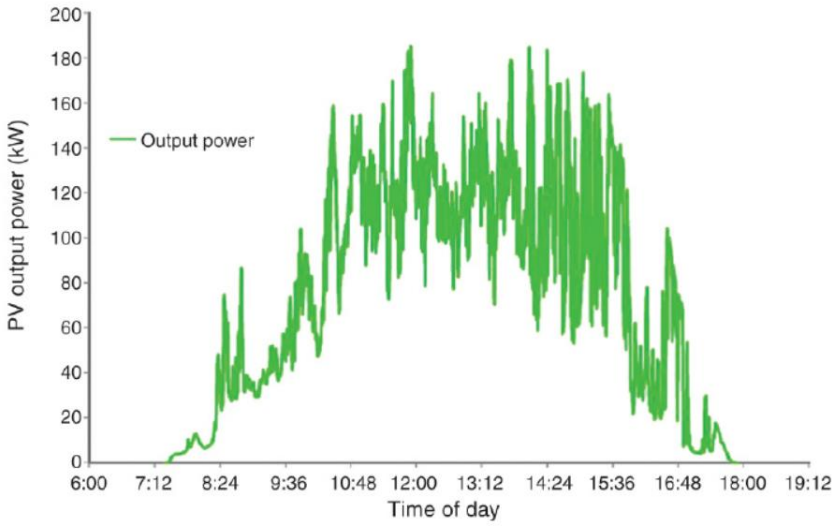

Figure 2.6: Solar power production profile over one day [10].

2.2.3 Operational regime changes

A synchronous generator situated in a conventional power plant could be subjected to significant effects of increased wind and solar penetration, as illustrated in Figure 2.7. The figure is an illustration that shows the before and after the so-called “German Energiewende”, where one can see significant changes to the active and reactive power [11] [2]. Still, most importantly, the distribution and changes in operational density are considerably affected. The difference in the operating regime as illustrated in Figure 2.7 can be considered an extreme scenario, especially for most conventional hydropower plants. In HPUs, the turbine usually limits the maximum and minimum active power production and will most likely not change significantly in the future. On the other hand, the future operating regime for hydropower plants may experience more significant fluctuations in production, more start/stop situations, and different operational density distribution. These changes may go at the expenses of reduced operating efficiency and more fatigue in several components.

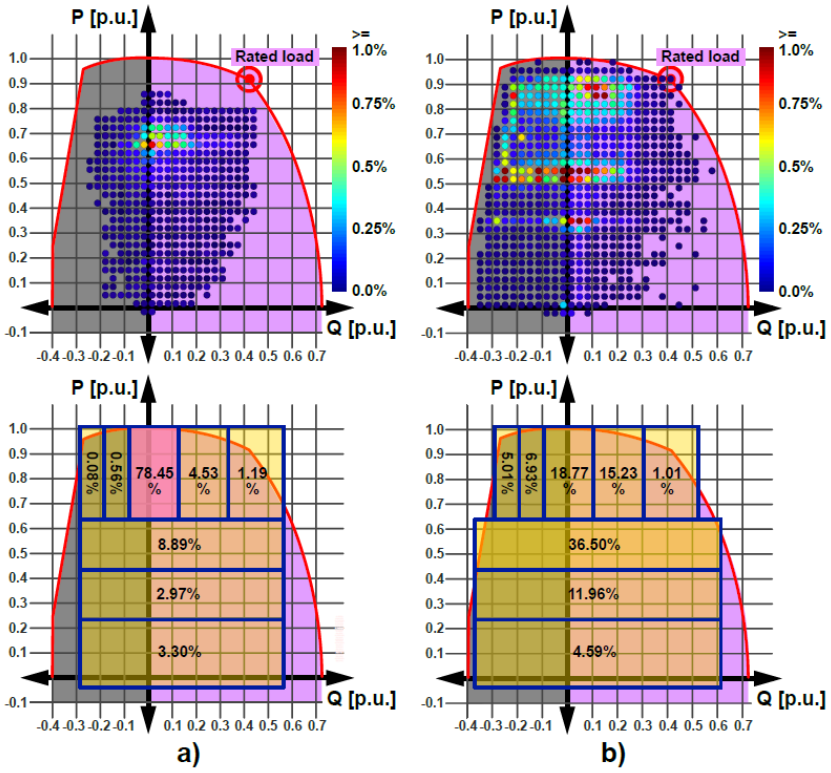

Figure 2.7: Distribution and density of load points of 300 MVA generator with highly volatile utilization, illustrating the situation before (a) and after (b) the "German Energiewende" [11] [2].

2.3 The energy markets

Nord Pool, the Nordic energy market, exchanges electric energy between the Nordic, Baltic, Central Western Europe and the UK. The function of Nord Pool is to stimulate the production and the demand to maintain a balanced grid. Nord Pool consists of three physical markets:

- day-ahead (Elspot)
- intraday (Elbas)
- balance services

where most of the energy sold is through the Elspot-market. In the Elspot-market, the power producers offer a given amount of power they would deliver the next day. At the same time, large industries and energy companies assess the consumption, which is likely to occur the next day. An algorithm then estimates the price based on the intersection between the aggregated supply and demand curves, as shown in Figure 2.8.

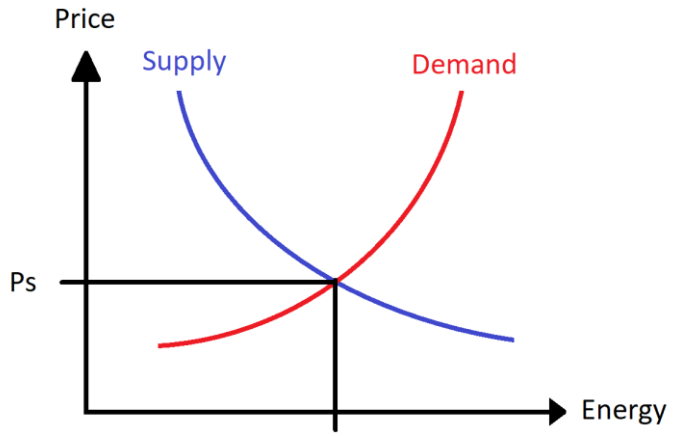

Figure 2.8: System price calculation, where Ps is the spot price.

The demand estimated the day ahead might not reflect the actual consumption and produce some errors balanced through adjustments in the Elbas-market. However, the price will not be equal for all countries or even within a nation as the price shall stimulate and balance the supply and demand. A typical situation is a power line connecting two areas that exceed its capacity, also known as a bottleneck. Thus, the two areas shall have a price differently from one another to retain balance by reducing the price in areas with surplus and decrease the deficit area's cost.

The last markets are the balancing services where power participants get paid either from delivered energy from automatic grid balancing (FFR, FCR or aFRR) or by manual grid balancing mFRR, also known as “regulerkraftmarkedet” (RK), see section 2.4.3. In addition, power participants can also be in the so-called capacity market or “regulerkraftopsjonsmarkedet” (RKOM), where they get paid for available capacity, often seasonal contracts.

2.4 Production requirements and guidelines

This section shall give an overview of the requirements and guidelines that briefly describe the operating regimes for production units, particularly hydropower units. All generators connected to the power grid is obligated to follow specific requirements. In Europe and the Nordic power grid, the ENTSO-E (European Network of Transmission System Operators for Electricity) is the authorized entity. For power producers, there is an under category in ENTSO-E called NC-RfG (Network Code on Requirements for Generators) [12], which are connection rules for power-generating modules[1]. In Norway, the NVE (The Norwegian Water Resources and Energy Directorate) is the national authorized entity based on the ENTSO-E with modifications customized to the Norwegian power grid. All power-generating modules connected to the Norwegian power grid shall follow the technical requirements provided by the national TSO (Statnett). Statnett guides producers to follow the regulations through guidelines, in particular, the new guideline NVF (National guide for functional requirements

[1] An installation which generates electricity, e.g., a hydropower plant.

in the power system) [13], which took over for the old guideline FIKS (Functional requirements in the power system) [14] in late 2020. The requirements for generator design and calculation/measuring methods are given by the IEEE standard C50.13 [15] and IEC (International Electrotechnical Commission) standard 60034 [16].

In the NC-RfG, the maximum capacity of an installation and its maximum voltage at PCC (point of common coupling) will determine which requirements to follow. The requirements in NC-RfG is structured so that type A power-generating modules have the least requirements, and B, C and D will have an additional set of rules in the respectful order. The power-generating modules for the Nordic area are categorised as shown in Table 2.1, which are also the origin of the models described in the national guideline NVF.

Table 2.1: Limits for thresholds for type A – D power-generating modules in the Nordic area [12] [13].

Type	Voltage level at PCC	Maximum capacity
A	$<$ 110 kV	0.8 kW
B	$<$ 110 kV	1.5 MW
C	$<$ 110 kV	10 MW
D	$<$ 110 kV	30 MW
	$\geq$ 100 kV	All installed capacities

2.4.1 Functional requirements - Voltage limits

NVF and NC-RfG have specified that all synchronous power-generating modules connected to a power grid shall be able to operate within the voltage range described in Table 2.2. The table shows the minimum periods during which a power-generating module must be capable of operating for voltages deviating from the reference 1 Pu value at the connection point without disconnecting from the network [12]. For the Norwegian power grid, the NVF has specified the continuous voltage boundaries for voltage levels of 66 kV and 420 kV, related to the reference voltage as seen in Table 2.3.

Table 2.2: Requirement for the minimum operative period for synchronous power-generating modules related to voltage limits [12] [13].

Synchronous area	Voltage range	Time period for operation
Nordic	0.90 Pu – 1.05 Pu	Unlimited
	1.05 Pu – 1.10 Pu	60 minutes

Table 2.3: Reference voltage related to the Norwegian grid voltage [13].

Nominal system voltage	0.9 Pu minimum continuous voltage	1.0 Pu Reference voltage	1.05 Pu Maximum continuous system voltage
420 kV	360 kV	400 kV	420 kV
300 kV	256 kV	285 kV	300 kV
132 kV	125 kV	138 kV	145 kV
110 kV	105 kV	117 kV	123 kV
66 kV	62 kV	69 kV	72.5 kV

2.4.2 Functional requirements - Reactive capacity

Synchronous power-generating modules must have a minimum reactive capacity to ensure high voltage stability. The minimum requirement for reactive capacity is given by the maximum power, P_{max} at nominal voltage, $U_{PCC} = 1.0\,Pu$, referred at PCC [13], see Table 2.4. The reactive power shall not be limited when $P < P_{max}$ [13]. In practice, one could assume a reactive consumption of about 12 % in for the transformer which results in a reactive capacity requirement as shown in

Table 2.5, which is a corresponding requirement referred to the generator terminals [13].

Table 2.4: General requirement to reactive capacity for synchronous power-generating modules, referred to PCC [13].

Requirements for type C and D, referred to P_{max}		
Capacitive capacity	$Q_{cap,max} = 0.46 \cdot P_{max}$	$cos\varphi_{cap} = 0.91$
Inductive capacity	$Q_{ind,max} = -0.46 \cdot P_{max}$	$cos\varphi_{ind} = 0.91$
Requirements for type B, referred to P_{max}		
Capacitive capacity	$Q_{cap,max} = 0.33 \cdot P_{max}$	$cos\varphi_{cap} = 0.95$
Inductive capacity	$Q_{ind,max} = -0.33 \cdot P_{max}$	$cos\varphi_{ind} = 0.95$

Table 2.5: General requirement to reactive capacity for synchronous power-generating modules, referred to generator terminals, assuming 12 % reactive consumption in transformer [13].

Requirements for type C and D, referred to P_{max}		
Capacitive capacity	$Q_{cap,max,g} = 0.51 \cdot P_{max}$	$cos\varphi_{cap,g} = 0.86$
Inductive capacity	$Q_{ind,max,g} = -0.33 \cdot P_{max}$	$cos\varphi_{ind,g} = 0.95$

2.4.3 Frequency requirements and energy reserves

Synchronous power-generating modules shall generally operate within the operating limits described in Table 2.6, which states that the power-generating module shall not be limited within the required time period. The requirement is vital to ensure a balanced power grid even under large contingencies, as a too high imbalance may result in a total blackout.

Table 2.6: Requirements for the minimum operative period for synchronous power-generating modules, related to frequency limits under the voltage range 0.9 – 1.05 Pu [13].

Frequency range	Time period for operation
47.5 – 49.0 Hz	30 minutes
49.0 – 51.0 Hz	Unlimited
51.0 – 51.5 Hz	30 minutes

One will achieve a balanced power grid or a constant frequency (50 Hz) when power production and consumption are equal. In contrast, a grid exposed to a higher consumption will have a lower frequency and vice versa when production is higher. According to the Nordic

system operation agreement, the frequency in the Nordic grid should be kept within 50 ± 0.1 Hz [17]. Designating power-generating modules into different energy reserves allows the grid to handle small and large grid imbalances with reduced risk. The reserves are also a part of the Nordic balancing services, as discussed earlier. The reserves categorized into:

- Fast Frequency Reserves (FFR)
- Primary reserve: Frequency Containment Reserve (FCR)
- Secondary reserve: automatic Frequency Restoration Reserve (aFRR)
- Tertiary reserve: manual Frequency Restoration Reserve (mFRR)

Fast Frequency Reserves (FFR): Are reserves with a rapid response to large frequency deviations, usually lower than 49.7 or 49.5 Hz [18]. The reserves shall secure the grid's stability during significant faults and therefore activated within a second. The FFR is mainly a substitute for the rotational inertia in power grids, where this is low.

Frequency Containment Reserve (FCR): The immediate change in load or production is balanced by the rotating mass's energy in the power system before the frequency begins to change. A frequency shift is handled first by the primary reserve FCR, an automatic controlled reserve used to constrain the frequency change [19]. FCR distinguish between regular operation (FCR-N), where the frequency is within a normal state and the process during disturbance (FCR-D). The response time is usually within few seconds.

Automatic Frequency Restoration Reserve (aFRR): Also known as load frequency control (LFC), where the reserves stabilise the frequency back to standard 50Hz. The TSO takes automatically control over the generators in aFRR market with a response time within 2 minutes.

Manual Frequency Restoration Reserve (mFRR): When there is a significant imbalance in the power grid or transmission bottlenecks, additional reserves will be activated manually by the national TSO. This market is known as the capacity market (RK). Every participant offers their mFRR price similar to the Elspot. During the activation, the cheapest reserves are first activated, with a response time under 15 minutes. The response time and the relationship between each energy reserve can be seen in Figure 2.9.

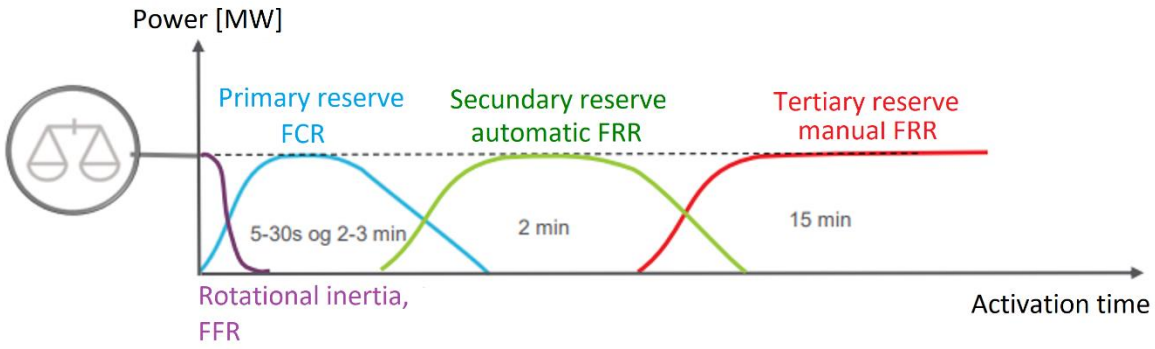

Figure 2.9: The response time of the different reserves [19].

3 System overview

This theory chapter provides an overview of the construction and stationary losses associated with a conventional hydropower unit (HPU). The main components which are covered are the waterway, turbine, generator and transformer. This thesis focuses primarily on HPUs with single generating units, i.e., HPUs with multiple generators, turbines, and waterways are not considered.

3.1 Waterway

A waterway is a generic term for a river, tunnel, pipe, or other construction elements to convey water from an upper to a lower reservoir. Waterway losses, often referred to as hydraulic losses, are usually measured in the head[2] [m] and proportional to the velocity squared, resulting in substantial losses under high flow rates. A typical waterway efficiency is usually well above 90 % [20], referred to as nominal flow rate, but depends on the flow rate and the construction of the waterway.

3.1.1 Construction

There are many components in a waterway construction, but the main components regarding losses are the headrace/conduit, penstock, tail race, valves, and trash racks.

1. **Headrace/conduits** are usually a tunnel or a set of tunnels used to convey a large amount of water, often over long distances of tens of kilometres, before connecting to the penstock. It is possible to reduce water losses by having large horizontal tunnels as the flow velocity become limited. In larger HPUs, tunnels will usually be blasting into the mountains resulting in a rough surface if not smoothed out by, e.g., concrete. One will often find one or more sand traps within the tunnels, as depicted in Figure 3.1. In the sand traps, the flow velocity is relatively low, allowing the sand and rock sediments to sink and accumulate at the bottom. The sand traps are essential, as sand and rock sediments could damage the turbine.
2. **Penstock** is the pipe or tunnel connected to the turbine and is often a close to vertical steel or concrete pipe with smooth surfaces, as depicted in Figure 3.2. The function of the penstock is to convey water under high pressure and at a high velocity with limited loss.
3. **Tailrace** is the tunnel or pipe which convey the water outflow from the turbine into the lower reservoir or river. A tailrace will only add losses in fully submerged turbines, like Francis and Kaplan, whereas a Pelton turbine would be unaffected.
4. **Valves and trash racks** are essential components in any conventional HPUs. When an HPU is out of service, the valves may block water flow, whereas trash racks remove any debris that may damage the turbine. Both valves and trash racks are small obstacles in the waterway, which provides small additional losses.

[2] Head is a synonym for height difference.

Figure 3.1: Cleaning process of a sand trap in Rosekrepp hydropower [21].

Figure 3.2: A multiple penstock arrangement [22].

3.1.2 Energy losses

As water moves through the waterway, energy loss, also known as hydraulic loss, accumulates under geometric changes[3] and friction forces in the water. The loss transforms the mechanical energy of water into heat, which is unusable in hydropower. With turbulent and high flow velocities, the magnitude of the loss will arise quickly. Hydraulic loss can be classified as [23] [24]:

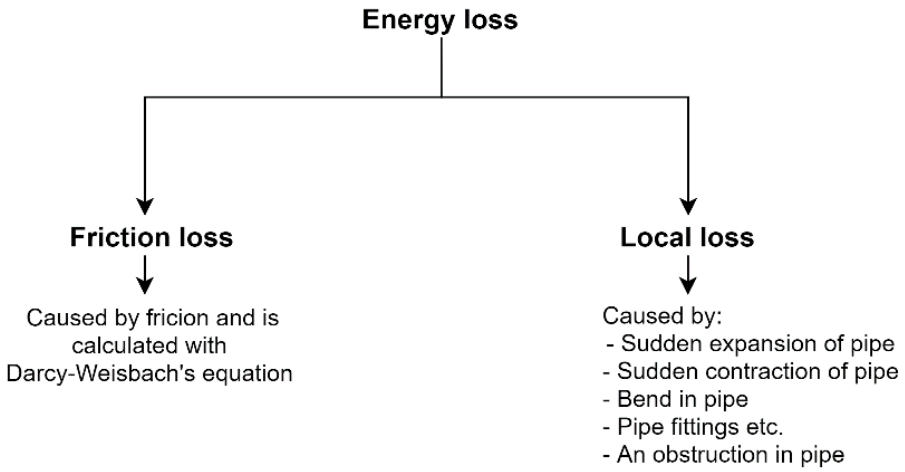

A typical illustration of head loss is seen in Figure 3.3, where the gross head (H_g) $[m]$ is the absolute difference in head between upper and lower reservoir, net head (H_n) $[m]$ is the available head for energy conversion and head loss (h_f) $[m]$ is the energy loss.

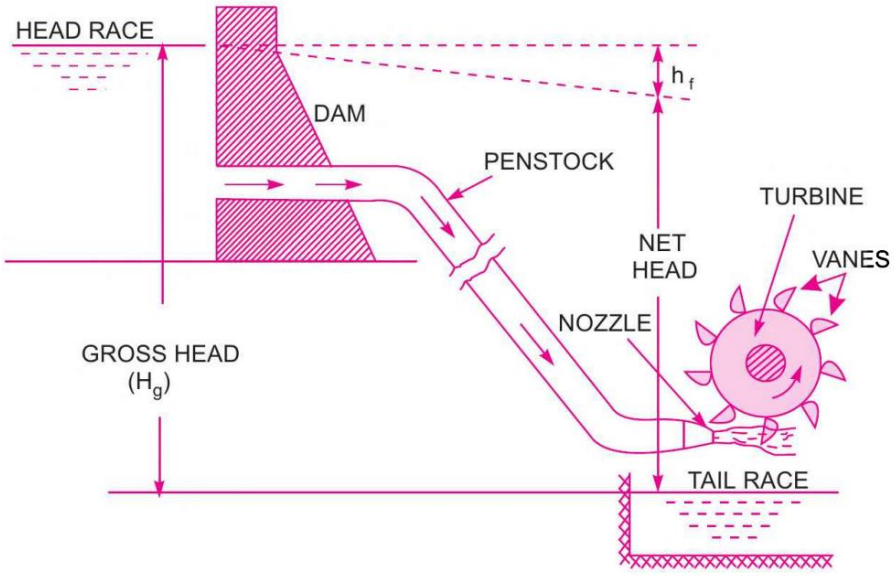

Figure 3.3: Layout of an HPU, illustrating the relationship between the gross head, net head and head loss [24].

[3] A change to the flow path like a bend or a change in cross section.

The friction losses arise from the water viscosity, molecular and turbulent effects [23]. Friction losses result from water molecules exchange their momentum, which occurs when molecules in motion have different relative velocities. When the surface roughness is high, the water becomes highly turbulent, causing friction losses to increase. A commonly used formula for friction losses is Darcy-Weisbach's equation [25] [26] [24]:

$$h_f = f \cdot \frac{L \cdot v^2}{2g \cdot D_h} \tag{3.1}$$

where h_f = head loss $[m]$, f = friction factor $[m]$, v = flow velocity $[m/s]$, L = tunnel length $[m]$, g = gravitational constant $[m/s^2]$ and D_h = hydraulic diameter $[m]$. A friction factor is a number describing the roughness of a pipe or tunnel, which can in some cases be obtained from tables. In tunnels where the surface roughness is high, the friction factor could be measured, like in the method proposed by Rønn and Skog [25], named IBA method. One can find more details about friction losses in Appendix C.

Local losses arise in the flow path due to varying geometry or obstacles from swirling water; this creates changes in the flow direction and localized pressure changes [23]. Local losses are losses calculated from a single part or location and are therefore independent of the length. Additional turbulence occurs whenever there is a change in the flow path, like pipe entrances or exits, pipe bends, pipe contractions or expansions, see Figure 3.4 [26]. The equation for head loss produced by local losses is given by [26]:

$$h_l = \frac{kv^2}{2g} \tag{3.2}$$

where h_l is the head loss in [m], v is the flow velocity $[m/s]$, g is the gravitational acceleration $[m/s^2]$ and k is the resistance coefficient for the pipe part/obstacle. The k-factor for different pipe and valves can be found in tables as depicted in Appendix C.

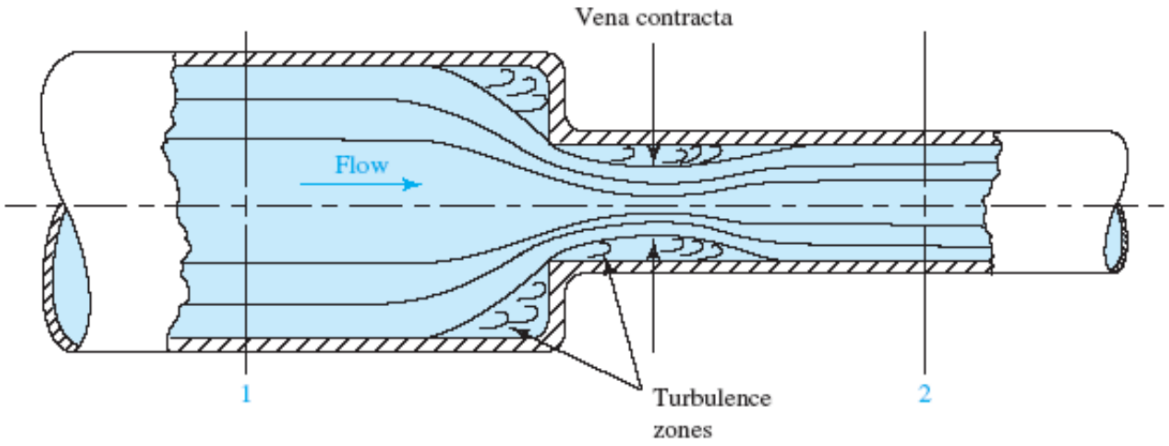

Figure 3.4: Illustration of local losses produced in a pipe with sudden contraction and the rise of additional turbulence [27]. "Vena contracta" is referred to as the point where fluid velocity is at its maximum.

In practice, one will often come across waterway losses represented by a single head loss coefficient (K). The coefficient (K) is a number describing the total friction and local losses in a waterway, given by the volumetric flow rate (Q_{flow}). Volumetric flow rate, also called water discharge, is regarded as the preferred unit as water velocity is relative to the pipe/tunnel size. In contrast, the volumetric flow rate is constant throughout the waterway, assuming water is incompressible. The equation for total head loss in a waterway based on the head loss coefficient (K) yields:

$$H_{loss} = KQ_{flow}^2 \qquad 3.3$$

Appendix D shows an example of the derivation of formula 3.3, based on equation 3.1 and 3.2.

3.2 Hydropower turbine

Hydropower turbines convert hydraulic power from the waterway into mechanical power, which drives the generator. In conventional HPUs, there are three main types of hydro turbines, called Pelton, Francis and Kaplan, where Francis is usually the turbine with the highest efficiency, up to around 95 %, often referred to as the turbines best efficiency point (BEP). If operated aside from the best point, it may reduce the efficiency significantly. Of course, the operation and efficiency characteristics will depend on the type of turbine used, where typical turbine characteristics are summarised [28] in Table 3.1.

Table 3.1: Typical specifications of turbines

Specification	**Pelton**	**Francis**	**Kaplan**
Net head $[m]$	200-2000	40-700	3-60
$Flow\ rate\ [m^3/s]$	1-30	2-1000	30-1000
Operation [%]	5-100	50-100	20-100
Efficiency [%]	<93	<96	<94

3.2.1 Main components – Francis and Kaplan turbines

A Francis and Kaplan turbine have almost identical construction, except the actual runner, as depicted in Figure 3.5. The main components for Francis and Kaplan turbines are:

The spiral casing is the inlet to the turbine, where all the water from the reservoir is going through. The design of the spiral casing is to guide the inlet water around the runner while maintaining a constant velocity/pressure, achieved by an ever-decreasing cross-sectional area.

Guide vanes are fully adjustable blades used to maneuverer the water into the runner at an optimal angle under an extensive range of operations with the additional ability to regulate the flow rate into the turbine. The flow rate is the main parameter that determines the amount of power the turbine will produce.

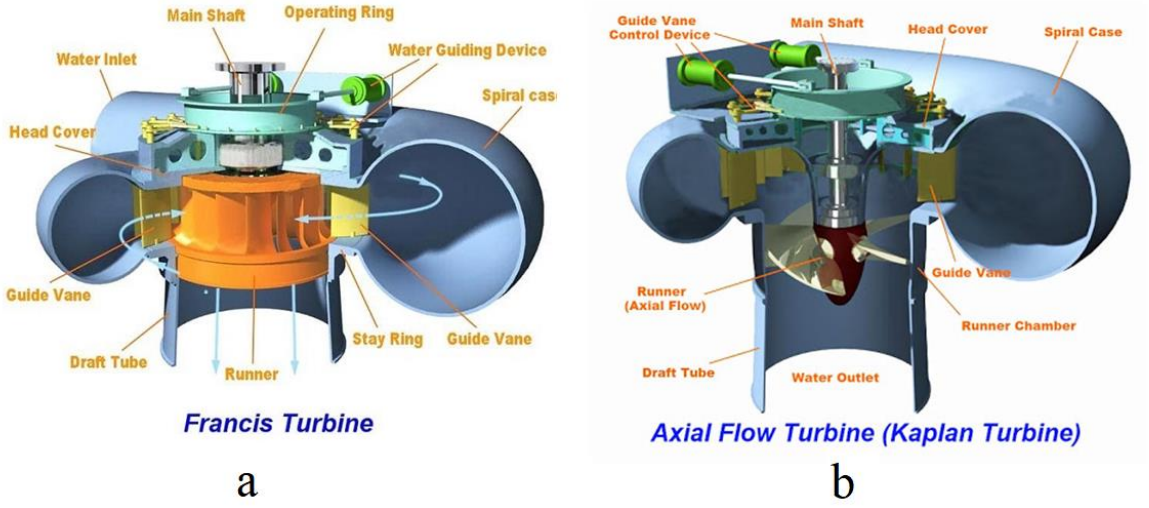

Figure 3.5: The cross-section and the components of a) Francis turbine and b) Kaplan turbine [29] [30].

The runner is the heart of the turbine, where the hydraulic power become converted to a mechanical rotation that drives the generator. In the Francis turbine, the runner blades are fixed and harness hydraulic power through lift and impulse forces. In comparison, the Kaplan turbine has adjustable blades in addition to guide vanes, allowing Kaplan to have a larger operational range than the Francis turbine. Kaplan turbines harness power only through lift forces.

The draft tube is only used by fully submerged turbines like Francis and Kaplan, connecting the runner exit to the tailrace tunnel or the lower reservoir. After the water exits the turbine, the backpressure will generally be less than atmospheric. By introducing an expanding tunnel, called a draft tube, the high kinetic energy of the water become converted to a higher water pressure that is useful as it increases the efficiency of the turbine before being discharged into the tailrace.

3.2.2 Main components – Pelton turbines

The construction of a Pelton turbine has some differences from the structure of the Francis and Kaplan turbine. The construction of a Pelton can be seen in Figure 3.7, and the main components of the turbine are:

The distribution pipe is the pipe connecting the water inlet from the penstock to the nozzles. It shares similar properties as the spiral casing, where the water pressure is maintained constant at all nozzles.

The nozzles convert the potential energy of the water into pure kinetic energy, i.e., increasing the velocity of the water as much as possible, resulting in a concentrated water jet. To regulate the production, one could either adjust the nozzles' opening or choose the number of nozzles. This feature allows excellent control of the flow rate while maintaining a constant water jet velocity.

Runners used in Pelton turbines have large set buckets, which converts the kinetic energy of the water into mechanical energy for what is known as impulse forces. The buckets could harness the hydraulic power by deflecting the water with an angle close to 180 degrees, as illustrated in Figure 3.6. By having a peripheral runner speed close to half the jet velocity, the exiting water jet will result in a limited velocity close to zero, relative to the surroundings, resulting in high efficiency.

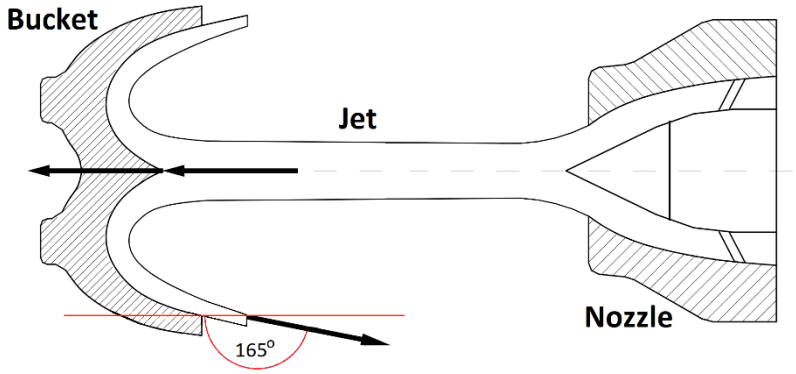

Figure 3.6: Cross-section of a Pelton bucket where the water jet reflects water at an angle of 165°. The figure is based on a figure given in [31].

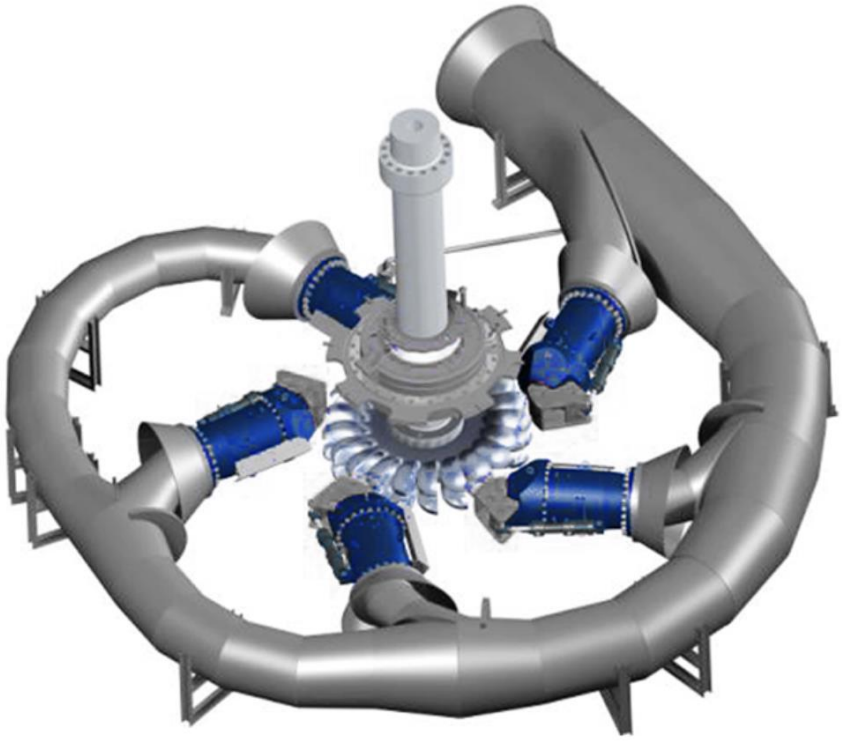

Figure 3.7: Construction of a five nozzle Pelton turbine [32].

3.2.3 Energy losses – turbines

In a turbine, most energy losses are hydro-mechanical losses, categorised as [33]:

Friction losses occur in the distribution pipe, nozzles and buckets. There would be high friction losses in the buckets due to the shear stresses between the buckets and the moving water produced by what is known as viscous adhesion [33].

Windage losses are due to the air around the runner, which produces a drag on a rotating runner

Swirling losses are related to the velocity of the exiting flow out of the runner. The loss arises from the existence of the rest kinetic energy that is present in the exit flow [33]. If the velocity of the exit flow is zero, the swirling losses will also be zero. Swirling water could be server in the draft tube of Francis and Kaplan turbines. Draft tube losses originate from swirling water, also known as helical vortices, which produce a large pressure drop over the draft tube. The minimal rotational motion of water exciting under BEP limits the size of the helical vortices, as depicted in Figure 3.8. The figure shows the helical vortices in the part-load and full-loaded condition in a test turbine [34].

Bearing losses are the losses produced by friction forces in the load-bearing to the runner. Hydrodynamic plain bearings are almost exclusively applied to all Pelton turbines, as these can handle high loads and stresses with minimal losses [33].

Erosion is an essential factor that may increase the friction losses after some years in service. Erosion is widespread in locations where a large amount of sand is present or in turbines where cavitation is present. Cavitation is a phenomenon produced by imploding water and occurs when water is subjected to localized under pressure zones, typically found on Francis and Kaplan turbines.

Leakage losses in Pelton turbines could be in the form of water that is not in contact with the bucket, illustrated in Figure 3.9. In Francis and Kaplan turbines, some water escapes between the runner and the sidewalls, thus wasting energy.

Impact losses are losses produced by water flowing in a direction that opposes the rotation of the runner [28]. For a Pelton turbine, the deflected water may impact the runner and resist its movement, whereas impact losses in Francis and Kaplan turbines occur at the runner's inlet.

One should have in mind that determining and make statements about the individual hydro-mechanical are difficult as there has been hardly any available and reliable equations to make it feasible with analytical and empirical formulas [33]. A common method is to use numerical simulation software like computational fluid dynamics (CFD), which can differentiate individual losses in turbines with high accuracies.

(a) part-load (b) full-load

Figure 3.8: Helical vortices formation in a draft tube at (a) part-load and (b) full-load regime [34].

3

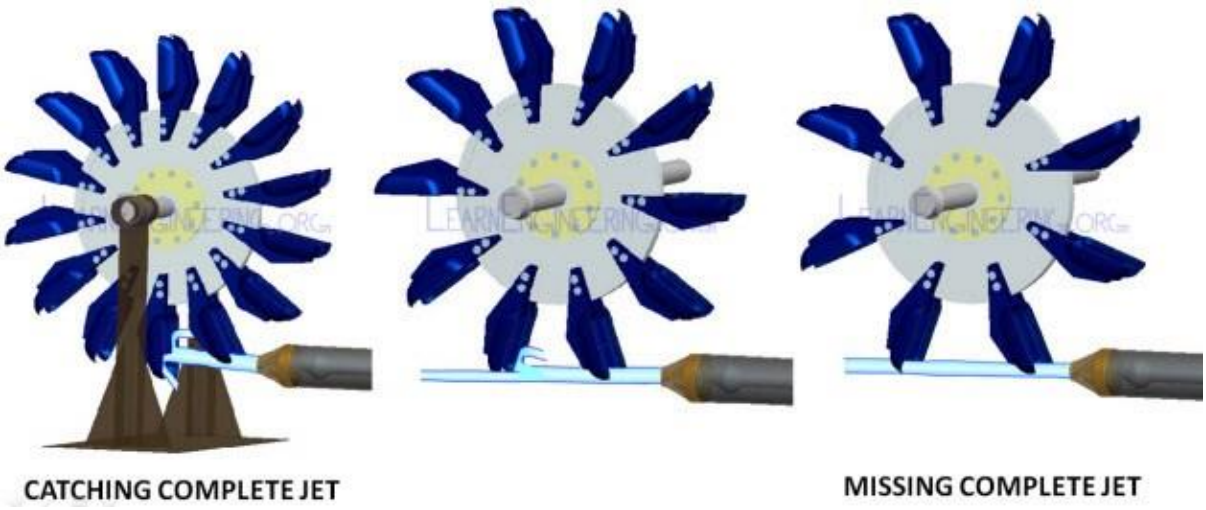

Figure 3.9: Energy loss in the form of leakage [35].

3.3 Generator

A generator converts the mechanical power from the turbine into electrical power. The efficiency of a large synchronous generator is in the order of 97-98.8% at nominal rating [20] [36]. Synchronous machines are the preferred choice for generators larger than 1 MVA [37]. The reason is that the machines can have a four-quadrant operation and thereby regulate the production of reactive power independently of the active power, making them superior to asynchronous generator regarding stability capacity and voltage control. A typical hydropower generator (salient pole) design is depicted in Figure 3.10.

Figure 3.10: Illustration of a salient-pole design of a large synchronous generator, used in an HPU [38]

3.3.1 Construction of synchronous machines

Synchronous machines come in two main types: cylindrical rotor and salient pole rotor, illustrated in Figure 3.11. A cylindrical rotor type often found in high-speed applications, e.g., steam turbines or few cases, with Francis and Pelton turbines. However, these generator types will not be discussed further. In contrast, salient pole rotor type machines are used for low-speed (125-500 rpm) applications and almost exclusively used in all large HPU.

The synchronous generator consists of armature (stator) windings and field (rotor) windings encased around an iron core made up from limitations of magnetic steel. Armature windings conduct the primary current, i.e., the current transported out of the power plant and into the grid. In comparison, the field windings conduct direct current to induce a magnetic field in the rotor, allowing the machine to regulate the magnetic field strength or, more importantly, reactive power production in the armature windings. With reactive power control, the generator will be able to maintain the voltage.

An automatic voltage regulator (AVR) are used to control and excite the field windings. Since the rotor is constantly rotating, the field windings are generally excited through what is known as slip rings, where the electrical contact between two points are maintained while one of the

points rotate. The slip rings usually have carbon (graphite) or metal brushes that slide or rubs the surface of a metal ring located on the rotating part (rotor). However, the brushes produce both friction and ohmic losses. Other technologies like brushless excitation systems use a secondary generator to maintain electrical contact without slip rings, but this will not be further discussed in this report.

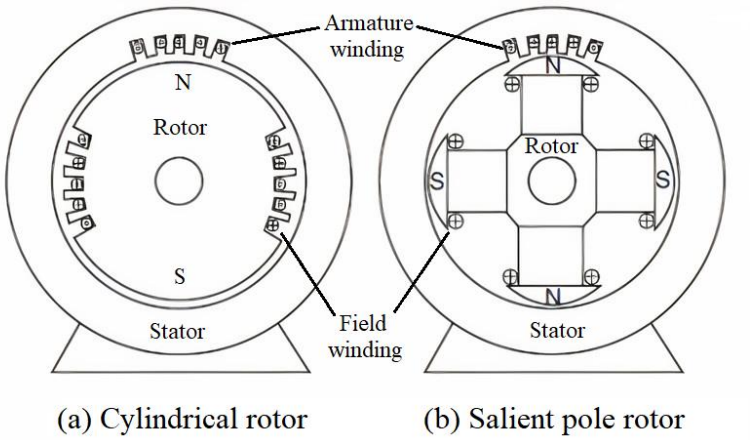

Figure 3.11: Design of (a) cylindrical rotor and (b) salient pole rotor [39].

3.3.2 Machine losses

In a generator, there are load-dependent losses considered variable, and there are constant losses that are independent of the loading. The IEEE standard [15] have a general categorisation of machine losses which is as follows:

- I^2R losses of stator winding
- I^2R losses of rotor winding
- Excitation system loss
- Stray load loss

Load-dependent

- Core loss
- Friction and windage loss
- Ventilation and cooling loss

Constant

Winding losses

The ohmic resistance in windings (stator and rotor) produces what is known as winding losses, also referred to as I^2R loss. The total winding loss in the stator is the sum of the winding resistance for each phase, expresses as:

$$P_S = 3 \cdot I^2 \cdot R_{s,stator} \qquad 3.4$$

On the other hand, the field winding losses have additional losses considering the total excitation system (e.g., AVR). One can assume the excitation losses to be a linear function of the field current (I_{fd}), with a contribution of about 10% (k = 1.1) that are added to the field winding losses [40] and [41], yielding:

$$P_R = k \cdot I_{fd}^2 \cdot R_{s,rotor} \quad 3.5$$

where $R_{s,rotor}$ [Ω] is the measured resistance (including bush resistance), P_R is the total rotor winding loss, k is the proportional constant for excitation system loss. I_{fd} is the field current and is usually given in the form of open-circuit characteristic (OCC) and air-gap characteristic. The air-gap characteristic represents the relationship between excitation voltage and field current when the core unsaturated. The OCC describes the relationship between excitation voltage and field current in both unsaturated and saturated situation. A calculation example of field current is found in Appendix E.

According to IEEE STD 115 [42], the winding resistance ($R_{s,stator}$ and $R_{s,rotor}$) should be given at specified temperature (normally 75 ℃). The formula for winding resistance under a given temperature, is expressed as:

$$R_s = R_0(1 + \alpha_t(T_s - T_0)) \quad 3.6$$

where

R_s is the winding resistance [Ω], corrected to the specified temperature, T_s

T_s is the specified temperature [℃]

R_0 is the nominal winding resistance [Ω]

T_0 is the nominal temperature [℃] of winding when resistance was measured, usually 20[℃]

α_t is the temperature coefficient for the winding material (0.00386 for pure copper or 0.00429 for aluminium)

Core losses

A generator with an applied voltage that is alternating (AC) will produce core losses. The induced alternating magnetic fluxes in the iron core produces what is known as hysteresis and eddy currents. These effects will then generate core losses in the form of heat. One can often assume the core losses to be constant by having minor voltage variations. In reality, the core loss is voltage-dependent, as depicted in Figure 3.12. It is possible to estimate the core loss by measuring the change in power draw with and without excitation under an open circuit operated at the constant nominal speed [15].

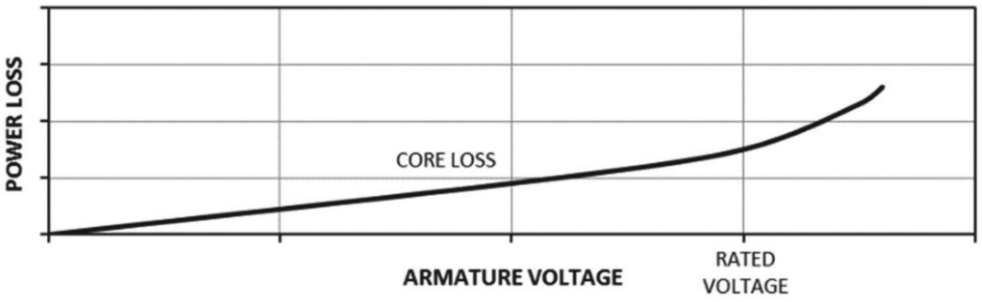

Figure 3.12: Armature core loss relative to the applied terminal voltage, as described in the IEEE STD 115 [42].

Over the years, numerous calculation methods have been proposed, like the well-known Steinmetz's equation, published by Charles Steinmetz in 1892 [43] or newer methods as shown in the study from Ionel [44]. Most core loss expressions estimate the energy loss based on the friction, flux density and material coefficients. However, advanced field simulations software like FEM (finite element method) are often required to achieve accurate results.

Hysteresis is a phenomenon observed in ferromagnetic materials like steel subjected to an alternating magnetic field. In ferromagnetic materials, the molecular structure can rotate to an adjacent field, and this motion requires energy, resulting in energy loss or heat. The polarisation of the structure is often illustrated in a hysteresis loop, as seen in Figure 3.13. The hysteresis diagram describes the relationship between the induced magnetic flux density (B) and the magnetisation force (H), often referred to as B-H loop [45].

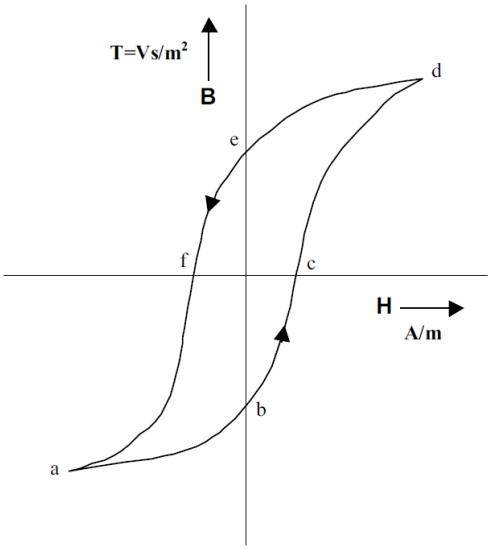

Figure 3.13**:** Illustration of a hysteresis loop [46].

Eddy currents are due to the induced circular currents conducted in the laminated magnetic steel that produces ohmic losses. Creating a core with laminated magnetic steel will decrease the electrically conductive path making a higher electrical resistance and reducing the induced eddy currents.

Stray-load loss

Under loaded conditions, the armature current induces an alternating magnetic field with a field strength directly proportional to the current, resulting in additional eddy currents in the armature windings and the iron core, often referred to as stray-load loss.

Copper stray-load loss: Alternating magnetic fields produces eddy currents inside the windings and give rise to a non-uniform current distribution in the windings. An effect is known as the skin-effect and proximity effect. The non-uniform current distribution decreases the effective cross-sectional area, resulting in increased resistance and ohmic losses proportional to the loading current squared, see Figure 3.14.

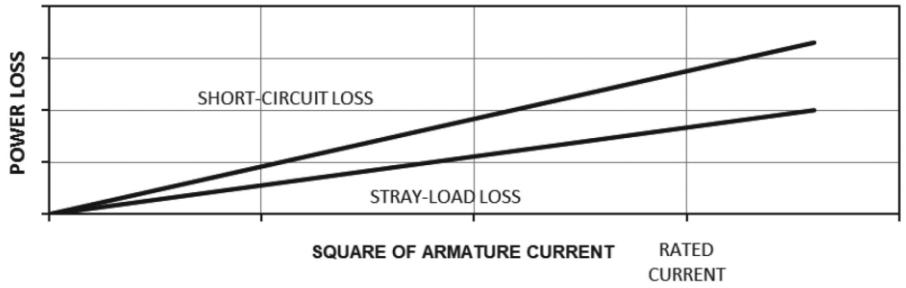

Figure 3.14: Armature winding loss and stray-load loss, as described in the IEEE STD 115 [42]

Core stray-load loss: Under the loaded condition, the iron core and teeth are highly saturated, allowing more flux to leak through the core that produces losses in the form of eddy currents in the shielding, stator cover and end frames [47].

Modelling stray-load losses are complex, and FEM simulation tools are often required, but the losses could be measured as described in the IEEE Std C50.13 [15].

Mechanical losses

Friction loss is the friction produced between the rotor shaft and generator bearings and the friction between the slip rings and brushes.

Windage loss (or viscous friction) is caused by air friction when the rotor rotates and is proportional to the rotor velocity cubed. A first approximation formula for windage losses has been proposed by J. Vrancik [48] in 1968, where the equation calculates the windage loss for a smooth cylinder rotating within a concentric cylinder and corrects for a salient pole design. For more detailed estimations, a CFD simulation would be required.

Ventilation and cooling losses are the power required to cool down the generator system, containing fans and circulation pumps [15].

3.3.3 Capability diagram

The operational boundaries to a generator are defined by the P-Q plane's limits, also known as the capability diagram. The capability diagram describes the maximum active and reactive power allowed for the generator to operate concerning thermal limits and stability limits under a constant (nominal) voltage. The limiting factors in the capability diagram are illustrated in Figure 3.15 and are given by:

- Armature current limit (c-d) and (e-f) produced by ohmic I^2R losses in the armature windings, where the upper temperature in the windings are the limiting factor.
- Upper prime mover limit (d-e) is determined by the maximum active power the HPU could continuously deliver, usually rated by the turbine.
- The lower prime mover limit (a-g) is the minimum power the turbine could produce continuously. A lower limit is only applicable for Francis and Kaplan turbines which have a limit of around 5-30 % of the rated output [49].
- Field current limit (f-g) produced by ohmic I^2R loss in the field windings, where the upper temperature in the windings are the limiting factor.
- End heating limit (a-b), localised heating in the end region of the stator laminations produced by electromagnetic fields entering and exiting perpendicular to the laminations [50]. In under excited operation, the field current is low, and the so-called retaining ring will not be saturated, resulting in high flux leakages. As a consequence, more eddy currents will be induced in the laminations that will be added to the eddy currents produced by the armature currents, and there will be excessive heating at the end laminations.
- Practical stability limit (b-c), a limit used to reduce the risk of losing synchronism, also known as skipping, when the generator is situated in an under-magnetised operation.

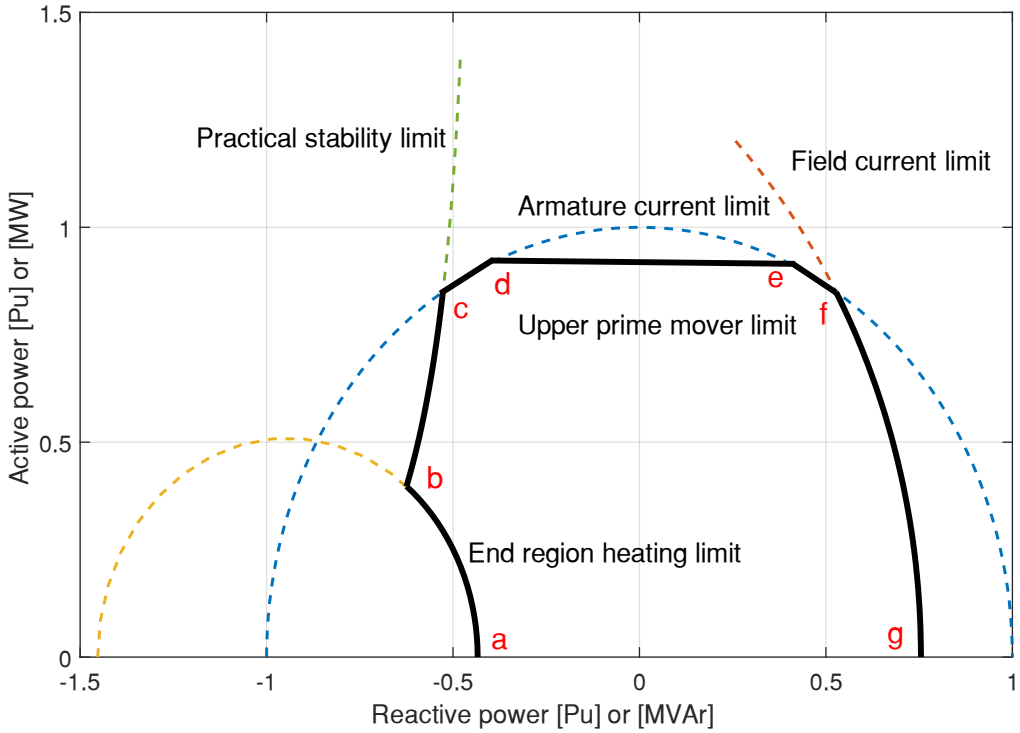

Figure 3.15: Illustration of a capability diagram to a salient pole generator.

3.4 Transformer

A transformer is an electrical component used to increase the relatively low voltage induced by the generator to reduce transmission losses. The transformer is a relatively simple component; it contains a primary and secondary coil wound around an iron core, see Figure 3.16. The ratio between the number of windings determines the ratio to which the voltage will increase/decrease. The transformer is the component in an HPU with the highest efficiency, usually close to 99.7% at nominal power. Due to the extraordinary high efficiency of the transformer, a simplified calculation model is seen as adequate and will only be described briefly.

3.4.1 Transformer losses

A transformer has a lot in common with generators when it comes to theoretical background and losses. In simplified terms, the transformer losses can be represented by no-load losses (P_0) and load losses (P_k) [46].

No-load losses (P_0), often referred to as magnetisation losses or core losses will be present as long as the transformer is energized. The no-load losses are usually assumed to be constant by not considering any voltage differences and flux leakages [46]. The magnetisation losses are produced by hysteresis and eddy currents, as described in section (0).

Load losses are produced under loaded conditions, where the load current and the resistance result in ohmic losses (I^2R). The load-dependent losses will, in addition, be affected by temperatures and stray-load losses, as described in section (0). For simplicity, one can represent the load losses as a proportional constant (P_k) that are multiplied to the loading ratio, seen in equation 3.7.

By combining no-load losses (P_0), and load losses (P_k), the total transformer loss (P_{loss}) and efficiency (η_{Tran}) can be expressed as:

$$P_{loss} = P_0 + P_k \left(\frac{S_{load}}{S_n}\right)^2 \quad 3.7$$

$$\eta_{Tran} = \frac{P_0}{P_0 + P_{loss}} \quad 3.8$$

where S_{load} is the load out of the transformer [MVA or Pu] and S_n is the transformer's rating [MVA or Pu].

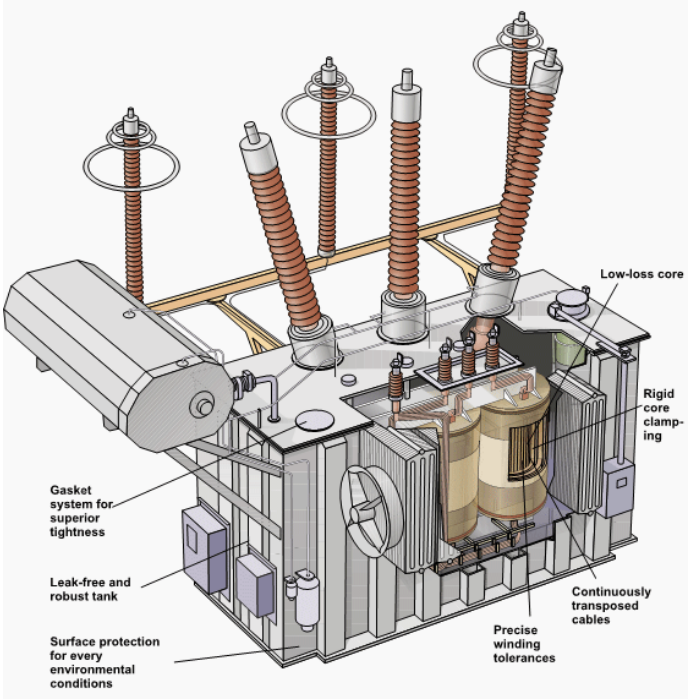

Figure 3.16: Design of a large power transformer (ABB's TrafoStar design) [51].

4 Power plant description

In this chapter, there will be a description of the two hydropower units analysed, namely Åbjøra and Sundsbarm. Both of the units are regulated impoundment types with a single generating unit. Åbjøra and Sundsbarm are owned or partly owned by Skagerak Kraft and are located in Nord-Aurdal and Seljord. A summary of the nominal specifications to Åbjøra and Sundsbarm can be seen in Table 4.1. The specifications depicted in Table 4.1 form the basis for most of the calculations used in the analysis. Additional details considering the generator and turbine characteristics relevant for simulation is found in Appendix F (Åbjøra) and Appendix G (Sundsbarm).

Table 4.1: Overview of the nominal specifications to Åbjøra and Sundsbarm hydropower station. * Mechanical losses in Sundsbarm contains windage, ventilation and bearing losses.

Åbjøra Value	**Sundsbarm Value**	**Specification**
442 m	493 m	Nominal gross head
24 m^3/s	24 m^3/s	Nominal discharge
5140 m	7750 m	Waterway length
550 GWh	430 GWh	Average annual production
0.016335	0.00893	Total head loss coefficient K (waterway)
95 MW	103MW	Nominal turbine power
94.26 %	93.86 %	Nominal turbine efficiency
103 MVA	118 MVA	Nominal generator power ($cos\varphi = 0.9, 0.85$)
98.8 %	98.6 %	Nominal generator efficiency
0.15253 Ω	0.24857 Ω	Field winding resistance (75℃)
0.003155 Ω	0.00390 Ω	Armature winding resistance (75℃)
11 kV	15 kV	Nominal voltage
172.92 kW	537 kW*	Mechanical losses (windage and ventilation)
211.92 kW	353 kW	Core losses
240.90 kW	–	Bearing losses (generator)
276.62 kW	333 kW	Nominal load losses
191.66 kW	226 kW	Nominal total excitation losses
1094.02 kW	1450 kW	Nominal total losses
103 MVA	118 MVA	Nominal transformer rating
52.5 kW	148.4 kW	No-load losses (P_0)
225 kW	281.4 kW	Load losses (P_k)

4.1.1 Åbjøra

Åbjøra hydropower station is located in Nord-Aurdal, Norway and owned by Skagerak Kraft. The station was first opened in the year 1951 with three Pelton turbines with a total rating of 81 MW. Åbjøra was later rebuilt in 2002, where all three Pelton turbines were replaced (Figure 4.1) by a single Francis turbine (Figure 4.2) with a rating of about 95 MW with an average annual production of 550 GWh. The increased power resulted from a more efficient turbine and changes to the waterway, as the new station was placed 15 meters below the old station. The hydropower utilizes multiple reservoirs joined to an intake reservoir at Bløytjern/Ølsjøen, which results in a nominal gross head of 442 m. Thought a year, the gross head only varies from about 439 m to 445 m or less.

Figure 4.1: Disassembly of the old Pelton turbines in Åbjøra (2007). *[Photo: Jan Erik Olsrud]*

Figure 4.2: Inside of Åbjøra power station, showing the generator. *[Photo: Skagerak Kraft]*

In the waterway, there is a 4.5 km headrace tunnel from the intake reservoir before entering a vertical pressure shaft of 380 m followed by an additional pressure shaft of 260 m before entering the turbine. After the rebuild in 2002, the losses in the waterway were measured. The measurements could be seen in Table 4.2, which shows the head loss coefficients (k_i) for each respectful element in the waterway, see Figure 4.3. The total head loss coefficient (K) of the waterway was estimated to $K = 0.016335$.

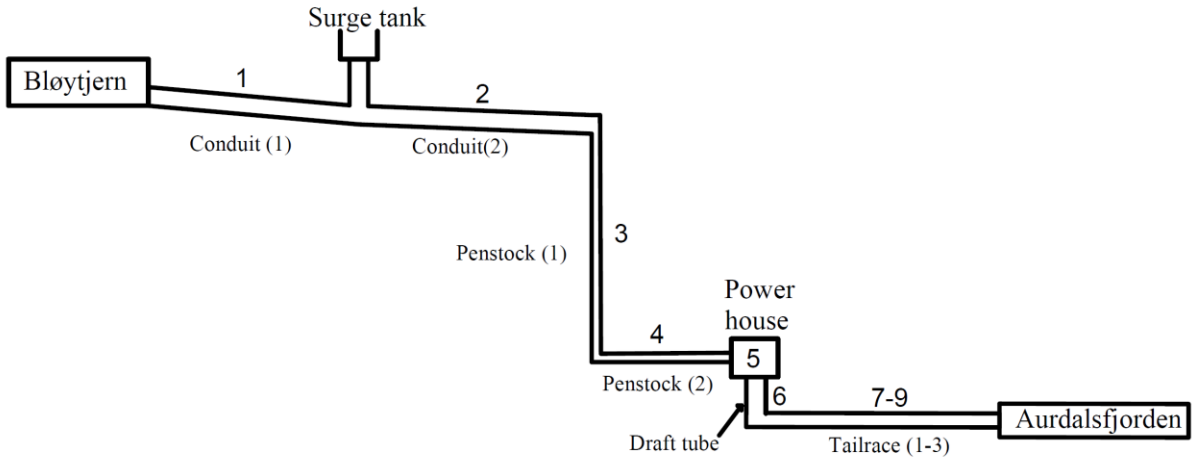

Figure 4.3: Simplified overview of the waterway in Åbjøra, where the numbers (1-9) represents the different elements used in the measurements found in Table 4.2. In the figure one can see the conduit and penstock is divided into two whereas the tailrace is divided into three elements.

Table 4.2 Head loss measurements of each element in the waterway from Åbjøra

Waterway elements and their respectful head loss coefficients			
Object Element	Element nr.	Head loss coefficient (k_i)	Power loss [%]
Conduit (tunnel part 1)	1	0.01	61.8
Conduit (tunnel part 2)	2	0.00009	
Penstock (part 1)	3	0.00069	5.7
Penstock (part 2)	4	0.000245	
Main valve + turbine	5	0.0022	13.5
Draft tube	6	0.00011	0.7
Tailrace (tunnel part 1)	7	0.0001	
Tailrace (tunnel part 2)	8	0.00015	18.4
Tailrace (tunnel part 3)	9	0.00275	
Total		**0.016335**	**100**

The Francis turbine operates under a nominal gross head of 442 m (net head of 433m) and a nominal discharge of about 24 m^3/s. Measurements from 2003 gave the results shown in Appendix F, which indicate a nominal efficiency of 94.26 % and a maximum efficiency of 94.56 % achieved around 86 MW under the nominal head. It has been assumed that the turbine efficiency correlates to the runner efficiency as the data includes both the main valve and turbine (spiral casing and guide vane) and draft tube as a part of the waterway.

4.1.2 Sundsbarm

Sundsbarm hydropower station is located in Seljord, Norway and is owned by Skagerak Kraft AS (91.5%). The station was put into operation in 1970 with a Francis turbine of 103 MW, depicted in Figure 4.4. Sundsbarm is a reservoir type hydropower, which uses the lake named Sundsbarmvatnet as a reservoir and utilizes few additional lakes interconnected through tunnels, resulting in a precipitation area of about 418 km^2. Throughout a year, the gross headwater could range from 455 m to 493 m, with and an annual production of about 430 GWh.

From the intake reservoir in Sundsbarmvatnet, the water in guided through a 6.6 km conduit tunnel before entering a vertical pressure shaft of 600 m. A simplified overview of the waterway is shown in Figure 4.5. In 2011, the head loss in the waterway was measured, these results can be seen in Table 4.3, which show the head loss coefficients for each respectful element in the waterway (Figure 4.5). The total head loss coefficient for the waterway is estimated to be $K = 0.00893$.

Table 4.3: Head loss measurements of each element in the waterway from Sundsbarm.

Waterway elements and their respectful head loss coefficients				
Object Element	Element nr.	Length [m]	Head loss coefficient (k_i)	Power loss [%]
Conduit (tunnel part 1)	1	3000	0.0026	61.6
Conduit (tunnel part 2)	2	3600	0.0029	
Penstock	3	600	0.00295	33.0
Draft tube and Tailrace	4	550	0.00048	5.4
Total		**7750**	**0.00893**	**100**

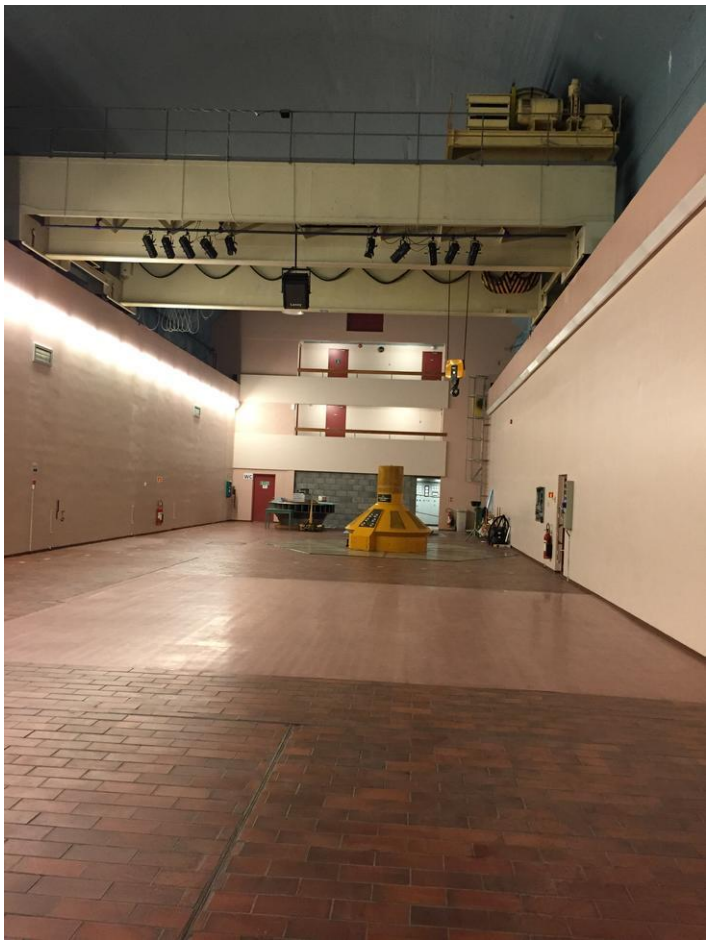

Figure 4.4: Inside of Sundsbarm power station, showing the generator. *[Photo: Skagerak Kraft]*

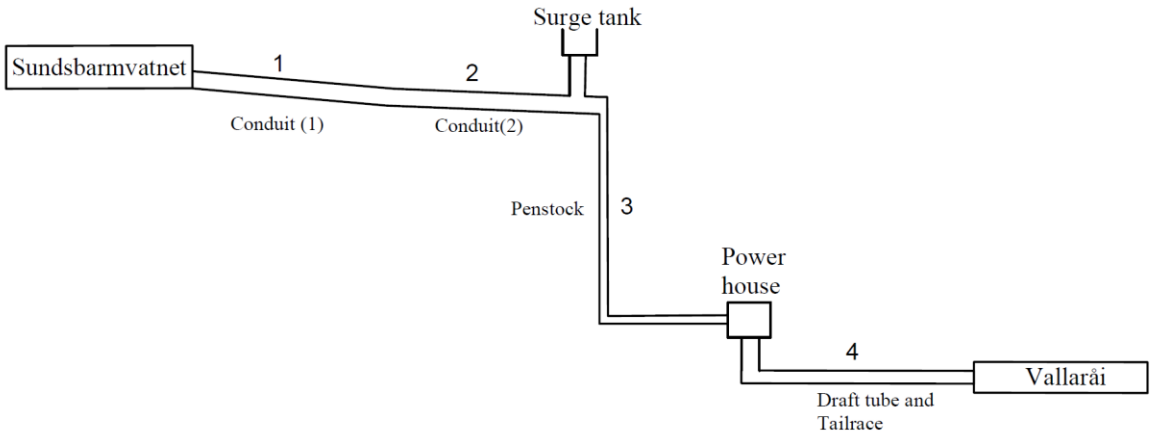

Figure 4.5: Simplified overview of the waterway in Sundsbarm. The element numbers (1-4) represents the object element found in Table 4.3.

The Francis turbine is operated under a nominal gross head of 480 m (net head of 487 m) and a nominal discharge of about 24 m^3/s. Estimates from 2011 gave the results shown in Appendix G, which indicate a nominal efficiency of 93.86 % and a maximum efficiency of 93.93 % achieved around 100 MW. Similar to Åbjøra, it has not been specifically defined what the turbine measurements evaluate, but it is assumed it contains only the runner efficiency.

The generator is a synchronous generator with nominal apparent power of 118 MVA and PF = 0.85 and a nominal voltage of 15 kV. In Appendix G, one can find the generator's load characteristics and measurements.

5 Methods

This chapter contains descriptions of the methods used to solve the analysis objectives. The main tool of this analysis is the simulation model of the HPU, created in the software MATLAB. The simulation model is used to map and assess possible optimal efficiency, also known as the best efficiency point (BEP). In addition, the model will be used for analysing the operational efficiencies and energy losses. The model uses input parameters from the waterway, turbine, generator and transformer, and uses operational data taken from the transformer (high voltage side) or generator to determine the losses in all of the components.

The basic structure of the simulation model is illustrated in Figure 5.1, which depicts all input parameters and variables, main functions and output variables. The input parameters are shown with their respective unit where data acquisition represents the filtered input variables, active power (P), reactive power (Q) and voltage (V).

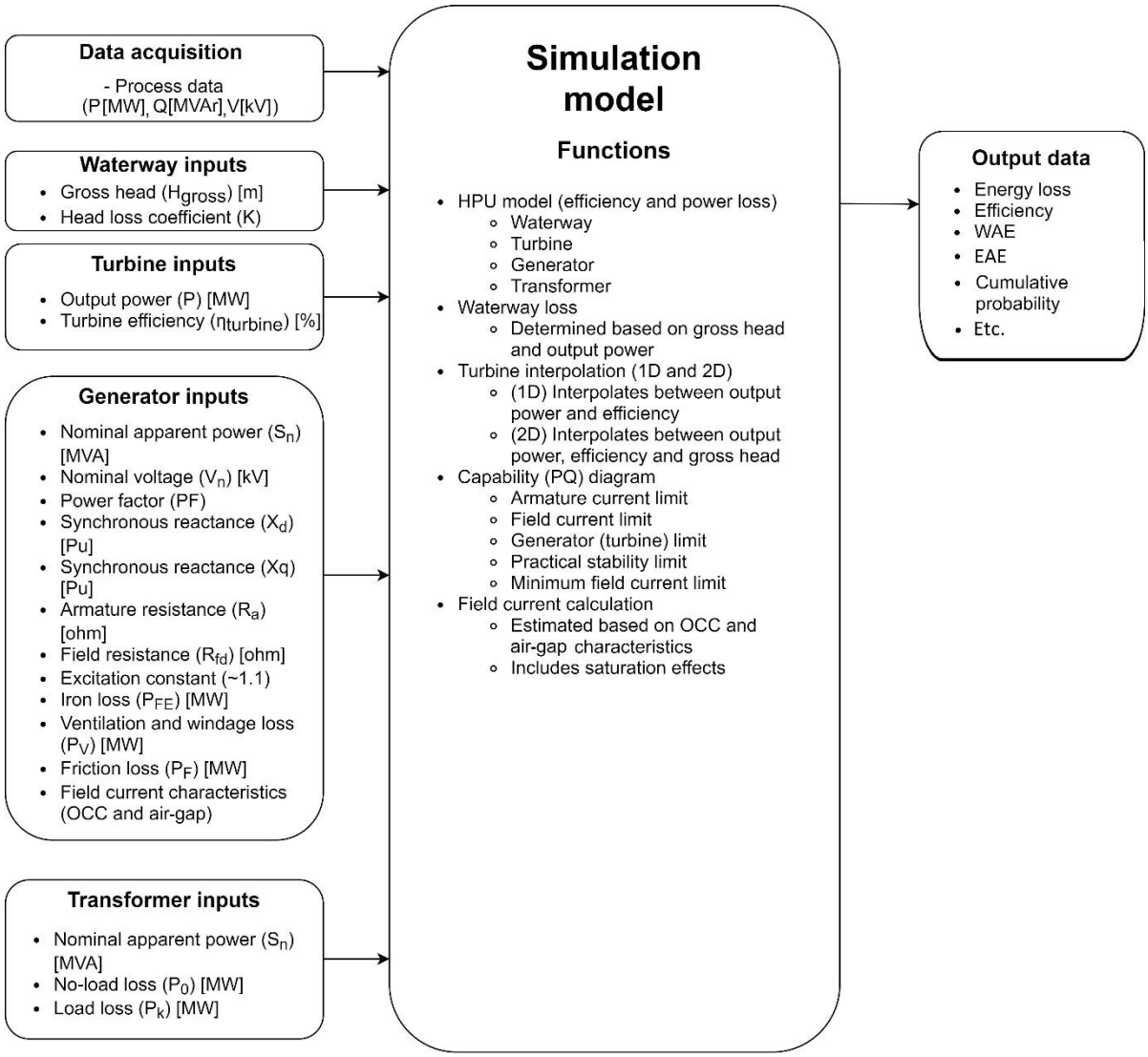

Figure 5.1: Diagram describing the structure of the simulation model.

5.1 Simulation model

In this report, the simulation (HPU) model is a general mathematical model coded in MATLAB and is used to calculate energy losses and efficiencies under static conditions given by operational data of active power (P), reactive power (Q) and voltage (V). The model has built-in features which allow an additional input of gross head (H_{gross}) to be added, but will not be used in this report as there was no available operational data about the head. The HPU model is a collection of several models (transformer, generator, turbine and waterway) which are combined into a single HPU model, illustrated in Figure 5.2. The figure depicts how each model is interconnected with its respective input parameters, variables and outputs.

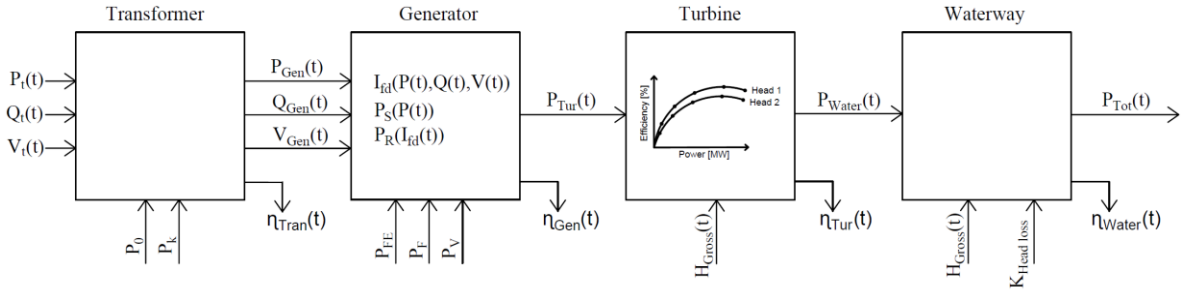

Figure 5.2: Structure of the HPU model.

The HPU model uses the production data from the transformer (or generator), as this data is widely accessible for most HPUs. Thus, allowing easy implementation of the model to, e.g., more extensive grid simulations. Knowing the efficiency of every component and having the production output of the transformer or generator accessible, one can simply predict the power flow through the turbine and the waterway and then determine the water or power consumption. Calculating from the production side to the input side causes the models closest to the production side (transformer) to transfer the least amount of power. However, the models furthest away (waterway) from the production side will transfer the most power as the losses for each model are added along the way, illustrated in Figure 5.3.

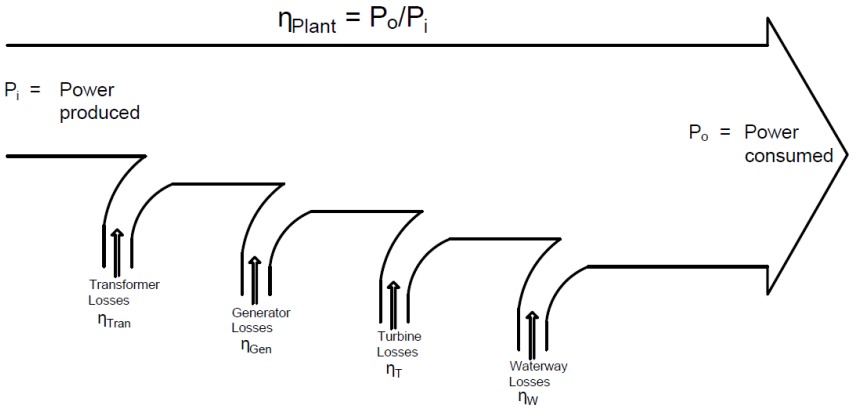

Figure 5.3: Power flow diagram, illustrating the calculation direction, where P_i represents the electrical production (input data) of the transformer and P_o represents the hydraulic power entering the waterway (output data from the model).

A single mathematical function can express how the efficiency of the HPU model and each sub-model is calculated, which yields:

$$\eta_{HPU}\left(P_{load}, Q_{load}, V_{load}, H_{gross}\right) = \eta_{Tran}(P_{load}, Q_{load}) \cdot \eta_{Gen}\left(\frac{P_{load}}{\eta_{Tran}}, Q_{Gen}, V_{Gen}\right) \cdot \eta_{Tur}\left(\frac{P_{load}}{\eta_{Tran} \cdot \eta_{Gen}}, H_{gross}\right) \cdot \eta_{Water}\left(\frac{P_{load}}{\eta_{Tran} \cdot \eta_{Gen} \cdot \eta_{Ttur}}, H_{gross}\right) \quad 5.1$$

where η_{HPU} is the total plant efficiency, η_{Tran} is the transformer efficiency, η_{Gen} is the generator efficiency, η_{Tur} is the turbine efficiency, and η_{Water} is the waterway efficiency. $P_{load}\ [MW], Q_{load}[MVAr], V_{load}[kV]$ are the input (operational data) at the transformer's high voltage terminals and $H_{gross}\ [m]$ is the gross head given at nominal value.

For this report, the operational data was measured from the generator terminals and not the high voltage terminals of the transformer, which the HPU model is designed for. Thus, the operational data was first adjusted by subtracting the energy loss of the transformer before implemented into the model, explained in detail in section 5.6. Since the inputs were given at the generator terminals, the absorption of reactive power in the transformer could be neglected, i.e., $Q_{load} = Q_{gen}$. In addition, due to the lack of data, the gross head was assumed constant and was set to nominal gross head for all operations. All parameters used for Åbjøra and Sundsbarm model is summarised in Appendix F and Appendix G, respectfully. A function description of the different functions used in the MATLAB model can be found in Appendix K. In addition, the MATLAB code all functions, including the code for Åbjøra with various plot functions, can be found in Appendix L.

5.2 Data acquisition and preparation

The operational data originates from the system called SCADA "Supervisory Control and Data Acquisition" and is the system used for measuring and transport information to the control centre [52], in this case, Skagerak Kraft. This data contributes to analysing the operational efficiency and energy losses of the respective hydropower plants.

5.2.1 Data format

Skagerak Kraft provided the data in CSV (Comma-Separated Values) format, a typical file format used to store measurements, where a comma separates each column. CSV files are plain-text files, which makes them compatible with most analysis/data programs and allow for easy transport of tables/measurements between different programs.

The data contained timestamps (date and time) and generator measurements of the active power [MW], the reactive power [MVAr] and the voltage [kV], given as average values over 1 hour periods. The operational data shows the operation period between (22.01.2020 – 31.12.2020), i.e., a total number of 8256 hours or data points.

5.2.2 Collecting and reading the CSV-files

CSV files are practical for transporting and storing measurements but are impractical for visualization and working with the data. Thus, the files was first converted to an excel-format with the help of the excel-functions named “From text/CSV” or “Text to columns”. Before the data could be implemented into MATLAB for analysis, the data file was filtered and corrected due to:

- Measurements with equal repetitive values were represented as “NaN” which needed to be replaced with actual values.
- Data were given as average values, which results in measurements of active power (P), reactive power (Q) and voltage (V) with highly inaccurate values that do not reflect actual operating regimes.
- The combination of measurements with average values and the repetitive values given as “NaN” resulted in a data set that did not differentiate between operation in the “on” and “off “state.

5.2.3 Data processing

The procedure for formatting and correcting the data was performed in excel and described in four steps where the original data set is gradually improved until the finished format. The full description with excel commands can be seen in Appendix H. The summary of each step goes as follow:

- Step 1: Convert all operating points marked “NaN” with actual numbers by assuming each “NaN” is equal to the previously known value.
- Step 2: Corrected for logical errors where it seems like the generator have multiple start/stop sequences between two stable regions, and these regions will be set to zero. A stable region is regarded as a region where the voltage is above a trigger point or a voltage that is considered close to “normal”.
- Step 3: Convert data from 1-hour resolution to 15-minute semi-resolution by copying each operation four times for differentiating between the “on” and “off” state during the start/stop region.
- Step 4: Estimate the data in the 15-minute semi-resolution. The duration of the on-state will be determined by the ratio between the operating voltage and trigger (“normal”) voltage. Assumptions during a start/stop sequence:
    - A voltage or active power value above or equal a maximum trigger value will be unchanged.
    - A voltage or active power below a maximum trigger point and active power above a minimum trigger value will be set to a chosen value that is considered normal.
    - A voltage or active power below a minimum trigger value will be regarded as an”off” state and set to zero.

- Reactive power will not be corrected as there is no "normal" operating point and can be both positive and negative.

An illustration of the filtering process is seen in Table 5.1, showing the result of each step. The illustrated example is taken from Sundsbarm, depicting the transition between full operation to off-state. Within the given period, 116 and 55 off-transitions have been identified, which accounts for about 1.4 % and 0.7 % of the total operations for Åbjøra and Sundsbarm, respectfully. Due to the assumptions stated in step 4, the filtering process may result in few incorrect evaluations. Still, with the low number of situations (1.4 % and 0.7 %), the effect could be assumed insignificant, in particular, to the energy loss and average efficiency.

Table 5.1: Example of the filtering process of the voltage to Sundsbarm. The "normal" value or the maximum trigger voltage is here chosen to be 14.4 kV. In operation nr. 2, the $duration = 9.59/14.4 = 0.67$ or rounded to 3/4, which can be seen in step 4.

Original	Step 1	Step 2	Step 3	Step 4 (Finished)
14.3667352	14.3667352	14.3667352	14.3667352	14.3667352
			14.3667352	14.3667352
			14.3667352	14.3667352
			14.3667352	14.3667352
9.5889163	9.5889163	9.5889163	9.5889163	14.4 (trigger voltage)
			9.5889163	14.4 (trigger voltage)
			9.5889163	14.4 (trigger voltage)
			9.5889163	0
NaN	9.5889163	0	0	0
			0	0
			0	0
			0	0

5.3 *Waterway model*

A single equation will represent the waterway model. The equation estimates the waterway efficiency and power loss based on the head loss coefficient (K) and the volumetric flow (Q_{flow}). From theory (section 3.1), it was claimed that the waterway is generally represented by the head loss [m]. However, describing the losses in terms of active power [MW] would be more practical for this model regarding compatibility between the other models.

For this report, the only known parameters for the waterway was the gross head (H_{gross}), the power output of the waterway ($P_{waterway,out}$) and the head loss coefficient (K). Under these conditions, a method was developed for determining the power loss [MW] in the waterway. The method is solely based on the standard hydropower formulas for hydraulic power plants. The method is as follows:

The total available power (output) of the waterway is [28]:

$$P_{waterway,out} = \rho g Q_{flow} H_n \qquad 5.2$$

where H_n = net head [m], ρ = water density and g = gravitational constant. Both Q_{flow} and H_n are unknown variables. $P_{waterway,out}$ will be known, as this power is given by the turbine.

From equation 3.6:

$$H_{loss} = KQ_{flow}^2 \tag{5.3}$$

Substituting H_n in (5.2) with gross head (H_{gross}) and head loss (H_{loss}) (5.3) gives:

$$P_{waterway,out} = \rho g Q_{flow}(H_{gross} - KQ_{flow}^2) \tag{5.4}$$

Rearrange (5.4) gives the expression of a cubic equation:

$$KQ_{flow}^3 - H_{gross}Q_{flow} + \frac{P_{waterway,out}}{\rho g} = 0 \tag{5.5}$$

Solving the equation with respect to discharge Q_{flow}, gives the flow rate required for yielding the output power under a given gross head and head loss coefficient. With the estimated discharge Q_{flow}, the power loss P_{loss} produced in the waterway is then calculated by using (5.2) and substituting H_n with head loss (5.3):

$$P_{loss} = K\rho g Q_{flow}^3 \tag{5.6}$$

Substituting (5.2) and (5.6) yields the total waterway efficiency:

$$\eta_{Water} = \frac{P_{out}}{P_{in}} = \frac{P_{waterway,out}}{P_{waterway,out} + P_{loss}} = \frac{P_{waterway,out}}{P_{waterway,out} + K\rho g Q_{flow}^3} \tag{5.7}$$

5.4 Turbine model

The turbine model will be represented by either a simple 1D interpolation or a 2D interpolation. Interpolation is an ordinary mathematical operation used to predict the value or line which is the most probable between two or more data sets. For the turbine, it has been provided operational data of the output power (P) and efficiency (η_{Tur}). With two data sets (P) and (η_{Tur}), one will have what is known as a 1D interpolation (linear, cubic or higher order), illustrated in Figure 5.4, where the blue circles and the orange curve represents the known data points and the interpolated curve, respectfully. MATLAB has implemented a simple function for 1D interpolation named “cubic spline” or simply “spline”, used in this report.

In the turbine model, bilinear interpolation (2D) have been added as an extended feature to the software. The bilinear interpolation allows the user to interpolate between output power (P), efficiency (η_{Tur}) and gross head (H_{gross}), which results in a three-dimensional plot, as depicted in Figure 5.5. Bilinear interpolation is an extension of linear interpolation where linear interpolation is first performed between, e.g., (P) and (η_{Tur}) for all known heads (H_{gross}). Then, bilinear interpolation will be achieved by interpolating again, but this time between all the interpolated curves.

The turbine model has the 1D interpolation implemented, which can be used for cases where one have only measurements from one head. In this report, the turbine measurements were given for multiple head, allowing 2D interpolation to be implemented.

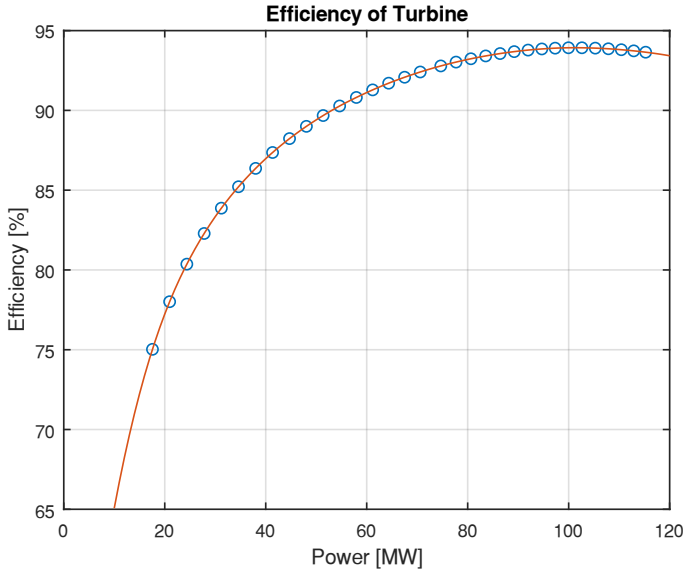

Figure 5.4: An illustration of the efficiency curve of a Francis turbine, where the dotted line is the given data points, and the red line is the interpolated curve.

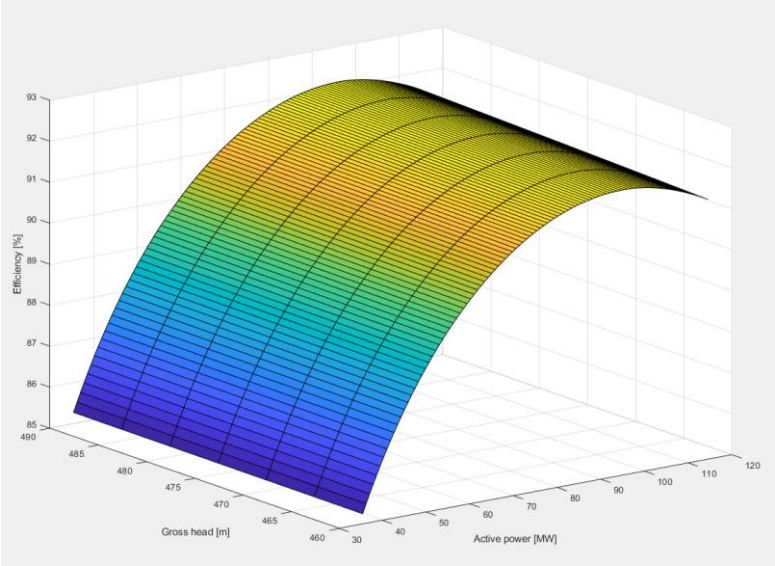

Figure 5.5: Efficiency mapping of Sundsbarm, with bilinear interpolation between active power (P), gross head (H_{gross}) and total plant efficiency (η_{HPU}).

5.5 Generator model

The generator model is based on the work form [40], and the IEEE standard [15], where the total energy loss in the generator is expresses as:

$$P_{loss} = P_S + P_R + P_{FE} + P_V + P_F \quad 5.8$$

where P_S is winding loss of stator windings, P_R is winding loss of rotor windings and excitation losses, P_{FE} is iron core loss, P_V is the ventilation and cooling loss, and P_F is friction and windage loss. Thereby, the total generator efficiency becomes:

$$\eta_{tot} = \frac{P_{load}}{P_{load} + P_{loss}(P_t, Q_t, V_t)} \quad 5.9$$

where V_t is the terminal voltage of the generator, P_t and Q_t is the active and reactive power produced by the generator, respectfully.

In this report, the iron core loss (P_{FE}), ventilation and windage (P_V) and friction loss (P_F) has been assumed constants for all operating regimes. These constant losses were fortunately provided, meaning the stator (P_S) and rotor (P_R) losses were the only losses that needed to be estimated. In the generator model, it was used the same equations for stator (P_S) and rotor (P_R) losses, as described in section (3.3), which yields:

$$P_S = 3 \cdot I^2 \cdot R_{s,stator}$$

$$P_R = k \cdot I_{fd}^2 \cdot R_{s,rotor}$$

where I is the armature/phase current, I_{fd} is the field current, $R_{s,stator}$ is the armature/phase winding resistance and $R_{s,rotor}$ is the field winding resistance. In this report, the $R_{s,stator}$ and $R_{s,rotor}$ are known parameters that have been measured and calculated (Eq. 3.6) to an operating temperature, in this case, 75 ℃ from 20 ℃. k is the excitation constant, assumed to be 1.1 [41] and [40]. In Åbjøra, the excitation constant k was approximated based on eight provided measurements of excitation loss under various operating conditions, see Appendix F. Thus, the well-known least square method was used to determine a more accurate estimate of the excitation constant k. The leas square method was used as follows:

$$\mathrm{k} = \min\left(error_i\right) = \left(P_{R,meas,j} - k_i \cdot I_{fd,j}^2 \cdot R_{s,rotor}\right)^2$$

where the excitation constant k is determined from a "random" value of k_i which produce the least error to the measurement $P_{R,meas,j}$. i represents the number for each value of k_i, $P_{R,meas,j}$ is the measurement of the total rotor loss, including excitation loss, where $I_{fd,j}$ is the representative field current at each measurement j. With the least square method, the difference between estimated and measured excitation constant showed a maximum error of about 2.5 %, with an average error of 0.2 %.

5.5.1 Approximation of field current

In this report, the field current was approximated with a method that was based on a method used by Bortoni [53] and combined with some assumption described in [54]. The method chosen considers saturation effects and can produce results with high accuracy. Compared to most other methods, the main benefit of this method is how saturation considered. Saturation can be implemented from the OCC by using either polynomials or an equation to represent the OCC. The last was the method of choice.

The method requires information about P_t [Pu], Q_t [Pu], V_t [Pu], and generator parameters X_d, X_q, X'_d, X_l, R_a, with air-gap line and OCC to calculate the field current using the Potier reactance. In this report, the generator parameters and characteristics were based on a document [4]where these parameters were estimated. The parameters used for Åbjøra and Sundsbarm can be found in Appendix F and Appendix G, respectfully. The document gives only an estimate of the parameters, and actual values may deviate slightly from these estimates. In Åbjøra, only X_q, X'_d, X_l were used from the document, as actual measurements were available for the other parameters and characteristics. It should be mentioned that the transient reactance X'_d was given as 0.29 Pu for Åbjøra but was adjusted to 0.15 Pu in this report to achieve similar estimations of OCC and field current as what was measured. For Sundsbarm, all parameters and characteristics were based on the document and could therefore be less accurate.

The following procedure has been used for field current approximation and is based on the work by Bortoni [53] and Kundur [50]:

- Calculating the armature current I and phase angle φ:

$$I_t = \frac{\sqrt{P_t^2 + Q_t^2}}{V_t} \tag{5.10}$$

$$\varphi = \tan^{-1}\left(\frac{Q_t}{P_t}\right) \tag{5.11}$$

- The internal rotor angle, or load angle δ_i can then be calculated [53],[50]:

$$\delta_i = \tan^{-1}\left(\frac{X_q I_t cos\varphi - R_a I_t sin\varphi}{V_t + R_a I_t cos\varphi + X_q I_t sin\varphi}\right) \tag{5.12}$$

  where X_q is the synchronous reactance on the q-axis, and R_a is the armature winding resistance.

- Calculating the internal excitation voltage:

$$E_g = V_t cos\delta_i + R_a I_t cos(\varphi + \delta_i) + X_d I_t sin(\varphi + \delta_i) \tag{5.13}$$

[4] The document is an excel sheet created by Prof. Hegglid, which estimates generator parameters based on factory data.

- In unsaturated operation or at open circuit, the field current I_{FU} have a linear characteristic, i.e., a constant relationship between the excitation voltage and field current. This relationship is usually known as air-gap line characteristic of the machine, yielding:

$$I_{FU} = \frac{E_g}{b_v} \tag{5.14}$$

where E [Pu] is the excitation voltage, I_{FU} is the unsaturated field current and b_v is the relationship between excitation voltage and field current in the air-gap, and determined by reading off the air-gap line.

- Under magnetic saturation, the machine requires a higher field current to induce the same voltage relative to the unsaturated operation. Thus, the so-called Potier reactance is used as used to represent the saturation effects of the machine. From [54] [55] the Potier reactance can be calculated with:

$$X_p = X_l + 0.63(X'_d - X_l) \tag{5.15}$$

and if X_l is not available, then Potier reactance for salient pole machines will be [54]

$$X_p = 0.7X'_d \tag{5.16}$$

where X_l is the leakage reactance and X'_d is the synchronous reactance.

- From [53], the Potier voltage will then be:

$$E_p = V_t cos\delta_p + R_a I_t cos(\varphi + \delta_p) + X_p I_t sin(\varphi + \delta_p) \tag{5.17}$$

where

$$\delta_p = \tan^{-1}\left(\frac{X_p I_t cos\varphi - R_a I_t sin\varphi}{V_t + R_a I_t cos\varphi + X_p I_t sin\varphi}\right) \tag{5.18}$$

- One could describe the curve with a high order polynomial equation by knowing the OCC, as used in [53] and [54]. Another method to describe the OCC was mention in [54], where it assumed most polynomial factors to be zero and was expressed as:

$$I_{OCC} = \left(E_p + C_n E_p^n\right) \cdot k \tag{5.19}$$

where I_{OCC} is the field current given by the approximated OCC, k is set to nominal field current ($I_{F,n}$), used to express the field current in [A] and not [Pu], E_p is the Potier voltage, n is the most significant polynomial order, often set to 5, 7 or 9 [54]. The C_n is a constant used to fit the approximated OCC curve, and in this report, it was determined by trial-and-error method.

- The additional field current caused by saturation will then become:

$$I_{FS} = I_{OCC} - \frac{E_p}{b_v} \tag{5.20}$$

- The total field current will be the sum of unsaturated field current and the saturated field current, yielding:

$$I_{fd} = I_{FU} + I_{FS} \tag{5.21}$$

A calculation example of this method and procedure can be seen in Appendix E.

5.5.2 Capability diagram

The capability diagram has been frequently used in this report to depict the boundaries of the generators. The procedure used in this report is based on the work by Pejovski [49], which shows how the capability diagram could be drawn and implemented in MATLAB. All capability diagrams depicted in the report refers to the nominal voltage. The procedure implemented is as follows:

- The armature current limit is drawn as a semicircle centred at the origin (0,0) with a radius equal to the machine's MVA rating (S_n), as illustrated in Figure 5.6. The nominal active power to the generator is depicted as a horizontal line marked as (P_{max}).

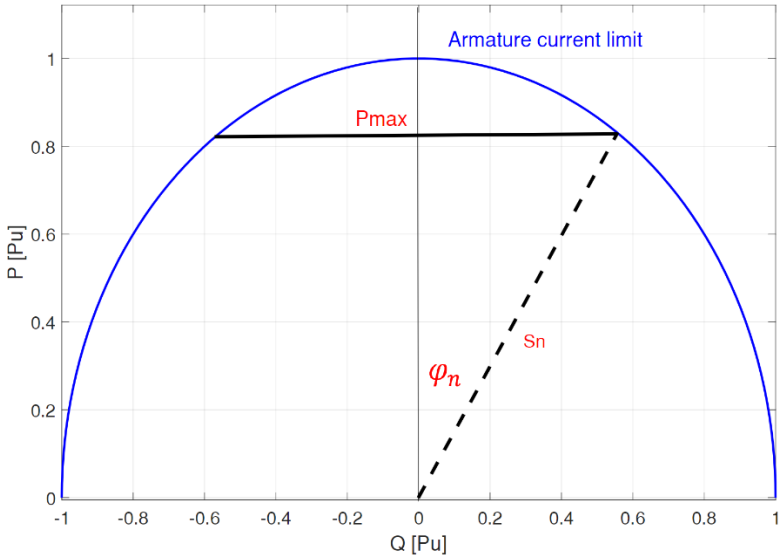

Figure 5.6: Armature current limit and maximum active power (P_{max}) where $P_{max} = S_n \cdot \cos\varphi_n$.The figure is based on [49].

- Field current limit is determined by the relationship between active power (P) and reactive power (Q) under a constant voltage (nominal) and excitation voltage (nominal), i.e., constant field current. By assuming zero resistance, the equations for determining the field current yields [49]:

$$P = \frac{EV}{X_d} sin\delta + \frac{V^2}{2} \cdot \frac{X_d - X_q}{X_d \cdot X_q} \sin\ 2\delta \quad 5.22$$

$$Q = \frac{EV}{X_d} cos\delta + V^2 \cdot \frac{X_d - X_q}{X_d \cdot X_q} \cos^2 \delta - \frac{V^2}{X_q} \quad 5.23$$

$$E = Vcos\delta + X_d I sin(\varphi + \delta) \quad 5.24$$

$$\delta = \arctan\left(\frac{Icos\varphi}{\frac{V}{X_q} + Isin\varphi}\right) \quad 5.25$$

where E is the generator's excitation voltage

V is the generator's phase voltage

I is the generator's phase current

X_d and X_q are the synchronous reactance's, given as construction parameters

δ is the load angle

φ is the phase angle between voltage and current

From equation 5.23, one can see the centre of field current circle on the abscissa point $(\frac{V_n^2}{2} \cdot \frac{X_d - X_q}{X_d \cdot X_q} - \frac{V^2}{X_q}, 0)$ or reduced to $\left(\frac{V^2}{X_d}, 0\right)$ as depicted in Figure 5.7. The field current limit can be drawn with equation (5.22) and (5.23) as coordinates, calculated under nominal excitation voltage $E = E_n$ at $\delta = \delta_n$. The filed current limit circle can then be drawn varying the load angle (δ) in the range from 0 to δ_n, see Figure 5.7.

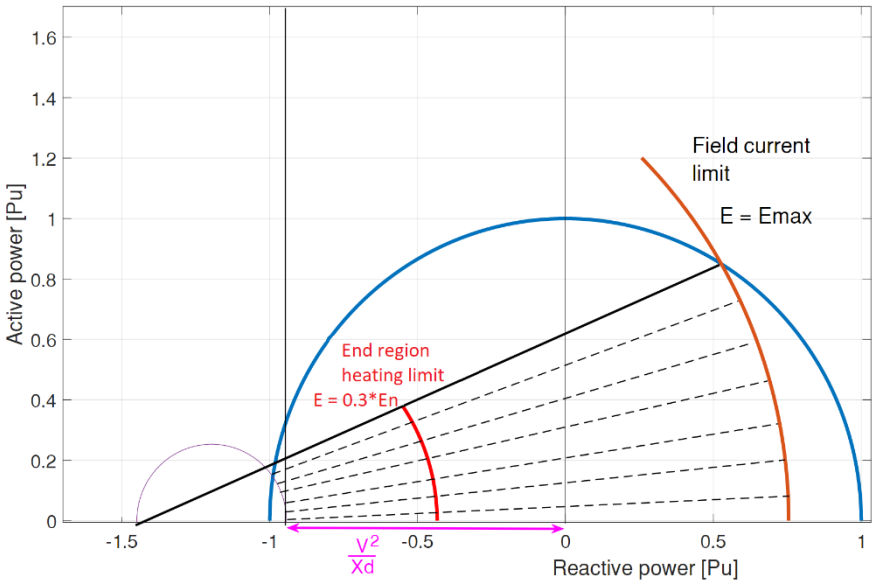

Figure 5.7: Field current limit. The figure is based on [49].

- The end region heating limit or minimum field current limit can be determined with equations equation 5.22 and 5.23, similar to the field current limit. Instead of using the nominal excitation voltage as used in field current limit (maximum), the excitation voltage is set to the minimum excitation voltage, given by:

$$E_{min} = k \cdot E_{max} \tag{5.26}$$

  where k-factor is $k = 0 - 0.3$ [49]. In this report, the k-factor have been set to 0.3, see Figure 5.8.

- The theoretical maximum power angle is $\delta_{max} = 90°$, and will be located at the point where active power in equation 5.22 peaks. The theoretical stability limit can therefore by found by [49] [56]:

$$\frac{dP}{d\delta} = \frac{EV}{X_d} cos\delta + V^2 \cdot \frac{X_d - X_q}{X_d \cdot X_q} \cos(2\delta) = 0 \tag{5.27}$$

  where $E \in (0,1)$.

  Solving 5.27 for each excitation voltage E gives the point where active power P peaks on the so-called Pascal curve, illustrated in Figure 5.7. The point where active power is at maximum is called the intersection angle δ, and can be used to draw the TLS from equation 5.22 and 5.23.

  Another approach to finding the theoretical stability limit is to use equation 5.28 and 5.29, derived from 5.27 [49] [56]:

$$P_{TSL} = \frac{\sqrt{2}\sqrt{k\sqrt{k^2 + 8d^2} + 4d^2 - k^2} \cdot (\sqrt{k^2 + 8d^2} + 3k)}{16d} \tag{5.28}$$

$$Q_{TSL} = \frac{k\sqrt{k^2 + 8d^2} + 4d^2 + 8dQ_0 - k^2}{8d} \tag{5.29}$$

$$k = \frac{EV}{Xd}; \quad a = \frac{d}{2} = \frac{1}{2} \cdot \frac{X_d - X_q}{X_d \cdot X_q} V^2; \quad Q_0 = -\frac{V^2}{X_q} \tag{5.30}$$

  where $E \in (0,1)$.

- The practical stability limit will have a reduced value to the theoretical stability limit. In this report, the practical stability curve is created by first drawing several excitation curves (Figure 5.7) with different values of (C), expressed in 5.31. The value of (C) is determined by the practical stability curve, which intersects the crossing point between armature and active power limit.

$$Q_{PSL} = \frac{k\sqrt{k^2 + 8d^2} + 4d^2 + 8dQ_0 - k^2}{8d} + C \tag{5.31}$$

$$P_{PSL} = \frac{\sqrt{2}\sqrt{k\sqrt{k^2 + 8d^2} + 4d^2 - k^2} \cdot (\sqrt{k^2 + 8d^2} + 3k)}{16d} \tag{5.32}$$

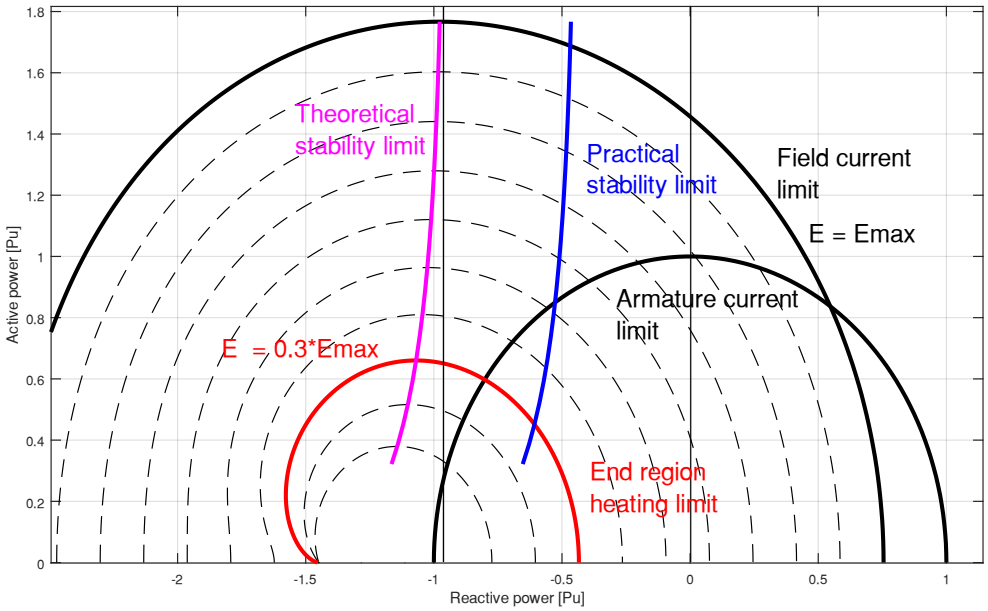

Figure 5.8: Capability diagram including practical stability limit, theoretical stability limit, end region heating limit (k=0.3), field current limit (k=1) and armature current limit. The dotted curves represent the field current under different excitation voltages (k=0.1-1). The figure is based on [49]

5.6 Transformer model

The transformer model is a relatively simple model consisting of a single equation presented earlier in section 3.4, which only depends on the loading [MVA]. The simple model was chosen as both no-load losses (P_0) and load losses (P_k) are excessively used parameters on power transformers nameplates. In addition, transformers usually have efficiencies in the range of 99.7 % under nominal rating, meaning an advanced model with higher accuracy will result in neglectable difference when compared to the entire HPU efficiency.

For this report, the operational data was measured from the generator terminals and not from the transformer terminals, which is assumed in the HPU model as it was initially developed with regards to being used in combination with other simulation tools in the future. Instead of changing the HPU model, the operational data was assumed to be measured at the high voltage

terminals of the transformer, meaning the transformer losses needs first to be subtracted. The operational data seen from the transformer side will then become:

$$P_{tran,out} = P_{tran,in} - P_{loss,tran} = P_{gen(original\ data)} - P_0 + P_k \left(\frac{S_{load}}{S_n}\right)^2$$

where $P_{tran,out}$ is the data used in the model, $P_{tran,in} = P_{gen(original\ data)}$ is the original data.

5.7 Evaluation of hydropower generation

In this report, the efficiency and energy loss is analysed with different methods, where methods like weighted average efficiency (WAE) and expected average efficiency (EAE) are used. The explanation of WAE and EAE will be described in section 5.7.1 and 5.7.2, respectfully.

5.7.1 Weighted average efficiency

The weighted average efficiency (WAE) is a method that has been used to evaluate the performance of the operational regime of hydropower. The WAE estimates the average efficiency that considers all loading conditions where each loading is weighted relative to the operational time [8]. Studies related to WAE can be seen in [8] and [53], where both are extensive work by Bortoni, who used the WAE method for evaluating the operational performance of different generators.

The WAE produces a single value η_w, a number considering all the loading conditions of the HPU, where efficiencies are weighed based on their probability of occurrence, i.e., the percentage of time the machine operates at a given load, illustrated in Figure 5.9 [8]. The weights are expressed as:

$$A_k = \frac{\Delta t_k}{T} \tag{5.33}$$

WAE is the summation of operational efficiencies with their respectful weights, yielding:

$$\eta_w = \sum_{k=1}^{n} A_k\, \eta_k \tag{5.34}$$

given that

$$\sum_{k=1}^{n} A_k = 1 \tag{5.35}$$

where Δt_k is the total duration of each loading point η_k, T is the total duration time (typically a day, month or year), η_w is the weighted average efficiency, and n is the number of loading points. If all operations provided were accounted for; T = $4 \cdot 8256$ hours (22.01.2020 – 31.12.2020). However, all operations with an active power of zero were neglected, resulting in

a value of T = 28452 for Åbjøra and T = 25089 for Sundsbarm. In this report, the duration Δt_k was determined based on the number of operations at a given efficiency.

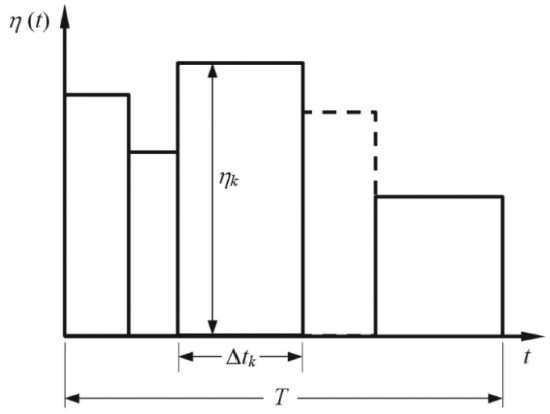

Figure 5.9: The time-depending efficiency trend for WAE calculation [8].

5.7.2 Expected average efficiency

Expected average efficiency (EAE) is a new term proposed in this thesis, which is a method that estimates the expected WAE for a reduced operating regime or operating points that are disregarded. With the EAE, one can determine which operating regions limit the WAE the most and what the WAE would be if certain regions are removed. The EAE is defined as the WAE within an expected operational area, determined from the least expected efficiency, as illustrated in Figure 5.10. The equation for EAE is in principle equal to the WAE where the summation area of (5.34) is replaced by η_{max} and η_{min}, yielding:

$$\eta_{EAE} = \sum_{k=\eta_{min}}^{\eta_{max}} A_k \eta_k$$

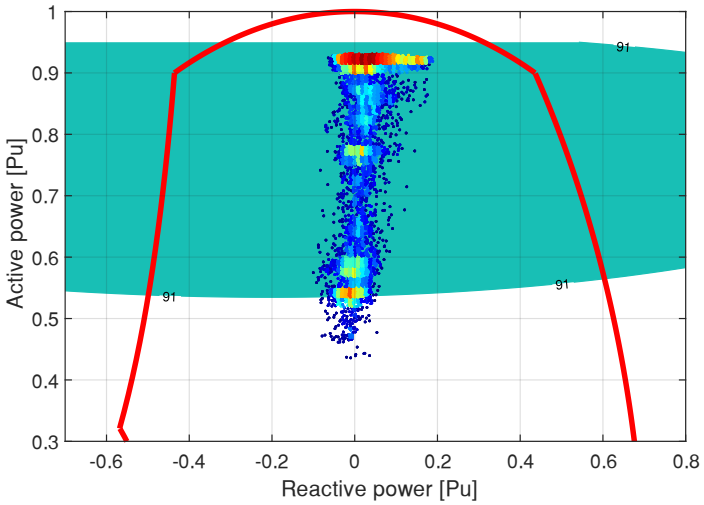

Figure 5.10: Illustration of EAE, where EAE is the WAE is estimated for all operations within the green area, here 91 %. [own work]

6 Power loss and efficiency analysis

In this chapter, the energy loss and efficiency of the Åbjøra and Sundsbarm HPU will be analysed and structured as shown in Figure 6.1. First, the losses in each component are compared under nominal operation to give an overview of the magnitude and distribution of losses. Then an in-depth loss analysis of each component where the effect of external influences and operations are analysed to determine the BEP for each component and for the entire HPU. Finally, a demonstration of the actual production of both HPUs will be analysed, where it will be shown the operational regimes with the respective losses. In addition, a comparison between both of the HPUs and their BEP will be provided to identify possible optimal and suboptimal operating regimes in terms of energy loss. A summary of the analysis results can be found in Table 6.1.

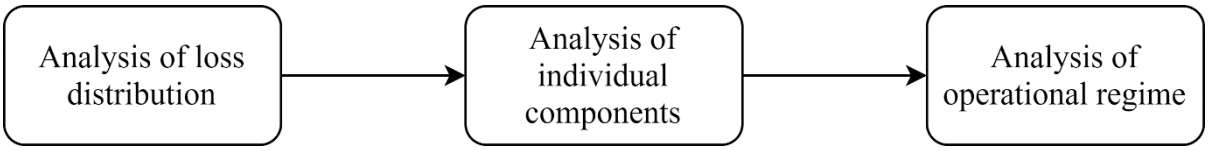

Figure 6.1: Chapter structure.

Table 6.1: Summary of operational statistics of Åbjøra and Sundsbarm. Operating time determined from nominal turbine power and total energy production. Results from the period (22.01.20 – 31.12.20).

Power plant	WAE [%]	Average P [MW]	Average Q [MVAr]	Energy production [GWh]	Energy loss [GWh]	BEP [%]	BEP location (Q,P) [Pu]
Åbjøra	91.6	79.31	1.03	579.6	53.1	92.25	(-0.22, 0.74)
Sundsbarm	91.87	94.4	3.54	602.8	52.2	92.14	(-0.30, 0.82)

6.1 Loss distribution

Analysis of the loss distribution is practised obtaining a better perspective on the size of the accumulated losses and the efficiencies in each component. The majority of all losses are in most cases determined by the active power [MW], and one could therefore depict the distribution of losses from the relationship between efficiency and the active power, as depicted in Figure 6.2. The figure shows the relationship between the power output (load) and the efficiency of Åbjøra under nominal generator ratings. For Sundsbarm, a representative figure can be seen in Appendix J. Figure 6.2 indicates a maximum HPU efficiency of 92.1 % achieved around 78 MW. From the figure, it is evident that the turbine is the dominating factor, in particular under low power levels as the turbine efficiency (max 94.5 %) is considerably lower than the other components. However, under higher power levels, one can expect waterway losses to become severe. The waterway efficiency in Åbjøra has shown to be about 1 % lower than Sundsbarm, under nominal rating, even though the flow rate is approximately 24 $[m/s]$ for both HPUs. In both HPU's, one could expect a transformer and generator efficiency above 99.5 % and 97 %, respectfully, which is typical for such large electrical machines.

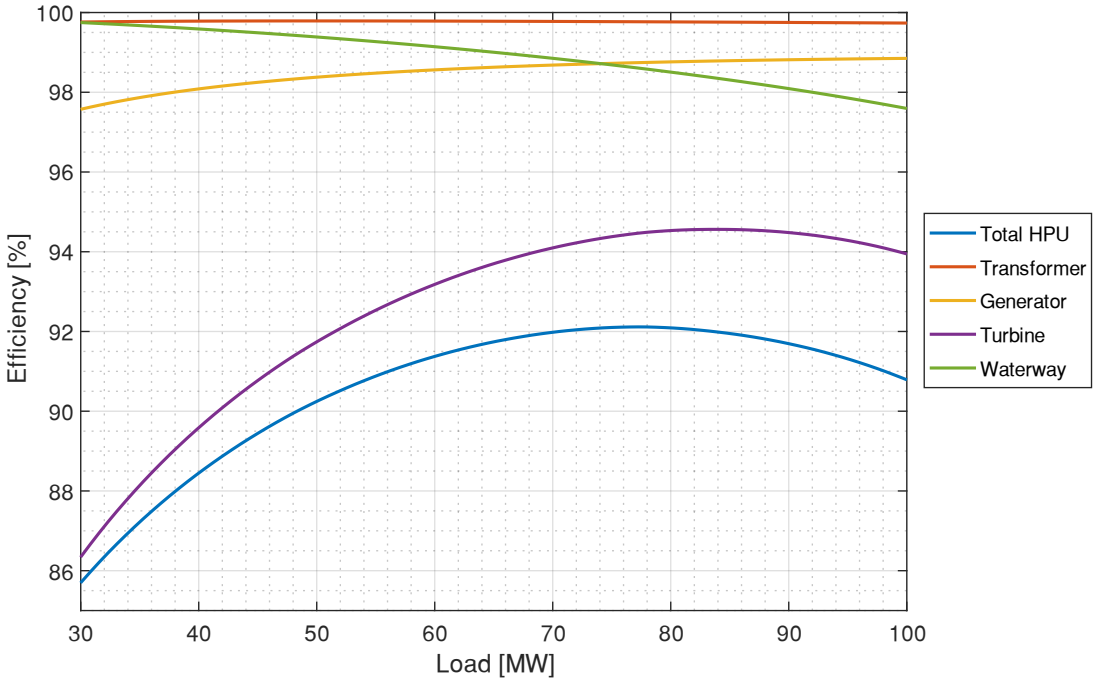

Figure 6.2: Efficiency curves in relation to power output (measured at transformer output) in Åbjøra. Calculated with: $(cos\varphi_{ind} = 0.9)$, $V = 11\ kV$ and $Gross\ head = 442m$.

In Figure 6.3, it is shown how the losses are distributed under nominal generator rating; Åbjøra (93 MW) and Sundsbarm (100 MW). Under nominal generator rating, the total power loss is 8.61 MW in Åbjøra, whereas the distribution indicates about 60% of all losses are related to the turbine. In Sundsbarm, the total power loss is 9.45 MW, whereas 69 % is produced by the turbine alone. In the figure, there is a clear difference in waterway losses between Åbjøra and Sundsbarm, which is caused by the high head loss coefficient (K) in Åbjøra. The head loss coefficient is about 1.83 times greater in Åbjøra, and since the nominal discharge (Q_{flow}) is about equal, one could expect an equally representative change in losses, as reflected in Figure 6.3. Under reduced load (0.3 Pu), the distribution of losses become significantly changed, like the losses related to the turbine, which account as much for as 82 % (Åbjøra) and 80 % (Sundsbarm) of the total losses.

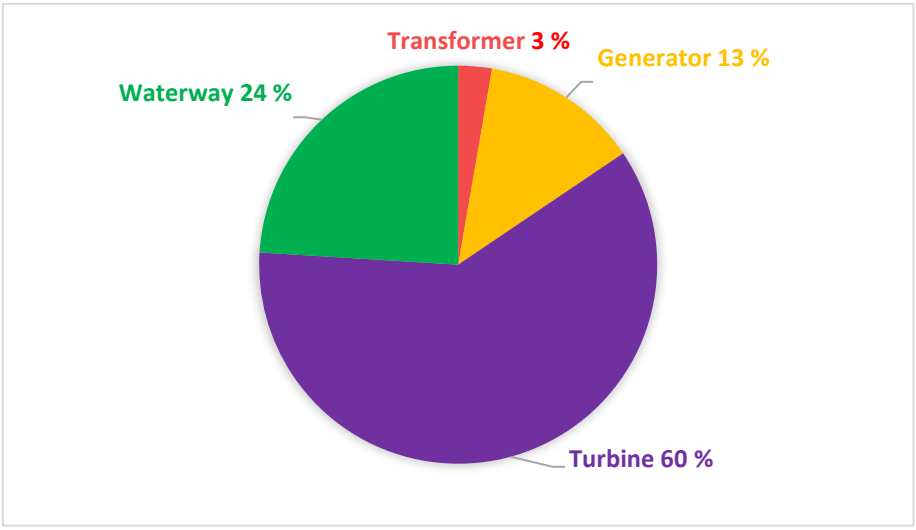

a)

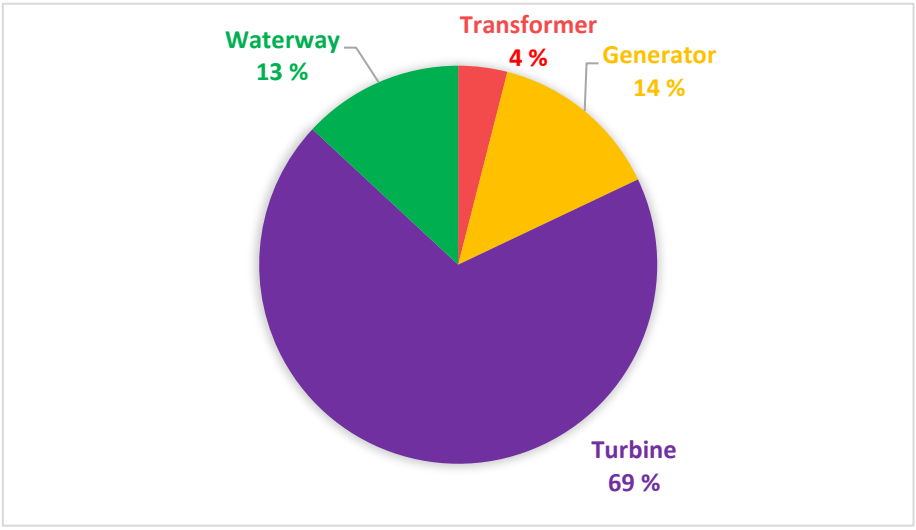

b)

Figure 6.3: Loss distribution under nominal generator operating point of a) Åbjøra and b) Sundsbarm.

6.2 Efficiency characteristics

The dominating factor regarding efficiency in an HPU is usually the active power, but external influences like change in head, temperature or other factors may affect the efficiency. Thus, in this section, the efficiency of the different components will be analysed with respect to external influences.

In general, one could expect power losses in the waterway that are proportional to the flow rate cubed, see equation 5.6. Under constant power output, there is a linear relationship between head and flow rate, i.e., the power loss related to change in the head will be significant, as illustrated in Figure 6.4.

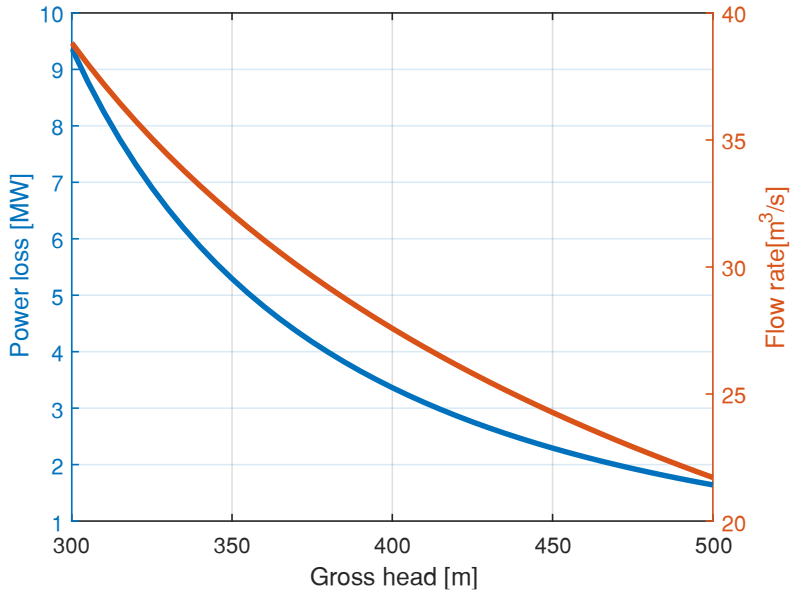

Figure 6.4: Power loss in the waterway (Åbjøra), showing the relationship between power loss $[MW]$ and flow rate $[m^3/s]$ relative to gross head $[m]$ under constant power (95 MW).

In Figure 6.5, it is shown an iso-efficiency contour map describing the turbine efficiency (Åbjøra) under varying power production [MW] and gross head [m]. A vital aspect of turbine efficiency is the flow velocity. The flow velocity is, of course, important and related to friction losses, but most importantly, the runner speed is design to operate at a fixed speed, and the flow velocity is proportional to the square root of the head. Thus, the turbine would have a specific head where the BEP is located, which can be seen from the hill-shaped map in Figure 6.5. Although the turbine has a specific optimum head, the difference in optimum efficiency is only 0.02 % (94.56 – 94.54 %) under the specific range in the head.

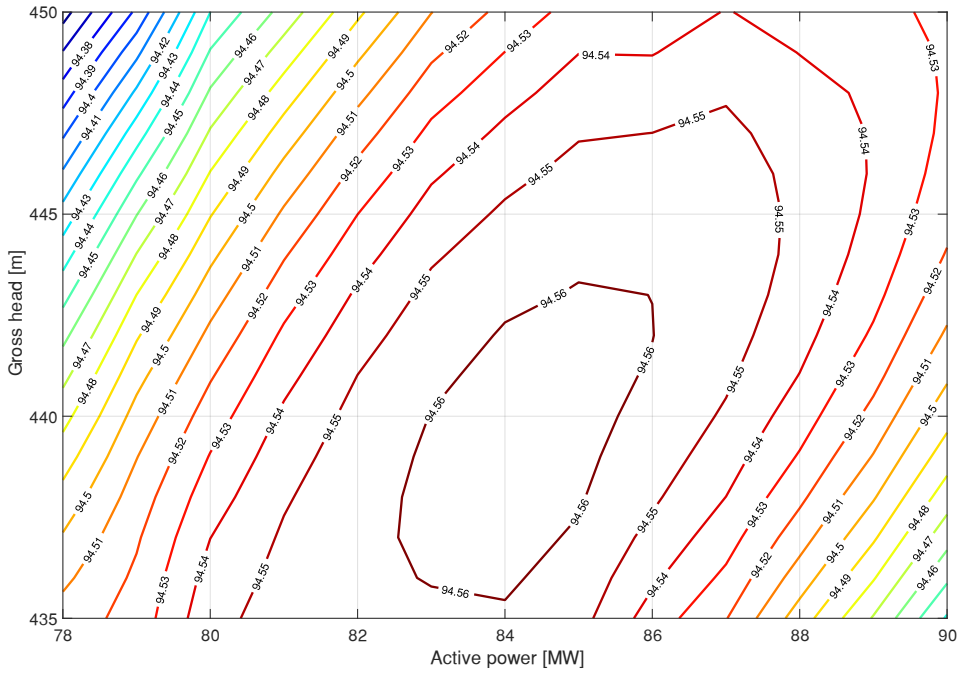

Figure 6.5: Iso-efficiency contour map of the Francis turbine used in Åbjøra.

Due to the dominating effect of the turbine on the entire HPU, the hill-shaped structure depicted in Figure 6.5 will also be present and similar to complete HPU efficiency, as seen in Figure 6.6. Figure 6.6 is an iso-efficiency contour map of the complete HPU in Åbjøra and Sundsbarm and reveals a maximum HPU efficiency of 92.12 % and 91.98 %, occurring at a production of 77.7 MW and 95.0 MW with a gross head of 442.6 m and >490 m, respectfully.

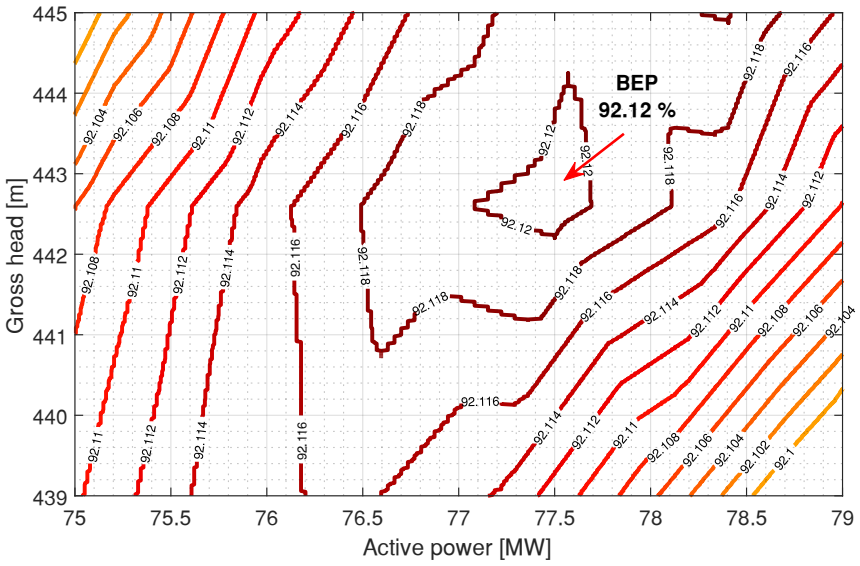

a)

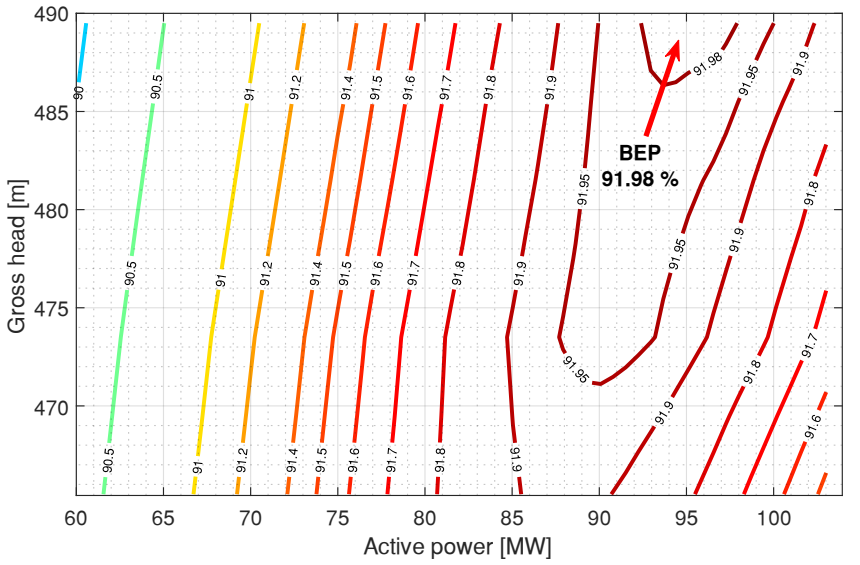

b)

Figure 6.6: Iso-efficiency contour map of the entire HPU, showing the relationship between efficiency, active and head in a) Åbjøra and b) Sundsbarm. Reactive power and terminal voltage are set to nominal values.

In the generator and transformer, there are load and no-load losses. The relationship between those losses produces an efficiency curve with a maximum efficiency at the point where load and no-load losses intersect. The transformer model is simplified and assumed to only depend on the absolute value [MVA] of the production. The transformer used in Åbjøra and Sundsbarm has a maximum efficiency of 99.79 % (50 MVA) and 99.65 % (85 MVA), respectively, where the results can be seen in Appendix I and Appendix J.

The optimum voltage has been found to be located at the nominal voltage for both HPUs (see Appendix I and Appendix J), which can be expected as the terminal voltage is usually a "free variable" during the designing process and selected based on the maximum efficiency point. In the following simulations, the generator voltage will be set to nominal voltage 11 kV (Åbjøra) and 15 kV (Sundsbarm).

The reactive power in a synchronous generator is fully controllable, which could be regulated independently of the active power and therefore have a maximum operating point relative to the excitation losses in addition to the active power. The iso-efficiency contour map of the generator efficiency of Åbjøra is shown in Figure 6.7, where the efficiency is depicted relative to the active and reactive power, overlayed with the representative capability diagram. The corresponding figure for Sundsbarm can be found in Appendix J. In Figure 6.7, one can see the generator having a BEP of 99.08 % achieved with an active power production of 1.4 Pu and reactive power of -0.22 Pu, or a PF of 0.988. The best operating point is a theoretical optimum and is not a practical optimum as the generator is limited by the capability diagram shown in red. Within the capability diagram, the Åbjøra generator is limited to maximum efficiency of 99.0 %, with an active power production of >0.93 Pu and a reactive power of about -0.2 Pu. For the generator efficiency, the influence of reactive power is relatively small compared to active power production. The reactive power can only influence the efficiency to about +/- 0.2% under the nominal active power.

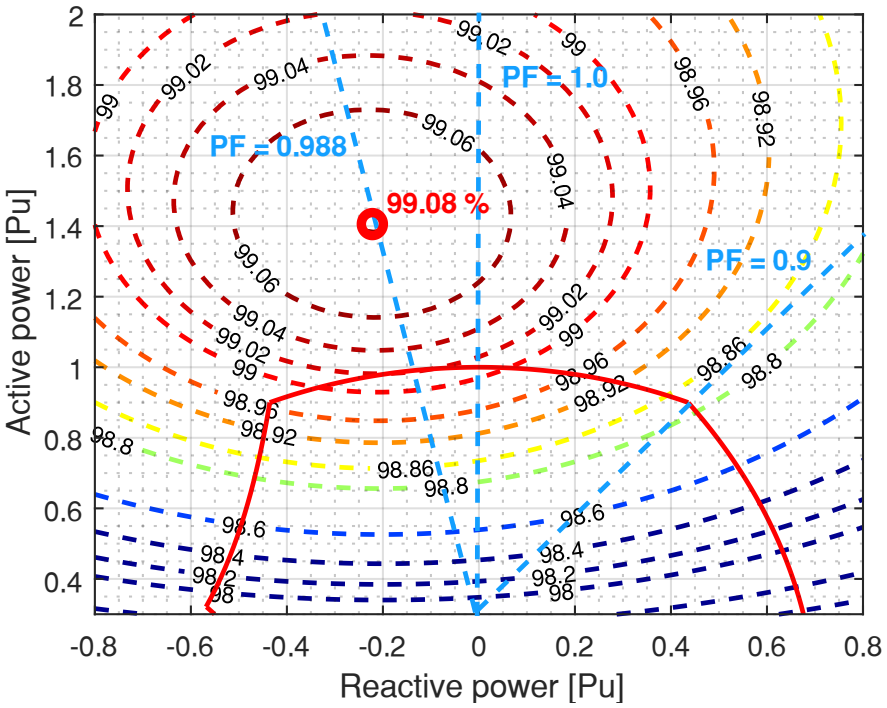

Figure 6.7: Efficiency mapping of the synchronous generator used in Åbjøra.

The BEP of the entire HPU has been obtained by plotting the active and reactive power combined with the optimum head given by the results from Figure 6.6. The results for Åbjøra and Sundsbarm can be seen in Figure 6.8. In Åbjøra, the BEP is 92.25 % achieved with a gross head of 442.6 m, active power production of 0.74 Pu (76.2 MW) and reactive power of -0.22

Pu (22.7 MVAr). In Sundsbarm, the BEP is 92.14 % achieved with a gross head of 490 m, active power production of 0.82 Pu (96.8 MW) and reactive power of -0.30 Pu (35.4 MVAr). It should be noted that the location of the BEP is different. The BEP of Åbjøra is located further down concerning active power, compared to Sundsbarm, which can be beneficial for HPUs that frequently operates with low production, but certainly a disadvantage for HPUs operating at rated power. In Sundsbarm, the BEP is located close to the rated power and does achieve higher efficiency for all operations above 0.8 Pu compared to Åbjøra.

Figure 6.7 and Figure 6.8 show that reactive power has a minor influence on efficiency, particularly compared to the total HPU efficiency, depicted in Figure 6.8. For both HPUs, on can expect about 0.2 – 0.3 % deviation in the HPU efficiency caused by the reactive power.

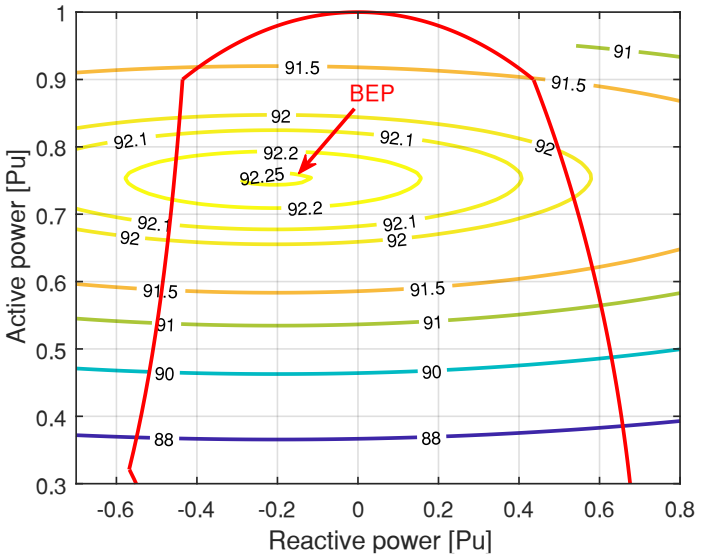

a)

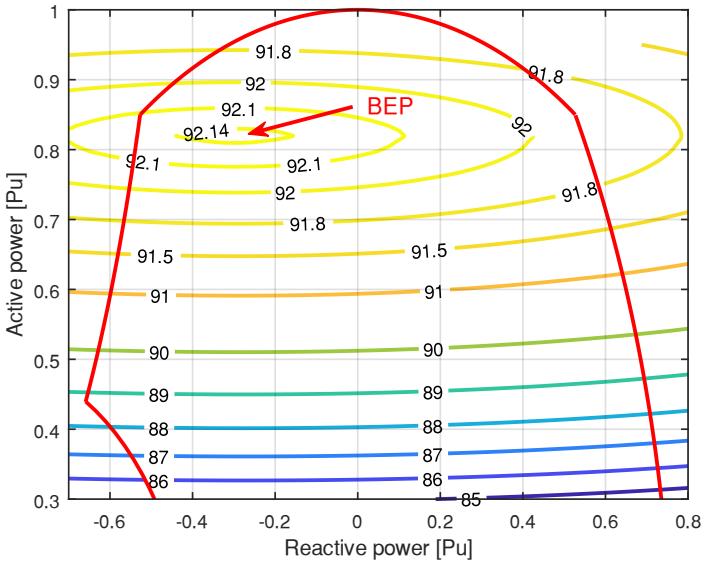

b)

Figure 6.8: Iso-efficiency contour map of the entire HPU, showing the relationship between efficiency, active and reactive power under the optimal gross head, in a) Åbjøra and b) Sundsbarm.

To summarise, there has been analysed three variables (headwater, active and reactive) that influence the efficiency. The results indicate a minor influence on the efficiency related to head and reactive power, as the active power dominates the variations.

All components will have their own local BEP efficiency and are usually different from the entire HPU. It is the sum of all efficiencies that result in the BEP for the HPU as a whole, which is clearly shown in Table 6.2 and Table 6.3. The tables are a summary of the results of Åbjøra and Sundsbarm.

Table 6.2: Optimum operation points at Åbjøra

Component	Optimum load (P) $[MW]$	Optimum load $(Q)[MVAr]$	Optimum head $[m]$	Maximum efficiency [%]
Waterway	0	–	High as possible	~ 100
Turbine	84	–	440	94.56
Generator	144	−22.7	–	99.08
Transformer	50 $[MVA]$		–	99.79
HPU (total)	76.2	−22.7	442.6	92.25

Table 6.3: Optimum operation points at Sundsbarm

Component	Optimum load [MW]	Optimum load [MVAr]	Optimum head [m]	Maximum efficiency [%]
Waterway	0	–	High as possible	~ 100
Turbine	100	–	490	93.91
Generator	212.4	−35.4	–	99.15
Transformer	85 $[MVA]$		–	99.65
HPU (total)	96.8	−35.4	490	92.14

6.3 Analysis of operational regime

The annual (2020) production regime of Åbjøra and Sundsbarm is shown in Figure 6.9 and Figure 6.10, respectfully. The figures show both the active and reactive power production measured at the generator terminals.

In Figure 6.9 and Figure 6.10, there are areas with high variations that could be a sign of frequency restoration reserve (FRR) control, where the generator is regulated to balance the grid. Areas with large spikes which shows zero production indicate the generator is situated in an on/off situation. In addition, areas with large variation in production could indicate the generator is turning on/off for a short period (under 1 hour), resulting in artificially low production. As discussed earlier in section 5.2, the data was given as average values from periods of 1 hour, making it difficult to distinguish between an on/off situation and a reduced operation. Thus, the results from the average efficiency may be affected and deviate from the actual operations.

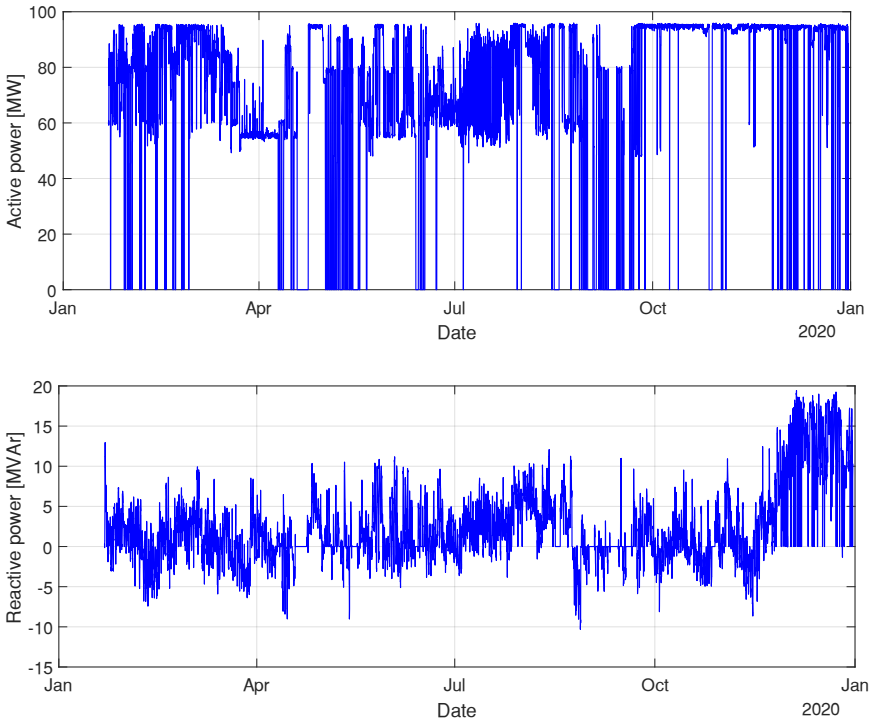

Figure 6.9: Production regime of Åbjøra, showing both active and reactive production.

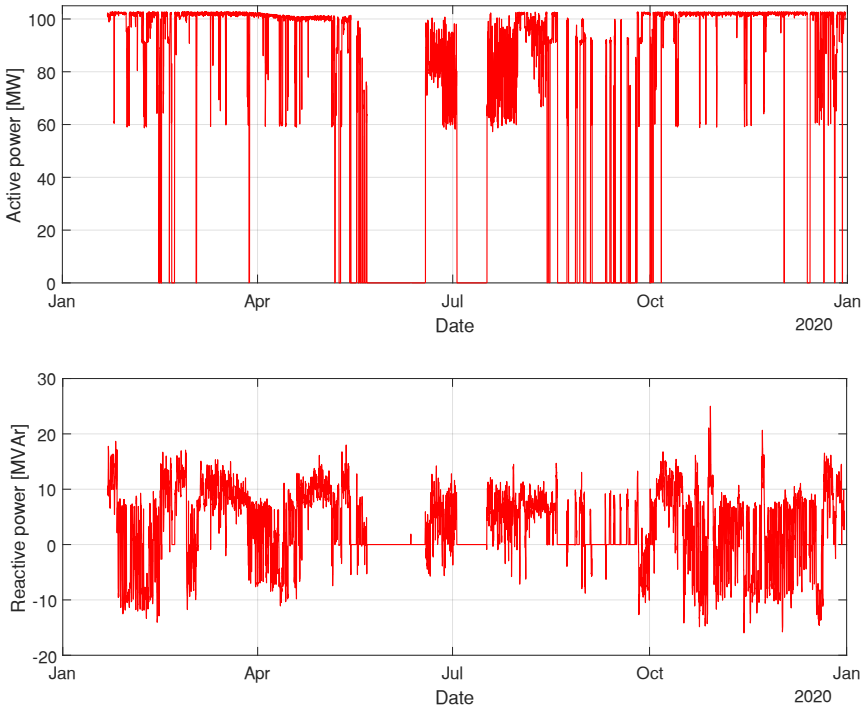

Figure 6.10: Production regime of Sundsbarm, showing both active and reactive production.

In order to have a better understanding of the operation, a so-called scatter diagram (left figure in Figure 6.11) has been used to show the distribution of all operational data points (active and reactive power). The figure to the left in Figure 6.11 depicts all operational data in relation to the representative capability diagram and the efficiency. A single operational point is marked as a blue dot in the scatter diagram, and areas with brighter colours represent a higher operational density. The operational density can also be seen in the figure to the right, which shows the percentage of all operations divided into given areas.

From Figure 6.11, there is a significant difference between Åbjøra and Sundsbarm when it comes to the distribution. Åbjøra has a larger number of operations at the lower end and more evenly distributed compared to Sundsbarm. Sundsbarm operates about 56 % of all operations in proximity to the maximum turbine rating, and only 20 % is neither close to maximum rating nor in the off state, resulting in an average operating point located at 0.8 Pu (active power) and 0.03 Pu (reactive power). For Åbjøra, the distribution of operations close to turbine rating is 40 %, whereas 46 % are found below the turbine rating, resulting in an average operating point located at 0.79 Pu (active power) and 0.02 Pu (reactive power). Although the distribution of operations differs from one another, the average operating point is about equal in terms of per unit. The reason is due to the high turbine rating in Åbjøra, which is partly due to a high nominal active power in the Åbjøra generator with a PF of 0.9, compared to 0.85 for Sundsbarm.

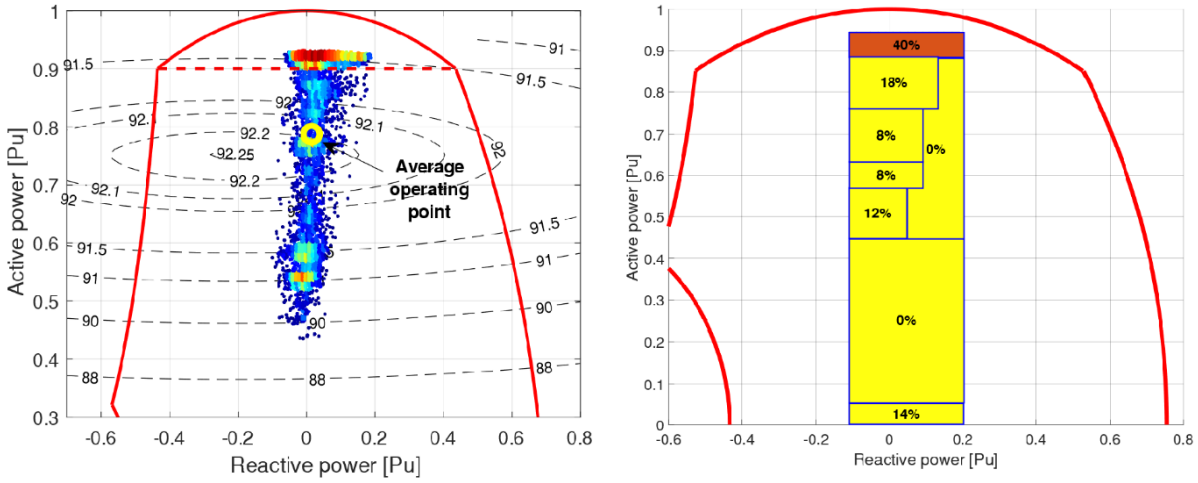

a)

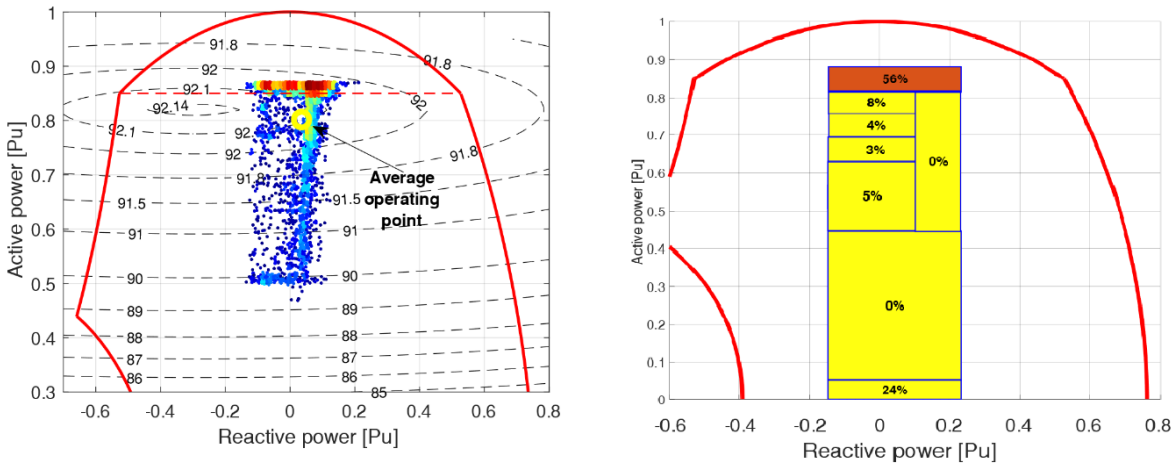

b)

Figure 6.11: Distribution of operational data for a) Åbjøra and b) Sundsbarm. The dotted horizontal line in the left figure represents the generator's nominal rating (active power). The figure to the right shows the rough distribution of all operating points.

The estimated WAE for Åbjøra is 91.6 %, and for Sundsbarm, it is 91.9 %, as shown in Figure 6.12. Figure 6.12 presents the operational efficiencies as cumulative probability and the expected average efficiency (EAE). The high WAE in Sundsbarm is clearly reflected in Figure 6.12, where one can see about 84 % of all operations are above 92 % efficiency, compared to Åbjøra with only 20 % of all the operations. About 50 % of all operations in Åbjøra are found in the region around 91.4 – 91.6 % efficiency, which is mainly represented by the production under maximum turbine rating and a large area with low production, seen in Figure 6.11.

The EAE depicted in Figure 6.12 is the new term proposed in this report and shows how the efficiency may be improved if one eliminates certain operations. For Åbjøra, one can see a close to linear EAE characteristic and shows that one must remove about the 20 % operations with the lowest efficiency to achieve only a 0.1% gain in WAE. For Sundsbarm, the EAE characteristic shows that by eliminating the 10 % operations with the lowest efficiency, one

may achieve a 0.15 % gain in WAE. Eliminating the 10 % operations with the lowest efficiency correlates to all operations below about 0.7 Pu (active power) for Sundsbarm, seen from Figure 6.11. One should notice that EAE does not include operations in off state, which is included in Figure 6.11.

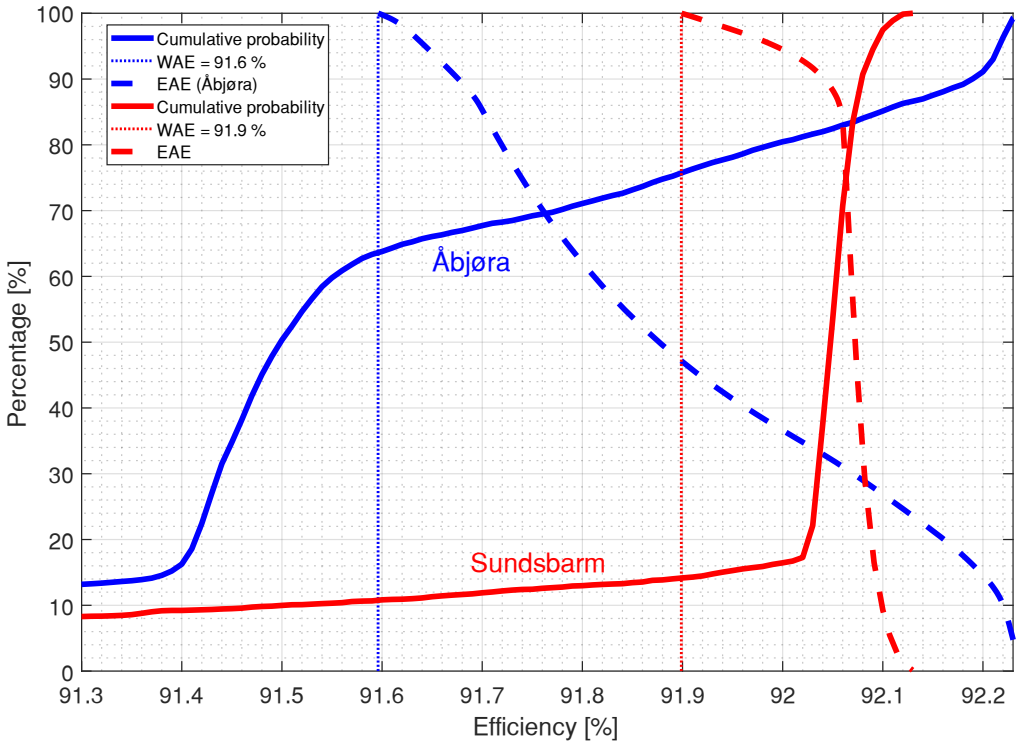

Figure 6.12: Cumulative probability of all operational efficiencies for both Åbjøra (blue) and Sundsbarm (red). The EAE is marked as large, dotted lines. Operations situated in off-state are not considered in the figure.

The smaller WAE of Åbjøra is reflected in Figure 6.11, where one can clearly see Åbjøra being operated far from the BEP, unlike the Sundsbarm, which have the BEP close to where most of the operations are originated. It has been speculated whether the WAE could have been improved if the efficiency curve of the turbine had shifted to a higher or lower active power level with equal characteristics, e.g., in the case of a new turbine. It is a purely hypothetical scenario, where the efficiency curve of Åbjøra and Sundsbarm turbine is shifted by multiplying the active power with a factor, e.g., 0.95, 1.0 and 1.05, depicted in Figure 6.13. It was discovered that the WAE did not improve when the efficiency curve was shifted in neither of the HPUs, but rather decreases significantly. Figure 6.13 shows that the original turbine characteristic is optimum for the given operational regime. As the turbine characteristic is shifted to lower production (0.95), the BEP increases, whereas the efficiency at the average operating point decreases and results in a lower WAE. Thus, the highest WAE will be determined by the turbine characteristic which has the highest efficiency at the average production. One should have in mind that the location of the average production determines which characteristic that results in the highest WAE but does not give any information about the magnitude of the actual WAE (e.g., Figure 7.4).

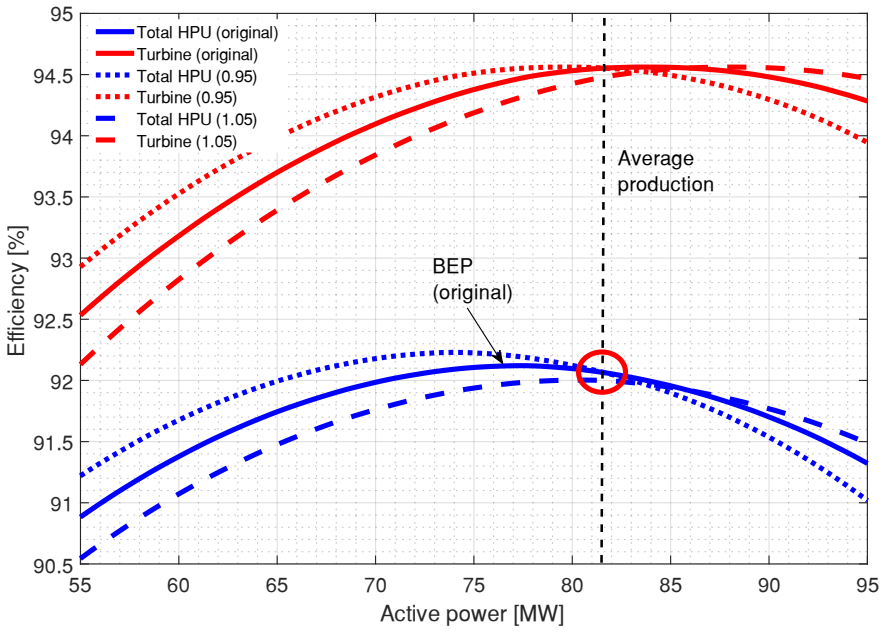

Figure 6.13: A hypothetical scenario of Åbjøra showing the effect of shifting the turbine characteristic curve. The turbine is given by interpolated measurements, which have been multiplied by 0.95, 1.0 (original) and 1.05 in order to move the turbine characteristic curve. The intersection point between HPU characteristic (blue) and average production is marked with a red circle.

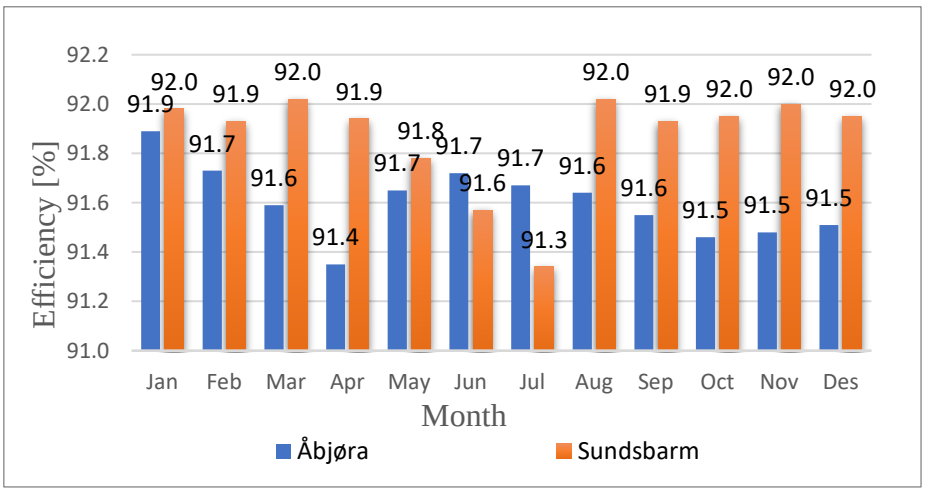

Figure 6.14: WAE of Åbjøra and Sundsbarm.

Analysis of the monthly average efficiency (WAE) gives the results shown in Figure 6.14, where Åbjøra is depicted in blue and Sundsbarm in orange. Åbjøra has the highest WAE in January (91.89 %) and the lowest in April (91.35 %), whereas Sundsbarm have the highest WAE in August (92.02 %) and the lowest in July (91.35 %).

The monthly operation with the highest and lowest WAE in Åbjøra and Sundsbarm is illustrated in Figure 6.15 and Figure 6.16, respectfully. The figures are uses to illustrated

relationship between average production and BEP. Although the highest WAE can be realised when the average production is close to the BEP, it does not imply that this is the case for all situations. In the left figure in Figure 6.15, the average operating point is about identical to the BEP, but most operations are either above or below the average point, resulting in a limited WAE compared to a situation where all operations are located at BEP. When it comes to the month (August) with the highest WAE in Sundsbarm, the difference between average production and BEP is larger than in Åbjøra but still obtains a higher WAE as a high number of operations is actually operating close to the BEP.

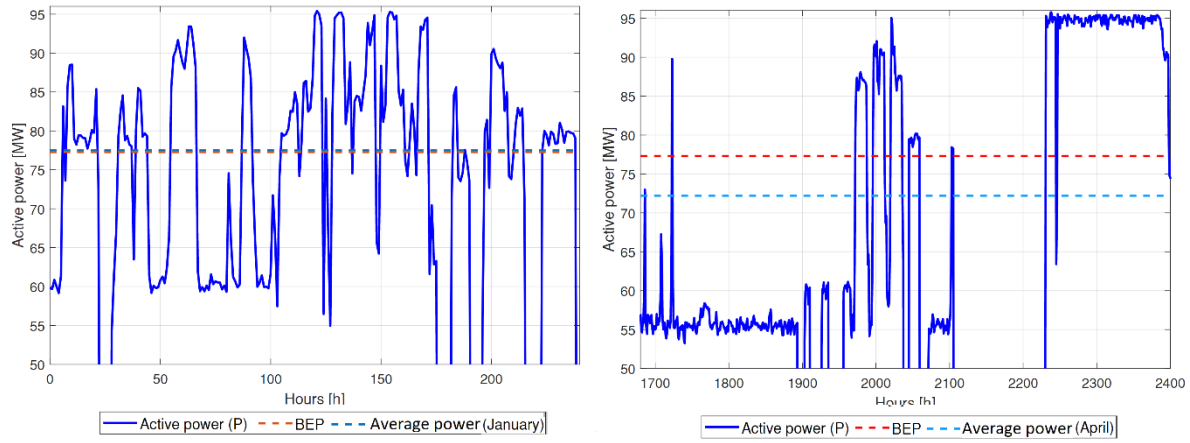

Figure 6.15: Production regime Åbjøra during January and April, with their representative WAE compared to the BEP. The hours are referenced from the first measurement (22.01.2020).

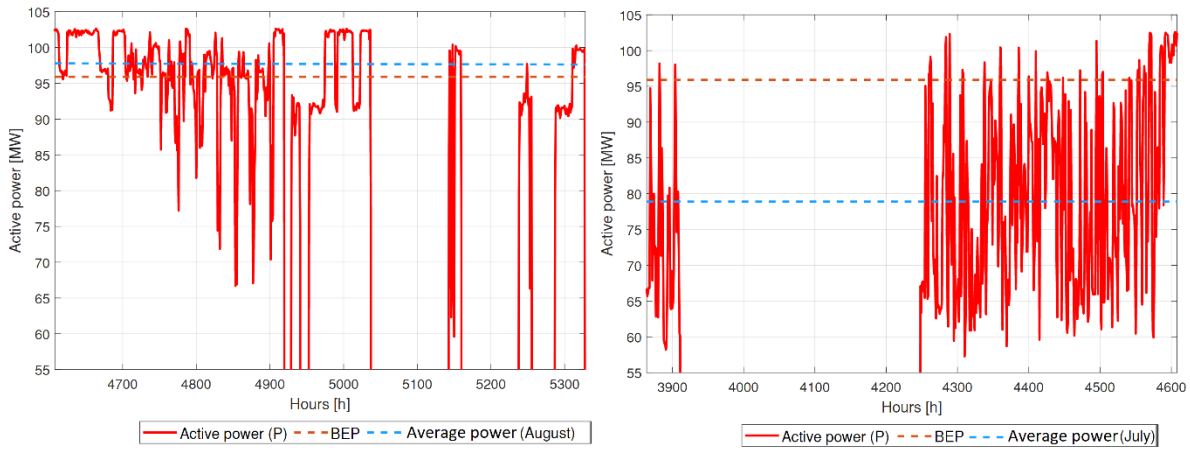

Figure 6.16: Production regime Sundsbarm during August and July, with their representative WAE compared to the BEP. The hours are referenced from the first measurement (22.01.2020).

In some situations, the WAE may not reflect the performance of the HPU as some months may have long or short periods with no operation. Thus, analysing the energy production and energy loss could give a better picture of the actual performance, as shown in Figure 6.17. In the figure, one can see the total energy production (blue) and energy losses (orange) for each month, which results in total energy consumption (water used). The annual (except the few days in January)

energy production of Åbjøra was 579.6 GWh with a total loss of 53.1 GWh, compared to Sundsbarm, which produced 602.8 GWh with a total loss of 52.2 GWh.

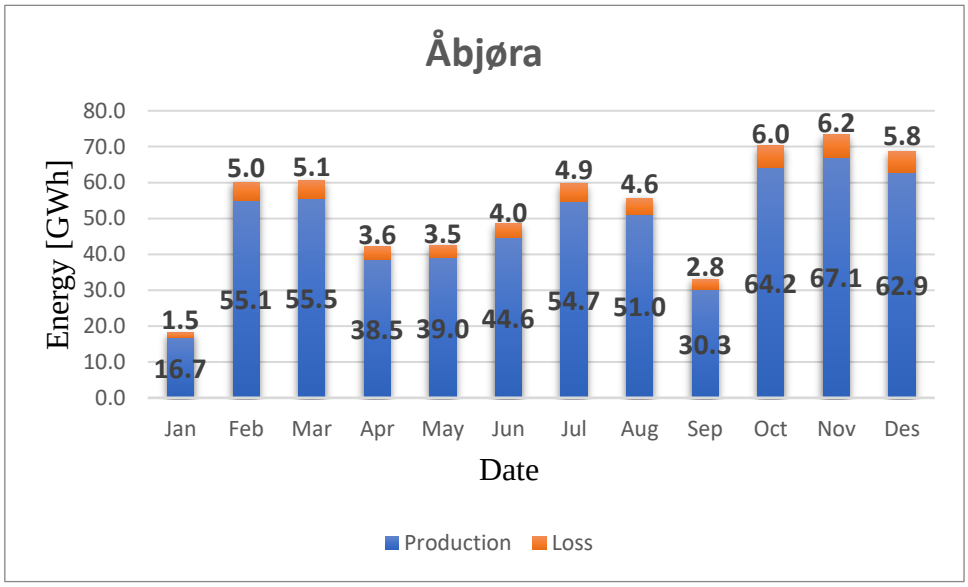

a)

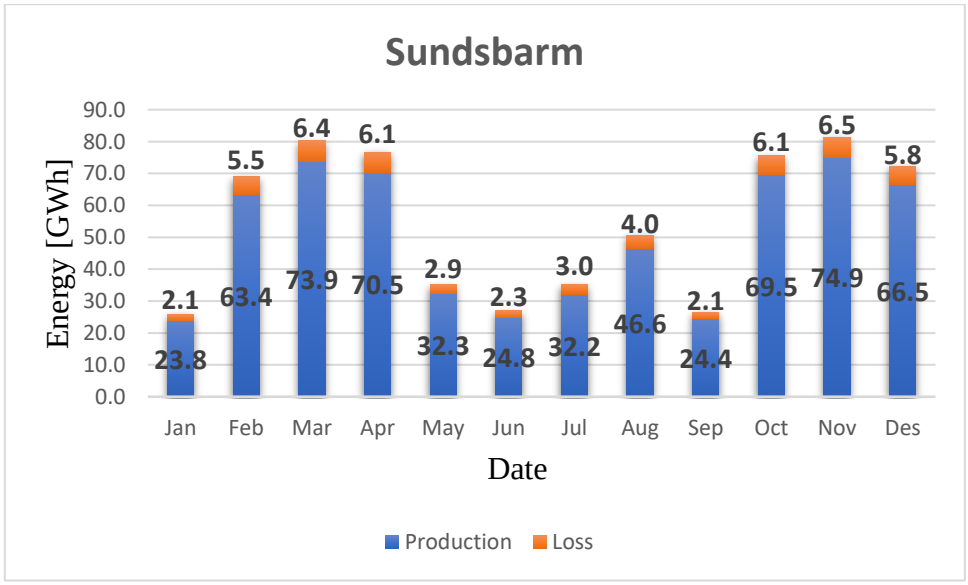

b)

Figure 6.17: The monthly energy production and energy loss in a) Åbjøra and b) Sundsbarm.

A comparison between actual and optimal energy loss is seen in Figure 6.18, where the optimal energy loss have been found by assuming both HPU's were operated at BEP with equal production. The results indicate a reduction in energy loss of 8.2 GWh and 5.4 GWh for Åbjøra and Sundsbarm, respectfully. By considering the average system Elspot price (Nord Pool), one can give a rough estimate of the possible savings related to energy losses. Due to the extraordinary low prices in 2020, the prices will be based on 2019, where the average system

price was 383 NOK/MWh, resulting in an annual savings of 3.14 million NOK for Åbjøra and 2.07 million NOK for Sundsbarm.

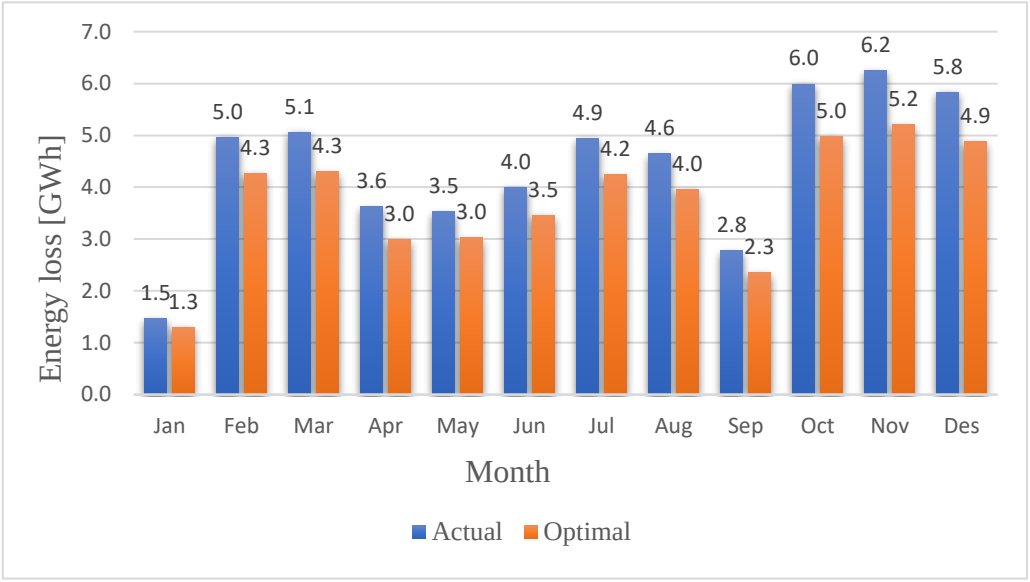

b)

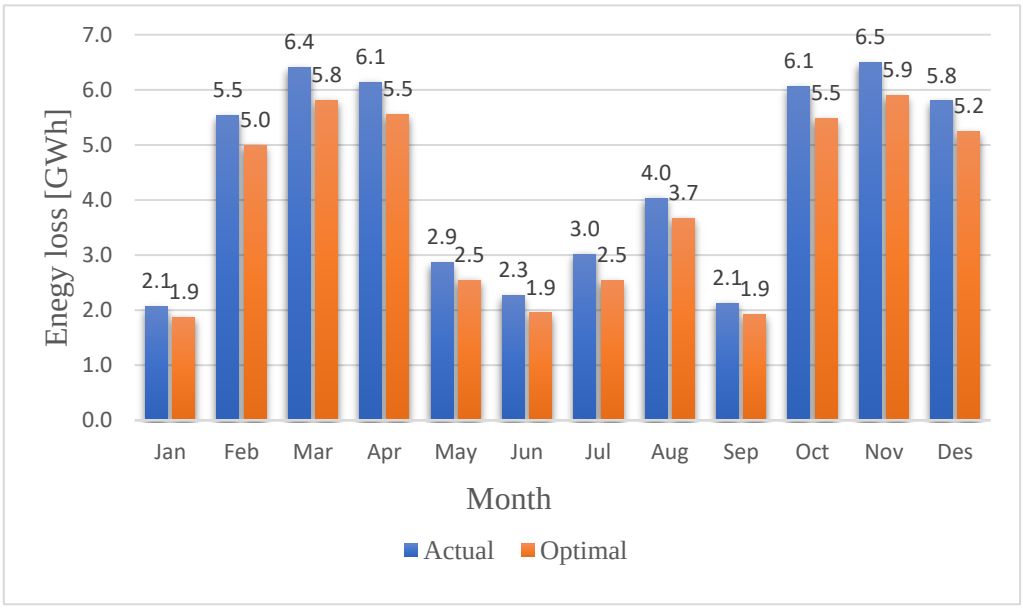

a)

Figure 6.18: Energy loss a) Åbjøra and b) Sundsbarm. The optimal energy loss represents the energy loss that would be obtained if operated at BEP under equal production as the actual data.

7 Sensitivity analysis

In this chapter, a short sensitivity analysis will be presented to identify the WAE under new operating regimes. In the future power grid, one may expect larger fluctuations in active and reactive power demand, partly caused by the intermittency of wind and solar. A sensitivity analysis could therefore be helpful for preparing for what to come in the future. It is difficult to determine the actual future operating regime, so in this report, there will be focused on two scenarios. Scenario 1) shall identify patterns in WAE by varying the active power production while maintaining the maximum production and reactive power constant, and scenario 2) shall vary the reactive power production while maintaining the active power constant, see Figure 7.1. Analysing the production of active and reactive power separately makes it possible to examine the effect each of them has on the WAE.
The result from this analysis indicates that one could expect a significant reduction in WAE, of which a 2 % reduction has been identified under severe changes in the active power regime. On the other hand, the influence of reactive power on the WAE has shown to be minor, with a maximum reduction of 0.02 % under large fluctuations of reactive power.

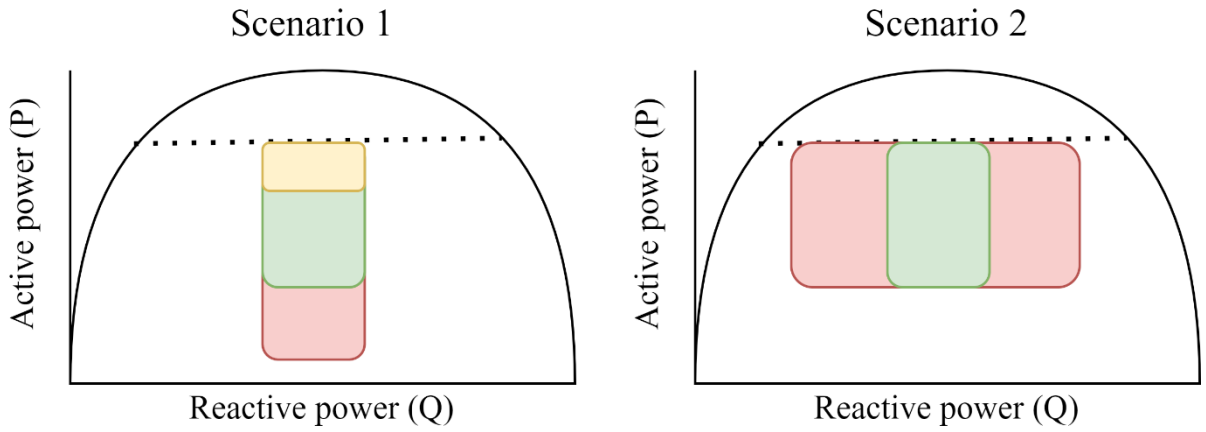

Figure 7.1: Illustration of the sensitivity analysis scenarios. The green area represents the original operational regime, whereas the red and yellow area represents expansion and contraction of the operational regime, respectfully.

7.1 Scenario 1 - Variation of active power

In this scenario, the active power is varied by expanding and contracting the operation points while maintaining the maximum active power, see Figure 7.2. The scenario is simulated ten times, and each test is numbered as P1 to P10, where P10 represents full extension ($a_i = 2$) and P1 represents full contraction ($a_i = 0.2$), where each test uses the following equation to vary the active power:

$$P_{new,i} = a_i \cdot P_{original} - b_i$$

where a_i is a factor that starts with a value of 0.2 and increases with increments of 0.2 up to 2 for each test i and b_i is a value used to maintain the maximum active power and is estimated by:

$$b_i = a_i \cdot P_{original,max} - P_{original,max}$$

where $P_{original,max}$ is the maximum active power, 95 MW and 103 MW for Åbjøra and Sundsbarm, respectfully. An overview of the numbers used for each test is shown in Table 7.1:

When performing this scenario, it is vital that all operations at off-state ($P = 0$) are removed, else the off-state operations are evaluated as operations.

Table 7.1: Overview of test values used

Åbjøra										
Test nr.	P1	P2	P3	P4	P5	P6	P7	P8	P9	P10
a_i	0.2	0.4	0.6	0.8	1.0	1.2	1.4	1.6	1.8	2.0
b_i[MW]	-76	-57	-38	-19	0	19	38	57	76	95.0
Sundsbarm										
Test nr.	P1	P2	P3	P4	P5	P6	P7	P8	P9	P10
a_i	0.2	0.4	0.6	0.8	1.0	1.2	1.4	1.6	1.8	2.0
b_i[MW]	-82	-62	-41	-21	0	21	41	62	82	103.0

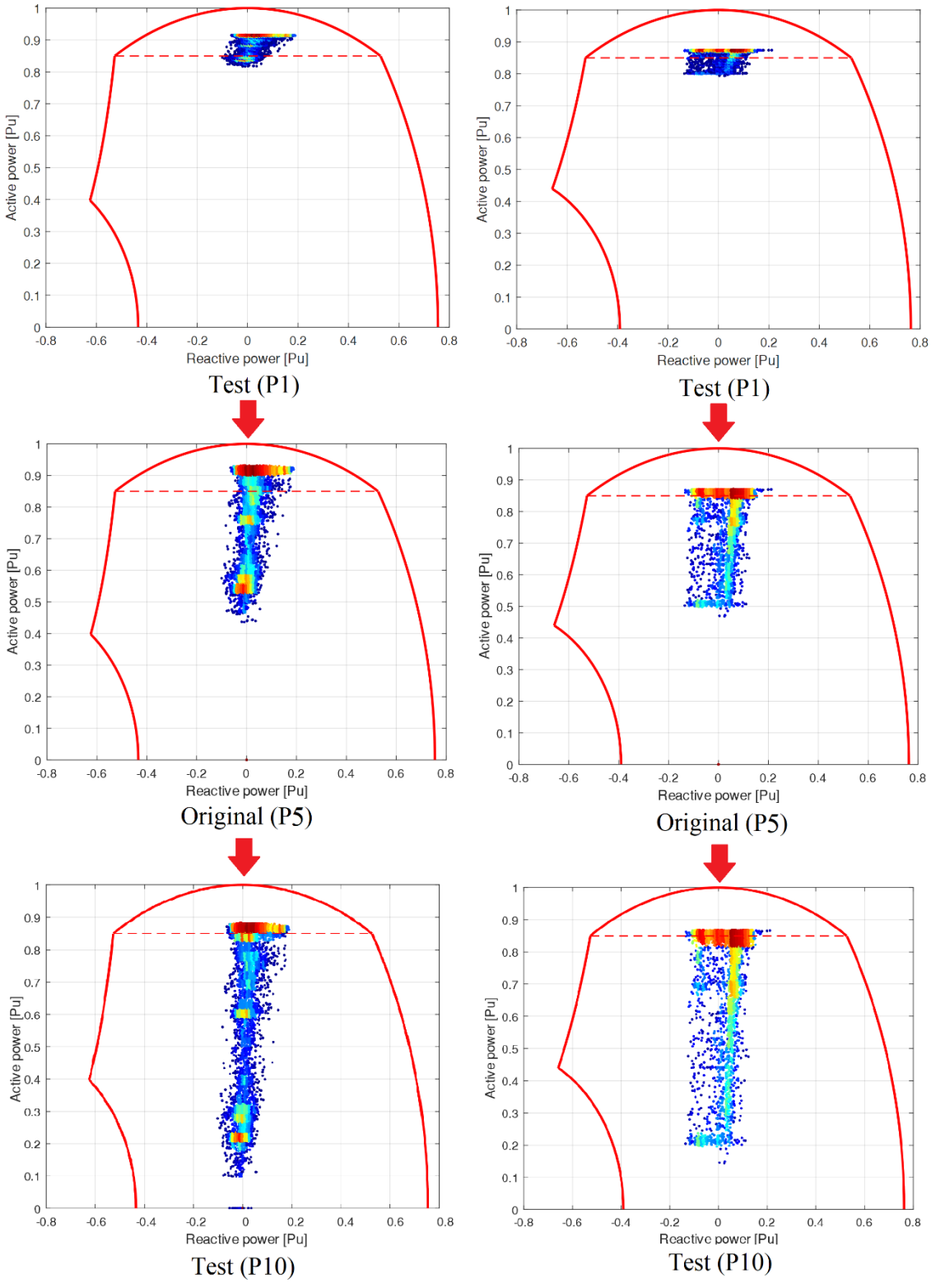

Figure 7.2: Scenario 1, variation of active power, where left figures represent operations of Åbjøra and right represents Sundsbarm. Test P1 shows full contraction ($a_i = 0.2$) and test P10 shows full extension ($a_i = 2$).

The test results indicate a change in WAE, as depicted in Figure 7.3. The figure shows a relatively large reduction in average efficiency when the operating regime has a higher density of low active power operations (P10). Between test P10 and original data (P5) for Åbjøra, the results show a WAE reduction from 91.6 % to 89.7 % or a difference of 1.9 %. For Sundsbarm, the WAE was reduced from 91.9 % to 90.9 % or a difference of 1 %. From the tests P1-P4, it was shown an increase in WAE for both HPU's, where Åbjøra increased the WAE by 0.19 % between maximum (P3) and original operation (P5), and Sundsbarm had a maximum increase between test P1 and P5 with an increase of 0.1 %. It should be noticed that Åbjøra have a more prominent change than Sundsbarm due to the difference in the original distribution of operational density. The function used to create each test influences the lowest power levels more than the highest, as these are maintained about constant.

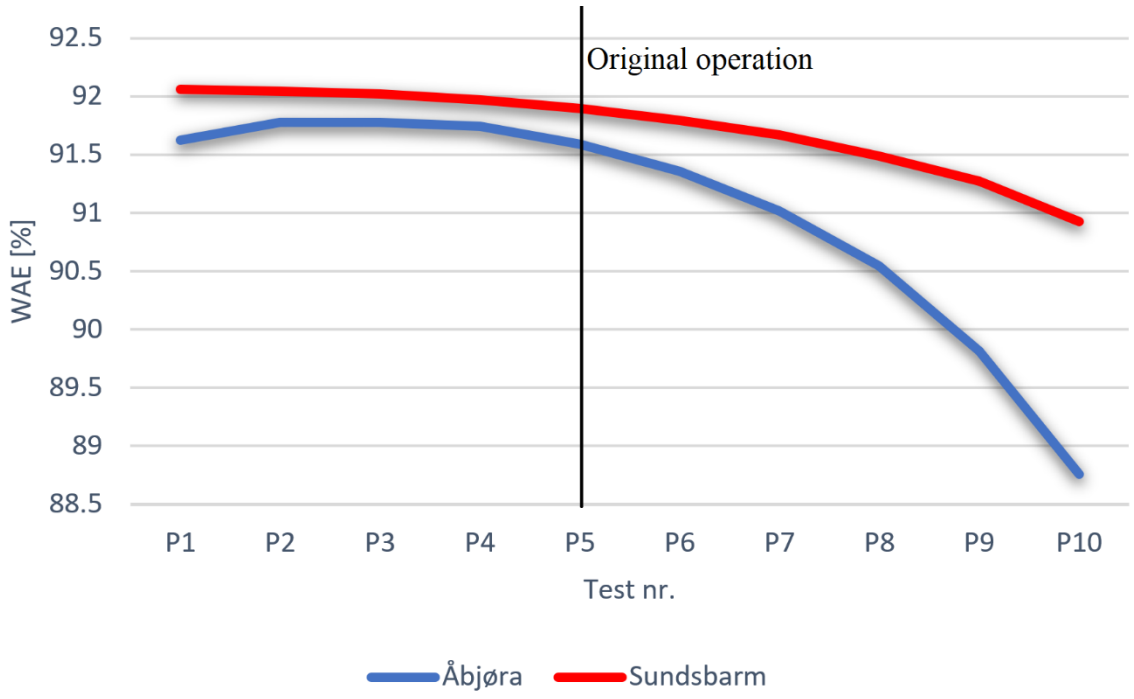

Figure 7.3: Estimated WAE for each test

In Figure 7.4 it is shown the correlation between average active power for each test, the WAE for each test and the BEP. The figure indicates no significant correlation between the average active power obtained for each test and the active power representing the BEP. Both HPUs achieved a maximum WAE under a higher average active power, see Figure 7.4.

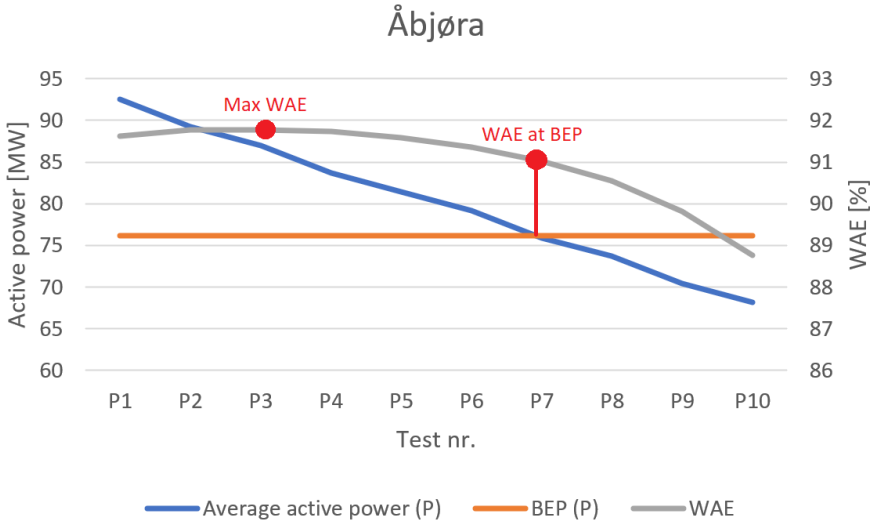

a)

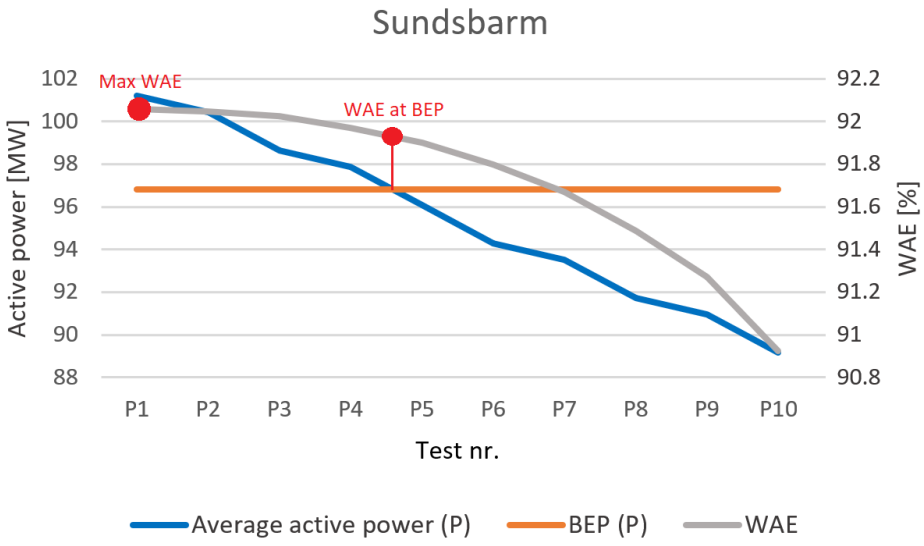

b)

Figure 7.4: Correlation between average active power, BEP and WAE obtained from each test for a) Åbjøra and b) Sundsbarm

7.2 Scenario 2 – Variation of reactive power

In this scenario, the magnitude of the reactive power will be changed, this by multiplying the reactive component of all operational points with a constant to achieve a higher variation of reactive power, illustrated in Figure 7.5.

Within this scenario, there will be 11 simulations numbered from $Q_1 - Q_{11}$, where Q_1 represents the original operation, and for each simulation, the multiplied factor k will increase in increments of 0.2. The change in reactive power can be expressed as:

$$Q_{new,i} = k_i \cdot Q_{original}$$

where k_i is the multiplication factor for each test i and ranges from value 1.0 to 3.0 with increments of 0.2.

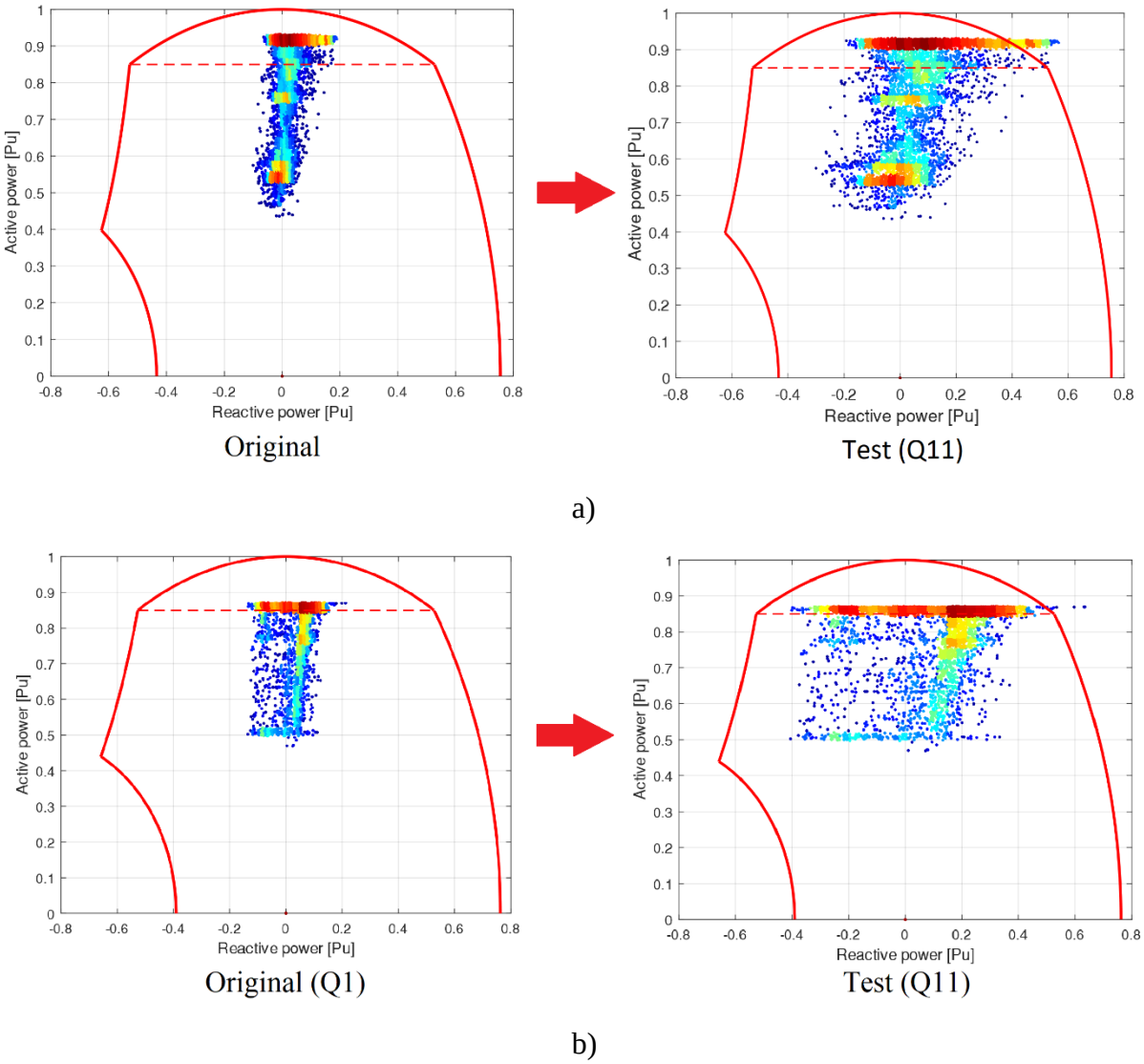

Figure 7.5: Increased variation of reactive power, where a) is the operation in Åbjøra and b) is Sundsbarm. Test Q11 represents a variation of reactive power three times the original.

From the simulations, the WAE only reduced by about 0.02% between test Q1 and Q11 for both HPUs. The corresponding annual energy loss would increase by 0.15 and 0.16 GWh for Åbjøra and Sundsbarm, respectfully. As discussed earlier (Section 6.2), the reactive power can only change the efficiency to about 0.2 – 0.3 % under all loading conditions. In this test scenario, the reactive power is amplified with a constant (1 - 3.0), meaning all reactive components that are negative (absorbing) will become closer to the BEP (-0.22 and -0.3 Pu) and improve efficiency and limit the changes in WAE.

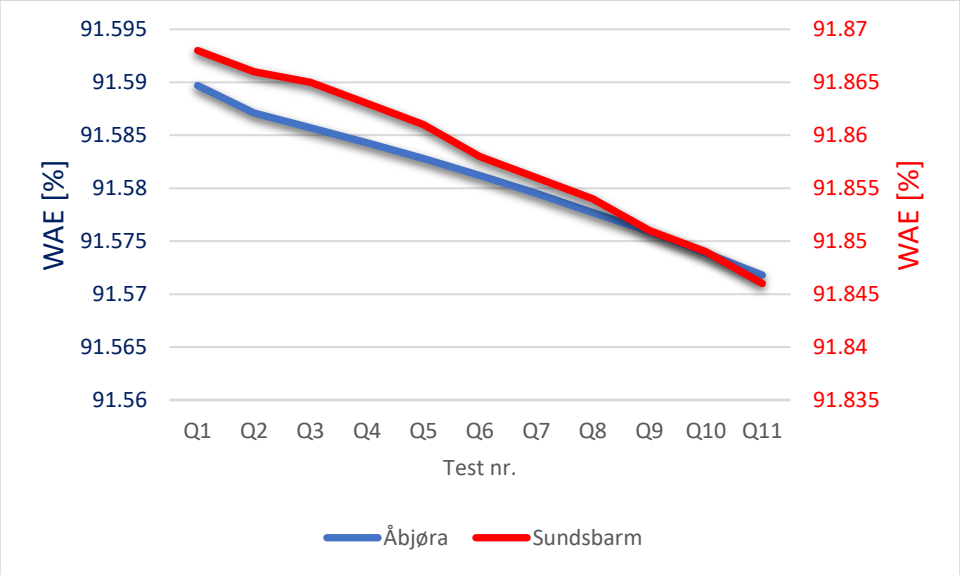

Figure 7.6: WAE obtained from each test for both Åbjøra and Sundsbarm. The test nr. represents each simulation where all reactive power measurements are multiplied by a constant ranging from 1.0 – 3.0.

8 Discussion

8.1 Data acquisition and filtering process

The operational data acquired contained information about the terminal voltage, active and reactive power production to both generators. The data could not be used without modifications as it had apparent errors or problems which needed to be sorted out. The main issues were:

- A large set of operations was represented with “NaN” instead of the actual value.
- All data was given as average values from 1-hour periods.

These problems influence the results in different ways, and one may expect the results to deviate slightly from reality. Average values may not directly affect the energy production, but the combination of “NaN” and average values made it difficult to distinguish between start/stop regions. The method used to differentiate between start/stop regions was by analysing the magnitude of the terminal voltage, indicated the possible duration of an operation point. Thus, an algorithm was created to filter the data based on given assumptions. Both HPUs frequently operated in FRR, i.e., the excessive use of start/stop operations and large fluctuations in active or reactive power. The combination of considerable variation in the active power and measurements from average values would result in some uncertainty to the estimated WAE and other efficiency calculations.

An example would be two operations operated both above and below the BEP with equal distance from the BEP, concerning efficiency. This scenario would result in an average value of active power close to the BEP. However, the average efficiency of those operations would be far from the BEP. Because of the efficiency and energy losses, average values may not be suited for this type of analysis, where one could expect a production with large fluctuations within the average period, here 1-hour.

8.2 Simulation model and assumptions

In this report, the headwater was set to nominal during the simulations due to a lack of accessible data. The effect of possible head difference have been analysed and indicate a BEP reduction of about 0.06 % and 0.1 % in Åbjøra and Sundsbarm respectfully, and should be considered in future work.

The HPU model was initially designed to use measurements from the high voltage side of the transformer. Instead, the provided data was given for the generator terminals. A quick solution to this problem was to calculate the power loss of the transformer ahead and add the power loss to original operational data (P) before implementing the data in the simulation model. This procedure will not affect the energy loss calculated in this report. In cases where the data is provided from the grid side, the transformer inductance shall be implemented to consider the reactive power absorption of the transformer, which was not necessary as the reactive power to the generator was already known.

It was discovered that the WAE obtained the same results as the general formula for average value, i.e., $\bar{x} = (\sum x)/N$. The reason is that all measurements have the same duration (15 minutes), resulting in weights (A_k) which are either equal or directly proportional to the number of operations. The WAE will differ from the general formula for average value if each duration is different or disproportionate to the number of operations.

8.2.1 Turbine and waterway model

The data provided for the turbine contained estimates of the efficiency under various operating conditions. The estimates were performed in 2011 for both HPUs, meaning the effect of turbine fatigue might be present but have been neglected in this report. In the turbine and waterway data, it was described that the spiral casing and draft tube was a part of the waterway. Therefore, it is uncertain whether or not the turbine data consists of only the runner efficiency or if swirling losses (helical vortices) in the draft tube are considered a part of the turbine or the draft tube. This detail may influence the accuracy of the waterway and turbine model.

The turbine model uses interpolation to estimate the efficiency, which is often a preferred method. However, interpolation methods are known for generating artificial oscillations in the data. In some of the iso-contour maps, the oscillations become prominent due to few data points related to the head.

8.2.2 Generator model

In the generator model, excitation losses are assumed to be a constant proportional to the losses in the field windings. The proportional constant of excitation may not reflect the reality but gives a valid approximation as the excitation losses are close to linear. The constant was set to the default of 1.1, the recommended value proposed by Westgaard [41]. For Åbjøra, excitation losses were set to 1.116, determined by the least square method from multiple excitation measurements to improve the accuracy. The accuracy had a maximum error of 2.5 % and an average error of 0.2 %, which will not contribute to any significant errors related to the entire HPU efficiency.

The field current calculations used a set of parameters and characteristics, which was provided from estimates and measurements. Thus, the simulation results from the generator may differ for the reality to a certain degree. In Åbjøra, the field current was determined from both estimated parameters and actual measurements, which means some adjustments to the estimated values were required to achieve results close to the actual measurements. The generator model of Åbjøra was compared to the measurements, and high accuracy was confirmed. However, there is no evidence of the accuracy of the estimated field current in Sundsbarm.

The generator model neglects all effects of temperatures as no temperature data was accessible. The temperature setting of armature and field windings was set to a constant value of 75 °C, i.e., the winding losses might differ marginally, particularly during lower power levels where the temperature is limited.

In the generator model, the voltage is only affecting the armature and field winding current. The effect of voltage in the iron core is neglected, which can be considered a valid assumption as the voltage fluctuations are negligible.

It has been assumed windage and friction losses to be constant, which is usually valid when the frequency is constant as both windage and friction heavily depend on the machine's rotational speed. In addition, the ventilation losses have been assumed constant and are considered a valid assumption, as the cooling of Åbjøra and Sundsbarm is unregulated air-cooled machines, i.e., fans mounted directly on the rotor.

8.2.3 Capability diagram

For this report, the capability diagrams are primarily used for illustrational purposes. The armature and maximum field limits can be regarded as reasonable. In contrast, the end heating limit and practical stability limit do not necessarily represent reality as these were based on some assumptions.

8.3 Discussion of results

The results have shown that the waterway losses in Åbjøra are considerable, as waterway losses accounted for 24 % of the total losses under nominal power, compared to only 13 % in Sundsbarm. The high waterway losses found in Åbjøra have a significant impact on efficiency but may also be the most expensive component of all to improve. The high waterway losses of Åbjøra are an essential factor contributing to moving the BEP to a lower power level which is not preferable if operating the HPU at higher power levels.

The BEP of Åbjøra (92.25 %) was found to be slightly higher than Sundsbarm (92.14 %), which is primarily due to the high turbine efficiency in Åbjøra. However, Åbjøra had a WAE of 91.6 %, which are lower than obtained in Sundsbarm (91.9 %), and is a result of having a BEP located at low power levels combined with large fluctuations in operation. Most of the large fluctuations seen in both HPUs are produced by what is recognized as FRR or mFRR operating regime, which means the HPUs are automatically or manually controlled by the national TSO (Statnett) to balance the power grid. During the summertime, Sundsbarm is primarily used for grid balancing, which also results in a significant operational efficiency reduction. In contrast, Åbjøra obtains a low operational efficiency during the winter, where the production is high.

8.4 Discussion of sensitivity analysis

The sensitivity analysis was performed to analyse how the WAE changes relative to operational patterns. The analysis was chosen to vary the active and reactive power based on the original regime and indicated a marginal increase in loss related to greater fluctuations of reactive power, assuming a proportional increase. If the generators operate more frequently in the inducive region, one could expect an improvement to the WAE. However, even in extreme scenarios, the influence of reactive power only influenced the WAE of about 0.02 % in both HPUs.

On the other hand, the change in WAE due to increased active power variation resulted in about 0.7 % and 2.8% change in Sundsbarm and Åbjøra, respectfully. The equation used to vary the active power did not affect all operating points equally, as operating points in proximity to the maximum power was almost not affected. In this sensitivity analysis, the variations in active power levels were increased, which is not realistic as both generators operate at a minimum setpoint. It is more likely that the operational density increase at the lower power levels or become more distributed. One could expect Sundsbarm to be most affected by the change as the location of the BEP is more favourable for high power levels, which is the opposite situation for Åbjøra.

9 Conclusion

The future power grid may experience severe changes due to the “green shift” which utilises intermittent energy sources like wind and solar power. With extensive use of intermittent sources, the power grid may experience severe challenges regarding grid balance, and hydropower units could be forced to change their operational regime to focus more on balancing the grid. This regime shift is expected to influence the hydropower units' operational efficiency, resulting in severe energy losses and lost revenue.

Therefore, this report will analyse the operational efficiency and energy losses in hydropower units to prepare for future challenges. The analysis was performed as a part of a larger research program collaborated by Skagerak Kraft and the University of South-Eastern Norway (USN). During this report, production regimes, regulations, and general hydropower theory has been introduced with a focus on energy production and related losses. In this report, a static hydropower model has been developed in MATLAB. The model combines basic fluid dynamic theory and electrical machine theory, allowing energy loss and efficiencies to be determined from parameters given by the hydropower unit and operational data from the generator (transformer). The model has been implemented in two hydropower units, namely Åbjøra and Sundsbarm. The analysis of these hydropower units is presented in two study cases. The first study case analyses and compares the individual components and the entire hydropower unit followed up with an analysis of the operational regimes. The second study case is a short sensitivity analysis where changes in the operational regimes are investigated for possible future grid changes.

From the analysis of Åbjøra and Sundsbarm, a total best efficiency point (BEP) was found with an efficiency of 92.25 % and 92.14 %, respectfully. The results show signs of frequent use of FRR in both hydropower units, which strongly correlates with reduced operational efficiency due to the large fluctuations of active power. Sundsbarm operates most efficiently under high power levels with a weighted average efficiency (WAE) of 91.9 %, whereas Åbjøra operates with a WAE of 91.6 %. From the report, it can be concluded that the impact of reactive power on efficiency will be minor and does not contribute to any significant change to the efficiency. On the other hand, operations with low active power should be limited due to the considerable impact on efficiency, which could occur with increased use of grid balancing.

10 Further work

To improve the accuracy of this analysis, one should use single measurements or average values with short time periods. Variations in the head should be implemented to account for the additional losses in the waterway and turbine. Additional losses related to start/stop and idle situations could be implemented, which may be significant for hydropower units with frequent start/stop operations. The generator in Sundsbarm should be implemented with more accurate parameters, preferably from measurements. The effect of fatigue in turbines should be investigated and implemented in the model. For the transformer, an improved model could be constructed, which includes the internal impedance for reactive power absorption.

The HPU model is only designed for single generating units and should be expanded for multi generating units as additional head loss calculations may be required. For the long run, the HPU model should be improved with a higher level of software usability.

References

[1] ‘Kraftproduksjon’, *Energifaktanorge*, Mar. 25, 2021. https://energifaktanorge.no/norsk-energiforsyning/kraftforsyningen/ (accessed Apr. 18, 2021).

[2] A. Joswig and M. Baca, ‘Extended requirements on turbo-generators and solutions for flexible load operation’, in *2016 XXII International Conference on Electrical Machines (ICEM)*, Lausanne, Switzerland, Sep. 2016, pp. 2649–2654. doi: 10.1109/ICELMACH.2016.7732895.

[3] E. F. Bødal, ‘Coordination of Hydro and Wind Power in a Transmission Constrained Area using SDDP’, Norwegian University of Science and Technology, 2016.

[4] ‘Hydroelectricity in the Nordic countries’, *Nordics.info*, Feb. 25, 2019. https://nordics.info/show/artikel/hydroelectricity/ (accessed May 12, 2021).

[5] ‘Meld. St. 25 (2015–2016): Kraft til endring - Energipolitikken mot 2030’, Det Kongelige Olje- og Energidepartement, Apr. 2016.

[6] ‘Egenskaper ved det norske kraftsystemet’, *Norges vassdrags- og energidirektorat (NVE)*, Aug. 26, 2020. https://www.nve.no/stromkunde/om-kraftmarkedet-og-det-norske-kraftsystemet#01 (accessed Apr. 18, 2021).

[7] I. V. Sem *et al.*, ‘Langsiktig Kraftmarkedsanalyse 2020-2040’, NVE (The Norwegian Water Resources and Energy Directorate), 37/2020, Oct. 2020. Accessed: May 13, 2021. [Online]. Available: http://publikasjoner.nve.no/rapport/2020/rapport2020_37.pdf

[8] E. C. Bortoni, R. T. Siniscalchi, S. Vaschetto, M. A. Darmani, and A. Cavagnino, ‘Efficiency Mapping and Weighted Average Efficiency for Large Hydrogenerators’, *IEEE Open J. Ind. Applicat.*, vol. 2, pp. 11–20, 2021, doi: 10.1109/OJIA.2020.3048989.

[9] A. Estanqueiro, ‘The Future Energy Mix Paradigm: How to Embed Large Amounts of Wind Generation While Preserving the Robustness and Quality of the Power Systems?’, in *Wind Power*, S. M, Ed. InTech, 2010, p. 23. doi: 10.5772/8359.

[10] S. Fereidoon and S. P. Fereidoon, *Future of utilities - utilities of the future : How technological innovations in distributed energy resources will reshape the electric power sector*, 1st ed. London, England: Academic Press, 2016.

[11] J. K. Noland, M. Leandro, A. Nysveen, and T. Oyvang, ‘Future Operational Regimes of Bulk Power Generation in The Era of Global Energy Transition: Grid Codes, Challenges and Open Issues’, in *2020 IEEE Power & Energy Society General Meeting (PESGM)*, Montreal, QC, Canada, Aug. 2020, pp. 1–5. doi: 10.1109/PESGM41954.2020.9282001.

[12] THE EUROPEAN COMMISSION, ‘COMMISSION REGULATION (EU) establishing a network code on requirements for grid connection of generators (NC-RfG)’, p. 68, Apr. 2016.

[13] Statnett, ‘NVF 2020 Nasjonal veileder for funksjonskrav i kraftsystemet’, p. 240, Jul. 2020.

[14] Statnett, ‘Funksjonskrav i kraftsystemet 2012’, p. 116, 2012.

[15] ‘IEEE Std C50.13™-2014, Standard for Cylindrical-Rotor 50 Hz and 60 Hz Synchronous Generators Rated 10 MVA and Above’, p. 63, Mar. 2014.

[16] K. Mayor, L. Montgomery, and K. Hattori, 'Grid code impact on electrical machine design', in *2012 IEEE Power and Energy Society General Meeting*, San Diego, CA, Jul. 2012, pp. 1–8. doi: 10.1109/PESGM.2012.6345292.

[17] T. Kallevik *et al.*, 'RME RAPPORT: Driften av kraftsystemet 2019', Norges vassdrags- og energidirektorat (NVE), 3/2020, 2019. [Online]. Available: http://publikasjoner.nve.no/rme_rapport/2020/rme_rapport2020_03.pdf

[18] Statnett, 'Fast frequency reserves FFR', *Statnett*, Jan. 22, 2021. https://www.statnett.no/for-aktorer-i-kraftbransjen/systemansvaret/kraftmarkedet/reservemarkeder/ffr/ (accessed May 16, 2021).

[19] 'Primærreserver - FCR', *Statnett*, Nov. 09, 2018. https://www.statnett.no/for-aktorer-i-kraftbransjen/systemansvaret/kraftmarkedet/reservemarkeder/primarreserver/ (accessed May 12, 2021).

[20] E. J. Ruud, 'Beslutningsstøtte med kontinuerlig virkningsgradsmåling i vannkraftverk', Norwegian University of Science and Technology (NTNU), 2017.

[21] 'ÅRSBERETNING OG ÅRSREGNSKAP /2018', Sira Kvina Kraftselskap, 2018. Accessed: May 14, 2021. [Online]. Available: https://www.sirakvina.no/getfile.php/132809-1559636215/Dokumenter/%C3%85rsberetninger/Sira-Kvina_%C3%A5rsberetning-2018.pdf

[22] 'How hyperlocal hydro energy can empower communities', *Grist.org*, Nov. 11, 2020. https://grist.org/Array/how-hyperlocal-hydro-energy-can-empower-communities/ (accessed May 14, 2021).

[23] I. E. Idel'chik, 'Handbook of Hydraulic Resistance', *Israel Program for Scientific Translations*, p. 526, 1960 1966.

[24] R. K. Bansal, *A Textbook of Fluid Mechanics and Hydraulic Machines*, 9th ed. New Delhi: Laxmi Publications, 2005.

[25] M. B. Bishwakarma, 'Computation of Head Losses in Hydropower Tunnels', p. 16, Nov. 2012.

[26] O.-I. Lekang, *Aquaculture Engineering*, 2nd ed. Ås, Norway: John Wiley & Sons, Ltd, 2013.

[27] A. N. Kamarudzaman, 'EAT 252: Fluid Mechanics Engineering: Chapter 6 - Minor Loss', School of Enviromental Engineering Universiti Malayssia Perlis. Accessed: May 16, 2021. [Online]. Available: http://portal.unimap.edu.my/portal/page/portal30/Lecture%20Notes/School%20of%20Environmental%20Engineering/Semester%201%20Sidang%20Akademik%202017 2018/RK01/EAT252%20Fluid%20Mechanics%20Engineering/EAT%20252%20CHAPTER%206%20Minor%20loss%20portal.pdf

[28] A. Kjølle, *HYDROPOWER IN NORWAY Mechanical Equipment*. Trondheim, Norway: Norwegian University of Science and Technology (NTNU), 2001.

[29] 'An Ultimate Guide to Francis Turbine', *Linquip Technews*, Dec. 13, 2020. https://www.linquip.com/blog/what-is-francis-turbine/ (accessed May 15, 2021).

[30] ‘Turbines’. http://www.eternoohydro.com/turbines/axial-flow-turbines.html (accessed May 15, 2021).

[31] ‘Design of Pelton turbines’, Norwegian University of Science and Technology (NTNU), 2006. [Online]. Available: http://www.ivt.ntnu.no/ept/fag/tep4195/innhold/Forelesninger/forelesninger%202006/5%20-%20Pelton%20Turbine.pdf

[32] ‘Pelton turbines’, *Voith*. https://voith.com/hu-hu/turbines-generators/turbines/pelton-turbines.html (accessed May 15, 2021).

[33] Z. Zhang, *Pelton Turbines*, 1st ed. 2016. Cham: Springer International Publishing : Imprint: Springer, 2016. doi: 10.1007/978-3-319-31909-4.

[34] S. Alligné, ‘Forced and Self Oscillations of Hydraulic Systems Induced by Cavitation Vortex Rope of Francis Turbines’, ÉCOLE POLYTECHNIQUE FÉDÉRALE DE LAUSANNE, 2011.

[35] S. Mathew, ‘Pelton turbine - working and design aspect’, *Lesics*, Aug. 21, 2013. https://lesics.com/pelton-turbine-wheel-hydraulic-turbine.html (accessed May 15, 2021).

[36] A. Alfredsson and K. A. Jacobsson, *Elmaskiner och elektriska drivsystem*, 3rd ed. Stockholm,Sweeden: Liber, 2016.

[37] A. Petterteig, O. Mogstad, T. Henriksen, and Ø. Håland, ‘Tekniske retningslinjer for tilknytning av produksjonsenheter, med maksimum aktiv effektproduksjon mindre enn 10 MW, til distribusjonsnettet’, Sintef, Trondheim, Norway, Technical report TR A6343.01, Nov. 2006. [Online]. Available: https://www.sintef.no/globalassets/project/distribution_2020/publikasjoner/tr_a6343.01.pdf

[38] ‘KAPLAN HYDRO GENERATOR UNIT’, *GE Renewable Energy*. https://www.ge.com/renewableenergy/sites/default/files/2020-01/hydro-cgi-kaplan-generating-unit-3000px.jpg (accessed May 15, 2021).

[39] ‘AC generator’, *Synchronous machines Design of synchronous machines*, Dec. 16, 2020. https://www.freeenergyplanet.biz/renewable-energy-systems/synchronous-machines-design-of-synchronous-machines.html (accessed Apr. 22, 2021).

[40] T. Øyvang, ‘Enhanced power capability of generator units for increased operational security’, PhD, University of South-Eastern Norway (USN), Porsgrunn, 2018.

[41] E. Westgaard and O. Andersen, ‘Dimensjoneringseksempel for synkronmaskin’, *NTH, Department of Electrical machines, Trondheim Norway*, p. 52, 1965.

[42] ‘IEEE Std 115™-2009, IEEE Guide for Test Procedures for Synchronous Machines’, IEEE, 2010.

[43] Chas. P. Steinmetz, ‘On the Law of Hysteresis’, *Trans. Am. Inst. Electr. Eng.*, vol. IX, no. 1, pp. 1–64, 1892, doi: 10.1109/T-AIEE.1892.5570437.

[44] D. M. Ionel, M. Popescu, M. I. McGilp, T. J. E. Miller, S. J. Dellinger, and R. J. Heideman, ‘Computation of Core Losses in Electrical Machines Using Improved Models for Laminated Steel’, *IEEE Trans. on Ind. Applicat.*, vol. 43, no. 6, pp. 1554–1564, 2007, doi: 10.1109/TIA.2007.908159.

[45] P. Parthasaradhy and S. V. Ranganayakulu, ‘Hysteresis and eddy current losses of magnetic material by Epstein frame method-novel approach’, *The International Journal Of Engineering And Science (IJES)*, p. 9, 2014.

[46] *Transformer Handbook*, 3rd ed. ABB, 2007.

[47] ‘Rotating Electrical Machines Losses and Efficiency Classification’:, *EEEGuide*. https://www.eeeguide.com/rotating-machines-losses-classification/

[48] J. Vranick, ‘Prediction of Windage Power Loss In alternators’, NASA Technical Note, Cleveland, Ohio, United States, NASA-TN-D-4849, Oct. 1968. [Online]. Available: https://ntrs.nasa.gov/search.jsp?R=19680027690

[49] D. Pejovski, B. Velkovski, and K. Najdenkoski, ‘MATLAB Model for Visualization of PQ diagram of a Synchronous Generator’, *ResearchGate*, p. 5, Nov. 2016.

[50] P. Kundur, *Power System Stability and Control*. McGraw-Hill, Inc, 1993.

[51] E. Csanyi, ‘Large power transformer tailored to customers’ specifications’, *Electrical Engineering Portal (EEP)*, Dec. 30, 2013. https://electrical-engineering-portal.com/an-overview-of-large-power-transformer-lpt (accessed May 15, 2021).

[52] E. Vaahedi, *Practical Power System Operation*. Hoboken, New Jersey: IEEE Press/Wiley, 2014.

[53] E. D. C. Bortoni, ‘EFFICIENCY MAP AND WEIGHTED AVERAGE EFFICIENCY FOR SYNCHRONOUS MACHINES FOR HYDROPOWER PLANTS’, FEDERAL UNIVERSITY OF ITAJUBÁ, 2019.

[54] J. Arrillaga and C. P. Arnold, ‘Power System Stability - Advanced Component Modelling’, in *Computer Analysis of Power Systems*, John Wiley & Sons, Ltd, 1990, p. 11.

[55] S. Beckwith, ‘Approximating Potier Reactance’, *Electr. Eng.*, vol. 56, no. 7, pp. 813–818, Jul. 1937, doi: 10.1109/EE.1937.6540240.

[56] I. Ilić, Maljković, and I. Gašparac, ‘Methodology For Determining The Actual PQ Diagram Of A Hydrogenerator’, vol. 56, no. 2, pp. p144-181, 2007.

[57] E. S. Menon, *Transmission Pipeline Calculations and Simulations Manual*. Sint Louis: Elsevier Science & Technology, 2015.

[58] H. Kudela, ‘Hydraulic losses in pipes’, *Wroclas University of Science and Technology*, p. 9, 2012.

[59] H. Belyadi, E. Fathi, and F. Belyadi, ‘Chapter Eight - Hydraulic Fracturing Chemical Selection and Design’, in *Hydraulic Fracturing in Unconventional Reservoirs*, Elsevier Inc., 2017, p. 13. [Online]. Available: https://doi.org/10.1016/B978-0-12-849871-2.00008-3

Appendix A

Task Description of the Master Thesis

This appendix contains the original task description and main goals for this thesis.

FMH606 Master's Thesis

Title: Hydropower generating unit – An analysis of weighted average efficiency

USN supervisor: Gunne J Hegglid and Thomas Øyvang

External partner: Skagerak Kraft AS

Student: Sigurd S Berg

Task background:

The hydropower unit (HPU) is the real workhorse of the Norwegian power supply system. Load is varying over the day and year with high rates of change and for units with reservoirs the loading will change almost every hour over its total operational time. This tendency is even more increased if units are contributing to the various balancing markets which are handling the frequency control of the power system.

Optimization of operational efficiency of the power system makes it favourable to know efficiency of each generating unit under their entire operational range. In recent time, there have been an increased use of wind and solar systems in the power grid, shifting the HPU into a more flexible operation that requires higher focus on energy losses with respect to suboptimal operation and Frequency Restoration Reserve (FRR).

Task description:

- Explore the losses (energy conversion) of a hydropower system.
- Review the existing regulation and requirements, and typical operating conditions of the Norwegian Bulk Hydropower.
- Identify the optimal operating point/pattern of the HPU regarding efficiency. This from operation statistic for specific units for one or some years.
- Build a suitable mathematical model of the HPU (waterway, turbine, generator and transformer) to identify energy loss and efficiency under stationary conditions.
- Run different cases based on FRR, droop control and setpoints to identify efficiency (WAE) under new operating regimes.
- Give recommendations on future operating conditions with respect to energy loss under suboptimal operation.

Appendix B

Minutes of meeting, second formal project meeting 13.04.2021

This appendix contains the minutes of meeting from the second project meeting, where the task description was formally changed.

MINUTES OF MEETING #2

To: Gunne J. Hegglid (main supervisor) and Thomas Øyvang

FMH606 Master's Thesis 2021
Title of thesis: Hydropower unit – An analysis of operational efficiencies and energy losses

Date : 13.04.2021
Time : 14:00 - 15:00
Venue : Zoom Meeting

Item 1 Approval of cases

1. **Approval of notice**
   a. Approved
2. **Approval of agenda**
   a. Approved
3. **Other issues?**
   a. -----

Item 2 Project status

1. **Project status**
   a. It with was a discussed about the typical operating conditions and the energy markets.
   b. Specifications (P_0, P_k and S_n) of the transformers used in Åbjøra and Sundsbarm will be provided shortly (if they exists).
2. **Simulation results**
   a. It was a discussion about the operational data, where it was concluded that the operational data should be formatted differently.
3. **Future work**
   a. -----

Item 3 Other issues

1. **Discuss changes to original task description and title.**

   a. There was given approval for changes done to the title of the thesis:

      Old Title: Hydropower generating unit – An analysis of weighted average efficiency.

      New Title: Hydropower unit – An analysis of operational efficiencies and energy losses

   b. There was also given approval for the changes done in the task description, as shown below:

      - The main goal of this project is to analyse the operational efficiency and ~~estimate the weighted average efficiency of specific hydropower units to improve voltage quality at a lower operational cost~~ energy losses of specific hydropower units based on todays and future operational regime. The objectives of this thesis are listed below.

        Reason for change: The weighted average efficiency (WAE) was too specific for the description, and was therefore changed to energy losses instead. In addition, there was not enough time for performing voltage quality analysis.

      - Run different cases based on ~~FRR, droop control and setpoints to identify efficiency (WAE)~~ future predictions to identify energy losses under the new operating regimes.

        Reason for change: There was not enough time for creating such a complex model that would be able to implement FRR, droop control and setpoints.

      - ~~Give recommendations on future operating conditions with respect to energy loss under suboptimal operation.~~

        Reason for change: It would not be achievable to give recommendations to the operation based solely on the efficiency and energy loss of a hydropower unit.

Meeting leader and secretary:
Sigurd Berg

Appendix C
Theoretical study of losses in a waterway

Estimation of friction losses

Calculation methods for estimating friction losses in waterway have been developed by numerous people, where each has its pros and cons. Hagen-Poiseuille is an analytical equation used to calculate pressure drop through waterways, where the flow is assumed to be a Newtonian fluid, laminar and incompressible. The assumptions in Hagen-Poiseuille will give incorrect results where the flow in headrace tunnels is turbulent and have high frictional losses due to the rough walls. Empirical formulas like Darcy-Weisbach's and Manning's equation are developed to achieve suitable accuracy for large tunnels with uneven surfaces. The use of Darcy-Weisbach's and Manning's equation to estimate head losses are recommended during the planning and design of the system, where both provide similar accuracy for a given range [25]. The Darcy-Weisbach would be used as an example, as this method is widely used [26].

Darcy-Weisbach's equation expresses the losses in terms of head losses [m] as shown:

$$h_f = f \cdot \frac{L \cdot v^2}{2g \cdot D_h} \tag{10.1}$$

where h_f = head loss $[m]$, f = friction factor, v = flow velocity $[m/s]$, L = tunnel length $[m]$, g = gravitational constant $[m/s^2]$ and D_h = hydraulic diameter $[m]$.

The friction factor f represents friction losses in a pipe/tunnel section or a valve, dependent on the type of flow; laminar or turbulent. Reynolds number is a measurement that determines the magnitude of turbulence in fluids. In circular pipes, where the velocity and pipe diameter are small ($R_e < 2000$), the flow is considered to be laminar or low turbulent [26], and the equation for friction factor f could be used as follows:

$$f = \frac{64}{R_e} \tag{10.2}$$

Reynold number is defined by:

$$R_e = \frac{\rho \cdot v \cdot D_h}{\mu} \tag{10.3}$$

where R_e = Reynold number, ρ = density of the fluid $[kg/m^3]$, v = velocity of the fluid $[m/s]$, D_h = pipe diameter $[m]$ and μ = dynamic viscosity of the fluid $[kg/(m \cdot s)]$.

When the Reynolds number is between 2000 and 4000, the flow is unstable, and turbulent and laminar conditions could occur [26]. For turbulent flow, one can use the Colebrook-White, an empirical formula used to estimate the friction factor used in the Darcy-Weisbach's equation based on Reynold's number the relative surface roughness found tables. The Colebrook-White equation, also referred to as the Colebrook equation, is defined as [57] [58]:

$$\frac{1}{\sqrt{f}} = -2\log_{10} \cdot \left(\frac{\varepsilon}{3.7D_h} + \frac{2.51}{R_e\sqrt{f}}\right) \tag{10.4}$$

where, f = friction factor solved numerically, ε = absolute surface roughness $[mm]$ and D_h = pipe diameter $[m]$.

It is essential to distinguish between absolute and relative roughness. Relative roughness e expresses the amount of roughness existing inside a pipe and is defined as the absolute roughness ε divided by the inside diameter D of a pipe, yielding [59]:

$$e = \frac{\varepsilon}{D} \qquad 10.5$$

A Moody diagram shown in the figure below, is an alternative method to estimate the friction factor when the relative roughness and Reynold's number is known.

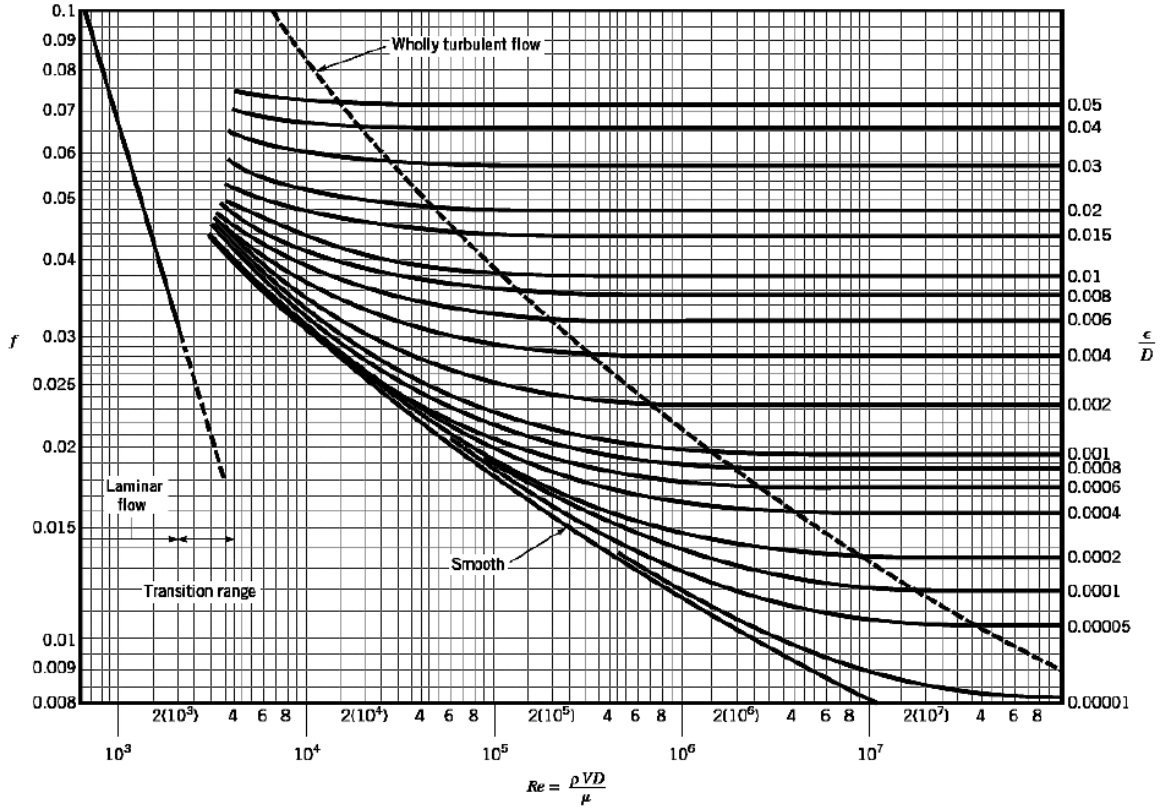

Moody diagram, a diagram used to determine friction factor (f) from the relative roughness factor and the Reynolds number [58].

Table for determining local losses in waterway

Typical resistance coefficients (k) for pipe fittings [26].

Fitting	*k*	Comments
Pipe entrance in a basin or in a river	0.05–1	Lowest value with rounded inlet pipes; highest with pipes with sharp edges. The value is increased when the pipe goes into the basin
Contraction of pipes	0.05–0.5	Lowest value with conical contraction and small alteration in the diameter
Expansion of pipes	0.05–1	Lowest value with conical expansion and small alteration in the diameter
Elbow		Increasing with reduction in the pipe diameter. Long smooth bends
90°	0.5–1	will have reduced *k* values. Smaller angles will have lower *k* values
45°	0.1–0.3	
T-pipe (divided flow)	0.3–1.8	Depends on the proportion divided from the main flow; increased with increased part flow
T-pipe (connection flow)	0.1–0.8	Depends on how much water is supplied via part flow in the T-pipe; increases with increased size
Valves		Values are highly dependent on the specification and the producer of the valve.
Ball valve	0.1	Values shown are for fully open valves
Angle seat valve	1.3	
Diaphragm valve	4	
Check valve	2	
Gate valve	0.2	

Appendix D

Derivation of head loss formula with a total head loss coefficient

An equation for head loss can be derived from the equations representing friction losses (3.1) and local losses (3.2). The following method has been used:

The relationship between volume discharge Q and velocity is:

$$v = \frac{Q_{flow}}{A} = Q_{flow}\frac{4}{\pi D_h^2} \qquad 10.6$$

Substituting (10.6) into the Darcy-Weisbach's equation (10.1) and introducing the head loss coefficient $k_{f,i}$, which yields:

$$h_{loss,i} = k_{f,i}Q_{flow}^2 \qquad 10.7$$

where $k_{f,i}$ is the head loss coefficient for friction loss to each component or section of the waterway and is given by:

$$k_{f,i} = f \cdot \frac{L_i}{2g \cdot D_{h,i}} \cdot \left(\frac{4}{\pi D_{h,i}}\right)^2 = f_i \cdot \frac{L_i}{8g\pi^2 D_{h,i}^3} \qquad 10.8$$

In a similar manner as the head loss coefficient based on friction losses (10.7 and 10.8), the head loss coefficient for local losses will be given by substituting (10.6) into (3.2), which yields:

$$h_{loss,j} = k_{l,i}Q_{flow}^2 \qquad 10.9$$

and

$$k_{l,i} = \frac{\mathrm{k_j}}{2\mathrm{g}}\left(\frac{4}{\pi D_{h,j}^2}\right)^2 \qquad 10.10$$

where $k_{l,i}$ is the head loss coefficient for local losses, k_j is the resistance coefficient and $D_{h,j}$ is the part diameter.

Summation of all the head loss coefficients $k_{f,i}$ and $k_{l,i}$ for $i = 1,2 \ldots, n$ and $j = 1,2 \ldots, m$, respectfully, would produce a single coefficient K representing the total head loss, expressed as:

$$H_{loss} = Q_{flow}^2\left(\sum_{i=1}^{n} k_{f,i} + \sum_{j=1}^{m} k_{l,j}\right) = KQ_{flow}^2 \qquad 10.11$$

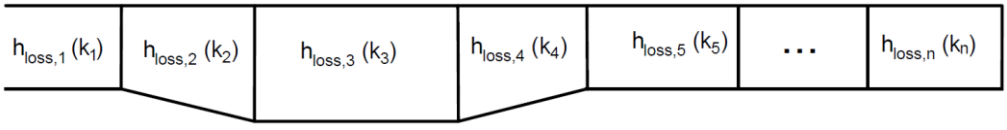

Illustration of head losses shown in sections.

Appendix E

Calculation example of field current

Input parameters to the generator: S_n = 103 MVA, $V_n = 11\ kV$, $X_d = 1.06$ Pu, $X_q = 0.69$ Pu, $X'_d = 0.15$ Pu, $X_l = 0.11$ Pu, $R_a = 0.0027$ Pu

Operation data: $P = 0.900$ Pu, $Q = 0.436$ Pu, $V = 1$ Pu

Field current is calculated with the following method, based on [53] and [54]:

1. $I_t = \frac{\sqrt{P_t^2+Q_t^2}}{V_t} = \frac{\sqrt{0.900^{\,2}+0.436^2}}{1} = 1\ Pu$
2. $\varphi = \tan^{-1}\left(\frac{Q_t}{P_t}\right) = \tan^{-1}\left(\frac{0.436}{0.900}\right) = 0.45\ (rad)\ or\ 0.9\ (deg)$
3. $\delta_i = \tan^{-1}\left(\frac{X_q I_t cos\varphi - R_a I_t sin\varphi}{V_t + R_a I_t cos\varphi + X_q I_t sin\varphi}\right) = \tan^{-1}\left(\frac{0.69\cdot 1\cdot\cos(0.45) - 0.0027\cdot 1\cdot\sin(0.45)}{1+0.0027\cdot 1\cdot\cos(0.45)+0.69\cdot 1\cdot\sin(0.45)}\right) = 0.44$
4. $E_g = V_t cos\delta_i + R_a I_t cos(\varphi + \delta_i) + x_d I_t sin(\varphi + \delta_i)$

   $E_g = 1\cdot\cos(0.44) + 0.0027\cdot 1\cdot cos(0.45+0.44) + 1.06\cdot 1\cdot sin(0.45+0.44)$

   $E_g = 1.73$
5. Air-gap line: $E_{g,o}$ is the excitation voltage at open circuit.

   $b_v = \frac{E_{g,o}}{I_F} = \frac{1}{556} = 0.0018$

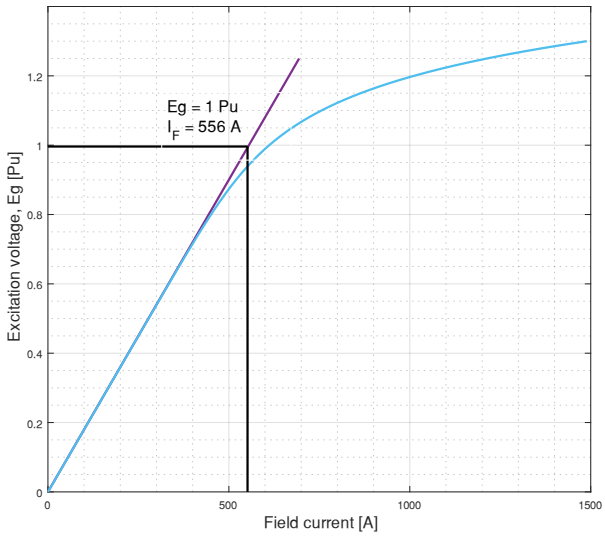

Open circuit characteristic (OCC) drawn in blue and air-gap line drawn in purple.

6. $I_{FU} = \frac{E_g}{B_v} = \frac{1.73}{0.0018} = 961.1\ [A]$
7. $X_p = X_l + 0.63(X'_d - X_l) = 0.11 + 0.63(0.15 - 0.11) = 0.135$ Pu

8. $\delta_p = \tan^{-1}\left(\frac{X_p I_t cos\varphi - R_a I_t sin\varphi}{V_t + R_a I_t cos\varphi + X_p I_t sin\varphi}\right) = \tan^{-1}\left(\frac{0.135 \cdot 1 \cdot \cos(0.45) - 0.0027 \cdot 1 \cdot \sin(0.45)}{1 + 0.0027 \cdot 1 \cdot \cos(0.45) + 0.135 \cdot 1 \cdot \sin(0.45)}\right)$

   $\delta_p = 0.113$

9. $E_p = V_t cos\delta_p + R_a I_t cos(\varphi + \delta_p) + x_p I_t sin(\varphi + \delta_p)$

   $E_p = 1 \cdot \cos(0.113) + 0.0027 \cdot 1 \cdot cos(0.45 + 0.113) + 1.06 \cdot 1 \cdot sin(0.45 + 0.113)$

   $E_p = 1.068$

10. $I_{FP} = \left(\sum_{i=1}^{n} b_i E_p^i\right) = (E_p + C_n E_p^n)k$

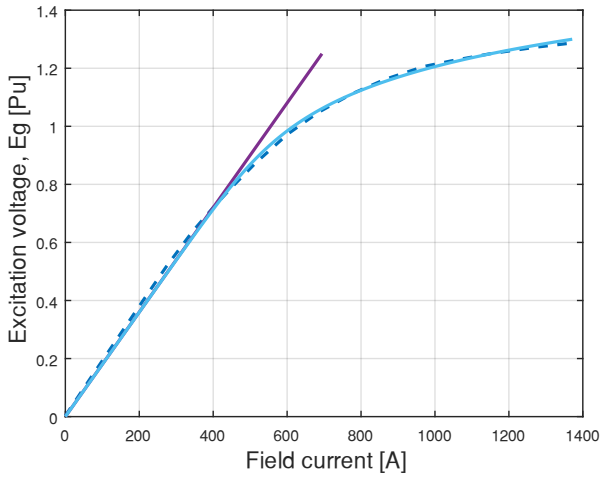

Dotted blue curve represent the actual OCC whereas the blue curve represents the fitted curve. Purple line represents the air-gap line

Find the coefficient C_n, n and k:

$k = I_{F,n} = 556$

n is usually set to 7 or 9.

C_n is found by plotting the relationship between the calculated field current (I_{FP}) and the voltage (e.g., 0-1.25) several times for different values of C_n until the curve is close to the measured OCC, as depicted above.

For this scenario: $k = 556$, $n = 9$, $C_n = 0.11$

$I_{FP} = (1.068 + 0.11 \cdot 1.068^9) \cdot 556 = 704.4\ [A]$

11. $I_{FS} = I_{FP} - \frac{E_p}{b_v} = 704.4 - \frac{1.068}{0.0018} = 111.1\ [A]$

12. $I_{fd} = I_{FU} + I_{FS} = 961.1\ [A] + 111.1\ [A] = 1072.2\ [A]$

Appendix F
Hydropower specifications and parameters for Åbjøra

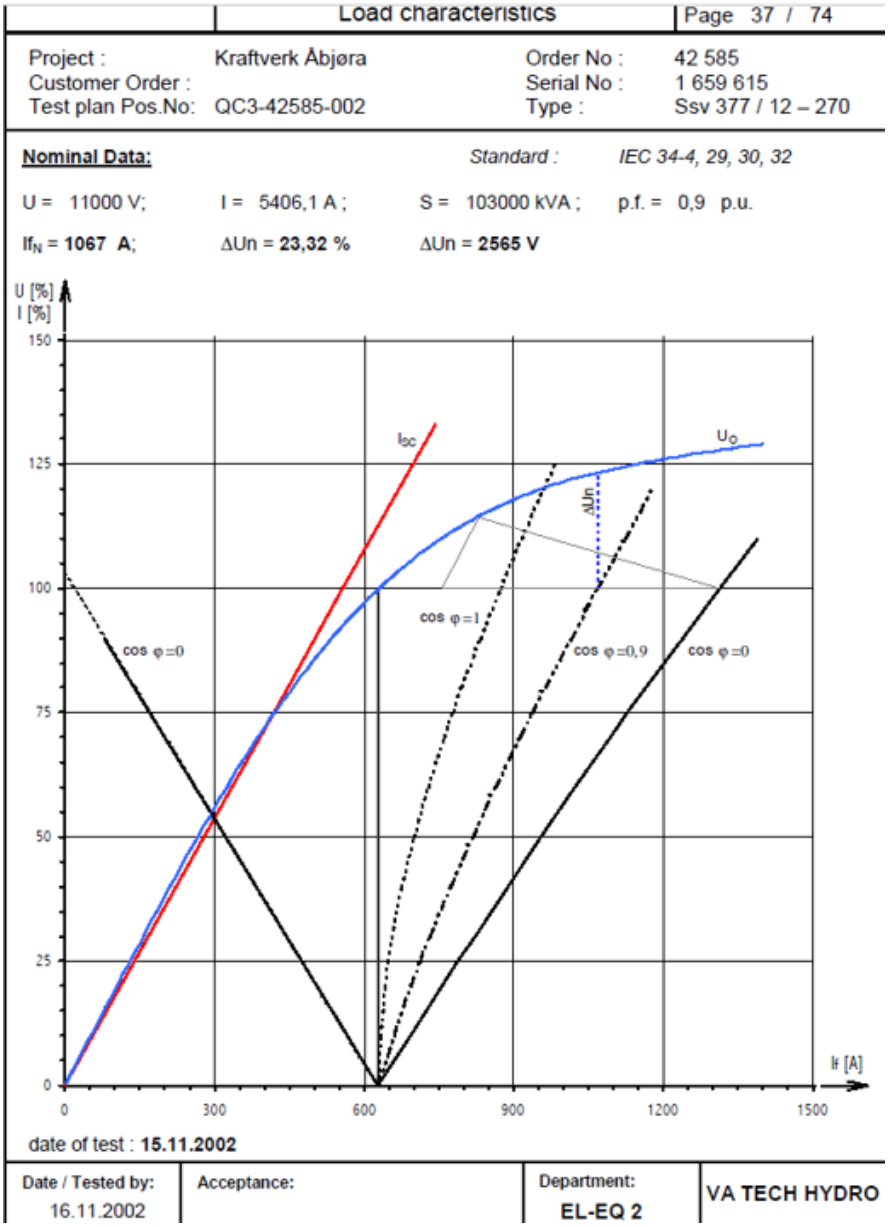

Project :	Kraftverk Åbjøra	Order No :	42 585
Customer Order :		Serial No :	1 659 615
Test plan Pos.No:	QC3-42585-002	Type :	Ssv 377 / 12 – 270

Field current I_f (at nominal data) : *Standard :* *IEC 34-4, 25-27*

No-load stator voltage **11000** V; I_f = **628,1** A
Short-circuit stator current **5406,1** A; I_f = **556,8** A

No-load- / short-circuit ratio : $K_C = \frac{OD}{OH} =$ **1,128** p.u. $X_{d\,unsat.} = \frac{AC}{BC} = \frac{OH}{OC} =$ **1,059** p.u.

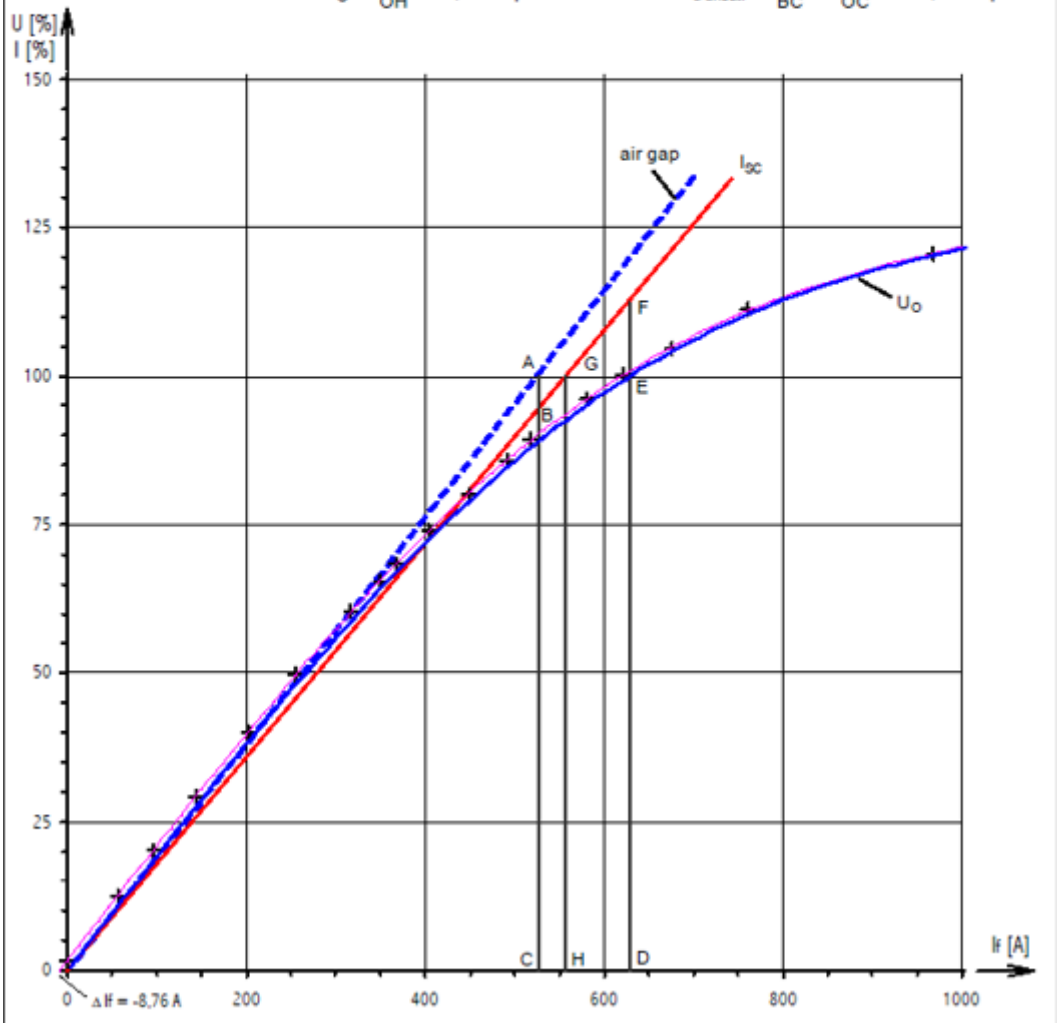

date of test : **7.11.2002**

ELIN

Synchronous machine
Efficiency

Page 68 / 74

Project :	Kraftverk Åbjøra	Order No :	42 585
Customer Order :		Serial No :	1 659 615
Test plan Pos.No:	QC3-42585-002	Type :	Ssv 377 / 12 – 270

Calculation of efficiency:

cos phi = **0,90**					
load	%	100,00	75,00	50,00	25,00
power	kVA	103 000,00	77 250,00	51 500,00	25 750,00
stator current	A	5 406,1	4 054,6	2 703,0	1 351,5
mechanical losses	kW	172,92	172,92	172,92	172,92
core losses	kW	211,92	211,92	211,92	211,92
bearing losses (related to generator)	kW	240,90	240,90	240,90	240,90
load losses	kW	276,62	155,60	69,16	17,29
total excitation losses	kW	191,66	148,55	113,96	87,48
total losses	kW	1 094,02	929,89	808,85	730,51
P out	kW	92 700,00	69 525,00	46 350,00	23 175,00
P in	kW	93 794,02	70 454,89	47 158,85	23 905,51
efficiency measured	%	**98,834**	**98,680**	**98,285**	**96,944**
efficiency gar.	%	98,650	98,450	97,950	96,310
efficiency tol.	%				

calculation of excitation losses					
field current	A	1 067,00	936,12	816,18	711,38
$Ip^2 * R$ (75°C)	kW	173,65	133,66	101,61	77,19
excitation losses	kW	15,88	13,02	10,72	8,87
brush losses (2V)	kW	2,13	1,87	1,63	1,42
total exc. losses	kW	191,66	148,55	113,96	87,48
R field at		20°C		75°C	
field resistance		0,12546 Ohm		0,15253 Ohm	

Date of test : **Nov. 2002**

	Efficiency	Page 69 / 74

Project :	Kraftverk Åbjøra	Order No :	42 585
Customer Order :		Serial No :	1 659 615
Test plan Pos.No:	QC3-42585-002	Type :	Ssv 377 / 12 – 270

Calculation of efficiency:

cos phi = **1,00**					
load	%	100,00	75,00	50,00	25,00
power	kVA	103 000,00	77 250,00	51 500,00	25 750,00
stator current	A	5 406,1	4 054,6	2 703,0	1 351,5
mechanical losses	kW	172,92	172,92	172,92	172,92
core losses	kW	211,92	211,92	211,92	211,92
bearing losses (related to generator)	kW	240,90	240,90	240,90	240,90
load losses	kW	276,62	155,60	69,16	17,29
total exc. losses	kW	129,69	103,47	84,54	73,03
total losses	kW	1 032,05	884,81	779,43	716,06
P out	kW	103 000,00	77 250,00	51 500,00	25 750,00
P in	kW	104 032,05	78 134,81	52 279,43	26 466,06
efficiency measured	%	**99,008**	**98,868**	**98,509**	**97,294**
efficiency gar.	%	98,840	98,660	98,210	96,720
efficiency tol.	%				

calculation of excitation losses					
field current	A	873,17	776,61	698,70	646,84
Ip^2 * R (75°C)	kW	116,29	91,99	74,46	63,81
excitation losses	kW	11,65	9,92	8,68	7,92
brush losses (2V)	kW	1,75	1,55	1,40	1,29
total exc. losses	kW	129,69	103,47	84,54	73,03
R field at		20°C		75°C	
field resistance		0,12546 Ohm		0,15253 Ohm	

Date of test : **Nov. 2002**

Turbine data from Åbjøra:

Gross head (nominal) = 445.3 m		
Turbine power MW	Water discharge m^3/s	Efficiency %
38.35	10.13	88.9
48.14	12.39	91.23
63.44	15.94	93.45
75.51	18.8	94.35
81.21	20.18	94.53
85.28	21.18	94.56
91.98	22.87	94.46
98.13	24.47	94.18

Gross head = 442.6 m		
Turbine power MW	Water discharge m^3/s	Efficiency %
38.81	10.18	88.95
48.7	12.46	91.26
64.17	16.03	93.46
76.36	18.89	94.35
82.12	20.28	94.53
86.24	21.29	94.56
93	22.98	94.45
99.21	24.59	94.17

Gross head = 439.2 m		
Turbine power MW	Water discharge m^3/s	Efficiency %
37.75	10.06	88.83
47.4	12.31	91.18
62.49	15.84	93.42
74.4	18.67	94.34
80.03	20.05	94.53
84.05	21.05	94.56
90.65	22.72	94.47
96.72	24.31	94.19

Input parameters

Parameter	Value
Waterway	
Nominal gross head	442 m
k_a (Total head loss coefficient K, waterway)	0.016335
Generator	
S_n (Nominal apparent power, generator)	103 MVA
V_n (Nominal voltage)	11 kV
R_f (Field winding resistance, 75℃)	0.15253 Ω
R_a (Armature winding resistance, 75℃)	0.003155 Ω
X_d (Synchronous reactance d-axis)	1.06 Pu
X_q (Synchronous reactance q-axis)	0.69 Pu
k_{ex} (excitation constant)	1.116
X'_d (Transient reactance)	0.15 Pu
X_l (Leakage reactance)	0.11 Pu
b_v (Air-gap reactance)	0.0018
n (generator OCC exponent)	9
C_n (Polynomial constant, OCC)	0.12
$I_{fd,n}$ (Nominal field current)	556 A
P_{FE}(Core losses)	0.21192 MW
P_V (windage and ventilation)	0.17292 MW
P_F (Bearing losses, generator)	0.24090 MW
Transformer	
Nominal transformer rating	103 MVA
P_0 (No-load losses)	0.0525 MW
P_k (Load losses)	0.225 MW

Appendix G

Hydropower specifications and parameters for Sundsbarm

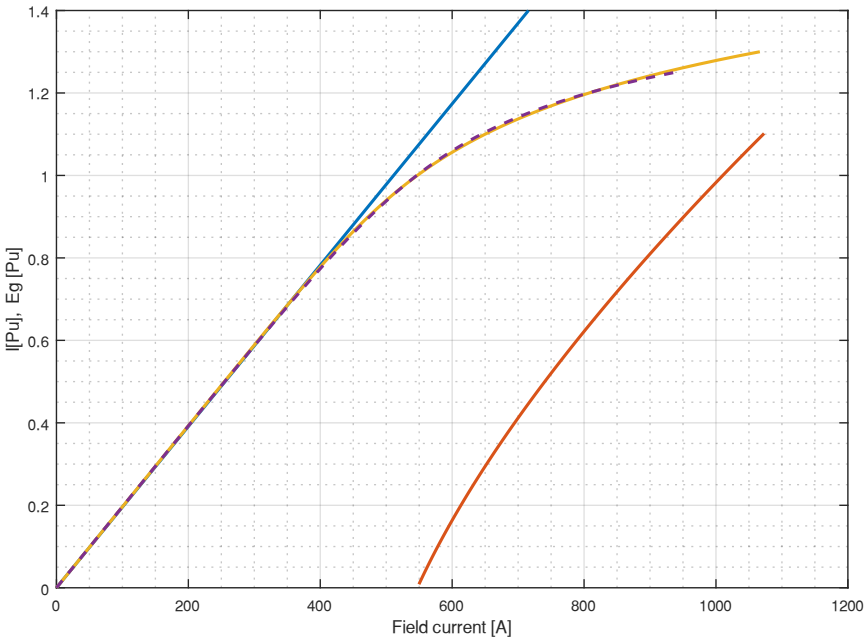

Characteristics of the generator in Sundsbarm: Open circuit characteristic (OCC), air-gap line and estimated field current relative to armature current (nominal terminal voltage).

Generator data from Sundsbarm (nominal)

$cos\varphi$ =0.85		
Load	%	100
Power	KVA	118 000
Stator current	A	4542.0
Mechanical losses	kW	537
Core losses	kW	353
Load losses	kW	333
Total excitation losses	kW	225
Total losses	kW	1450
P out	kW	100 300
P in	kW	101 750
Efficiency	**%**	**98.575**

Calculation of excitation losses		
Field current	A	1001
$I_{fd}^2 \cdot R(75℃)$ Loss	kW	205.45
Excitation and brush losses	kW	19.55
Total excitation losses	**kW**	**225**
R field at	20℃	75℃
Field resistance	0.20504 Ω	0.24857 Ω
Armature resistance	0.00322Ω	0.00390 Ω

Turbine data from Sundsbarm:

Gross head = 465.5 m		
Turbine power	Water discharge	Efficiency
MW	m^3/s	%
33.993	8.7741	85.832
47.048	11.643	89.527
55.854	13.575	91.156
68.021	16.259	92.688
76.869	18.236	93.389
86.809	20.5	93.813
97.158	22.94	93.83
105.24	24.92	93.563

Gross head = 473.7 m		
Turbine power	Water discharge	Efficiency
MW	m^3/s	%
35.177	8.9043	86.024
48.65	11.815	89.664
57.735	13.775	91.267
70.284	16.497	92.77
79.408	18.502	93.454
89.655	20.799	93.862
100.32	23.273	93.865
108.64	25.277	93.593

Gross head (nominal) = 493 m		
Turbine power	Water discharge	Efficiency
MW	m^3/s	%
38.005	9.2073	86.366
52.475	12.215	89.885
62.226	14.24	91.43
75.686	17.052	92.87
85.465	19.122	93.516
96.44	21.493	93.886
107.87	24.046	93.862
116.79	26.114	93.58

Input parameters

Parameter	Value
Waterway	
Nominal gross head	490 m
k_a (Total head loss coefficient K, waterway)	0.00893
Generator	
S_n (Nominal apparent power, generator)	118 MVA
V_n (Nominal voltage)	15 kV
R_f (Field winding resistance, 75℃)	0.24857 Ω
R_a (Armature winding resistance, 75℃)	0.00396 Ω
X_d (Synchronous reactance d-axis)	1.13 Pu
X_q (Synchronous reactance q-axis)	0.61 Pu
k_{ex} (excitation constant)	1.1
X'_d (Transient reactance)	0.29 Pu
X_l (Leakage reactance)	0.12 Pu
b_v (Air-gap reactance)	0.00196
n (generator OCC exponent)	9
C_n (Polynomial constant, OCC)	0.075
$I_{fd,n}$ (Nominal field current)	509 A
P_{FE}(Core losses)	0.353 MW
P_V (windage, ventilation and bearing)	0.537 MW
Transformer	
Nominal transformer rating	118 MVA
P_0 (No-load losses)	0.1484 MW
P_k (Load losses)	0.2814 MW

Appendix H

DATA FORMATTING:

The procedure for formatting the data is performed in excel and described in four steps where the original data set will be gradually improved until the finished format in step four.

- Step 1: Convert the data set from "NaN" values to numbers.
- Step 2: Add data (assumed) points at locations with no numbers (only the first few days).
- Step 3: Convert data from 1-hour resolution to 15-minute semi-resolution to improve the accuracy in start/stop regions.
- Step 4: Estimate the data in the 15-minute semi resolution.

1. In the data set, there are originally numerous cells with "NaN", which says that there is no change in value relative to the previous cell. This "NaN" value must be replaced with actual values in order to do the calculation. The procedure to convert the data set is as follows:

   I. Converts all "NaN" values with a unique constant like "999999"

   II. Use the excel command for all cells for $A_{old} \in$ (1,n):

   =If(A_{old} <999999; A_{old}; $A_{new,i-1}$)

   where A_{old} is a value (P,Q or V) at row (1 - n), and $A_{new,i-1}$ is the previously calculated value (0 – n-1) illustrated in the table below. The method requires an initial value, namely $A_{new,0} = A_{old,0}$.

$A_{old,0}$	$A_{new,0}$
$A_{old,1}$	$A_{new,1}$
$A_{old,2}$	$A_{new,2}$
$A_{old,3}$	$A_{new,3}$

   Exception for Åbjøra HPU: NaN is used differently where:

   - Active power (P) and reactive power (Q): NaN = 0
   - Voltage (V): NaN = 0 or 11 kV.

   With these findings, one could determine if the NaN at the voltage should equal 0 or 11 by comparing the with the active power (P). The excel command will therefore be:

   $$V_{new,i} = IF(AND(V_i = 9999; P_i > 0); 11; IF(V_i < 11; V_i; 0))$$

where $V_{new,i}$ is a new column for the filtered voltage column, V_i is the original voltage column, where NaN is first replaced with a random value like 9999 in order for performic the numeric command, P_i is the column for active power (P) and 11 is representing the nominal voltage 11 kV.

2. Corrected for logical errors where it seems like the generator have multiple start/stop sequences between two stable regions, and these regions will be set to zero. A stable region is regarded as a region where the voltage is above a trigger point or a voltage that is considered close to "normal".

   I. The table will be corrected for logical errors where it seems like the generator have multiple start/stop operations during few hours, as shown below:

i	Voltage [kV] $V_{i,old}$	Voltage [kV] $V_{i,new}$
1	14.3	14.3
2	14.4	14.4
3	6.4	6.4
4	6.4	0
5	6.4	6.4
6	14.3	14.3

   The generator will be regarded as disconnected (off) when the voltages close to the measurement are substantially lower than the rated voltage. The excel command for this correction is as follows:

$$V_{i,new} = IF(AND(V_{i-1,old} < V_{trig}; V_{i,old} < V_{trig}; V_{i+1,old} < V_{trig};); 0; V_{i,old}$$

   where V_x is the cell number (voltage) and V_{trig} is the minimum voltage recognised as a possible non-operation situation. For the active power (P) and reactive power (Q), the command is quite simple:

$$X_i = IF(\$A_i = 0; 0; X_i)$$

   which states that P or Q (X_i) shall be 0 if the voltage (V_i) is zero, else P or Q shall remain unchanged.

3. Since each value in the data set is an average value measured over one hour, there are unrealistically low measurements. An example could be a voltage measurement of 5 kV (average) occurring at a generator with a nominal voltage of 10 kV. The actual situation would probably be 10 kV for the first 30 minutes and then 0 kV for the next 30 minutes, giving an average of 5 kV.

   In order to have a compatible data set with the MATLAB program, each time step must have the same length. Thereby, it will be created a new column where each data point is used four times, i.e., time steps of 15 minutes.

   I. A new row will be created. This will be used for counting each value four times.

Cell nr.	C
1	1
2	1
...	...
4	1

5	$= C_1$+1
...	...
n	$= C_{n-4}$+1

II. With the help of the counting row previously made, and the following excel command, copy the value in column "A" and paste the same value in four rows in the "B" column, shown in the table below. (A and B are just cells representing old values of P,Q and V, se table below).

$$B_j = INDIRECT(\text{"A"} \,\&\, \$C_i)$$

The "INDIRECT" function will create a value in B_j equal to A_i, where "A" is nothing more than the column name in excel and C_i the number in counting row. The first C_i will be 1,1,1,1,2,2,2,2,3…n, as shown in the table below. The number of data rows in data set (1 hour) created in (3,I), have a length of $n = 8746$, and the new data set (15 minutes resolution) will have a length $m = 4 \cdot n$.

Data set (1 hour)	Data set (15 minutes)	Counting row
A	B	C
$A_{old,1}$	$A_{new,1}$	1
$A_{old,2}$	...	...
$A_{old,3}$	$A_{new,1}$	1
$A_{old,4}$	$A_{new,2}$	2
$A_{old,5}$	...	...
$A_{old,6}$	$A_{new,2}$	2
...	...	...
$A_{old,n}$	$A_{new,m}$	n

4. From the table with 15 minutes resolution, there will be added two additional columns. These columns will be used to determine how many of the four (15 minutes) operations that will be used.

I. The first column represents the probable duration of an operation (0-1) given by the voltage ratio:

$$duration = \frac{V_i}{V_{normal}}$$

where V_i is the operating voltage and V_{normal} is the voltage with a high probability of occurrence (14.6 kV for Sundsbarm).

II. The second column is only a repetitive pattern named "REP" and is as follows [0.25 0.50 0.75 1.00 0.25 ...]. The column is used in combination with the duration (4, I) to determine the number of operations (1-4) to be used.

III. The final step is to apply the "Duration" and "Rep" columns into the table from (3, II).

The full table will look like:

V [kV]	P [MW]	Q [MVAr]	Duration [%]	Rep	V_{final}	P_{final}	Q_{final}
$A1$	$A2$	$A3$	D	E	AA	BB	CC
14.6	102.0	18.1	1	0.25	14.6	102.0	18.1
14.6	102.0	18.1	1	0.50	14.6	102.0	18.1
14.6	102.0	18.1	1	0.75	14.6	102.0	18.1
14.6	102.0	18.1	1	1.00	14.6	102.0	18.1
8.0	101.5	15.0	0.5	0.25	14.6	101.5	15.0
8.0	101.5	15.0	0.5	0.50	14.6	101.5	15.0
8.0	101.5	15.0	0.5	0.25	0	0	0
8.0	101.5	15.0	0.5	0.50	0	0	0

From the table above, the final table will be created with this excel command:

$$X_{var,i} = IF\Big(D_i > 0.75; X_i; IF\Big(OR\Big(AND\big(D_i = 0.5; E_i < 0.75; AND(D_i < 0.75; D_i > 0.5; E_i < 1)\big); X_i; IF(AND(D_i > 0.25; E_i < 0.5; E_i < 0.75); X_i; IF(OR(D_i < 0.25; D_i = 0.25); 0; 0)\Big)\Big)\Big)$$

$$AA_i = IF\Big(AND\big(X_{var,i} < V_{trig}; X_{var,i} > 0\big); V_{trig}; IF\Big(X_{var,i} = 0; 0; IF\big(OR\big(X_{var,i} = V_{trig}; X_{var,i} > V_{trig}\big); X_{var,i}; 0\big)\Big)\Big)$$

$$BB_i = IF\Big(D_i = 1; X_{var,i}; IF\Big(AND\big(D_i < 1; X_{var,i} = P_{trig,max}; X_{var,i} > P_{trig,max}\big); X_{var,i}; IF\Big(AND\big(D_i < 1; X_{var,i} > P_{trig,min}; X_{var,i} < P_{trig,max}\big); P_{trig,max}; IF\big(OR\big(X_{var,i} < P_{trig,min}; X_{var,i} = P_{trig,min}\big); 0; 0\big)\Big)\Big)\Big)$$

$$CC_i = X_{var,i}$$

where $X_{var,i}$ is a variable to determine the value based on the duration, used here to make the command more readable (and used directly for reactive power), $X_i \in [A_i, B_i, C_i]$, V_{trig} is the minimum voltage recognised as a possible non-operation situation (used in (3, I), AA_i, BB_i, CC_i are column vectors for voltage (V), active power (P) and reactive power (Q), respectfully, $P_{trig,max}$ is the assumed active power for all operations where $D_i < 1$ and P is in the range between $P_{trig,max}$ and $P_{trig,min}$, and $P_{trig,min}$ is the absolute minimum active power any operation can be. In addition, the reactive power will may result in

values different from zero when both P and V are zero. This was solved by setting Q = 0 if P = 0.

Explained in short:

- If the voltage is above trigger voltage, then the V, P and Q will be on for 4 periods (60 min), and all values remains the same.
- If the voltage is under trigger voltage, then the duration will determine the period for which V, P and Q are on. The voltage will also be set to the trigger voltage for the "on" period.
  - If active power P is below min trigger P, then P = 0.
  - If active power P is above min trigger P and below Max trigger P, then P = max trigger P.
  - If active power P is above max trigger P, then P = P (old)
- Q will always be set to the original value, but will be zero for all periods where P is zero.

To summarise, the assumed values for Åbjøra and Sundsbarm are:

	Normal voltage	Trigger voltage	Max trigger P	Min trigger P
Åbjøra	11	10	45	20
Sundsbarm	14.6	14.4	75	20

Appendix I

Additional results from Åbjøra

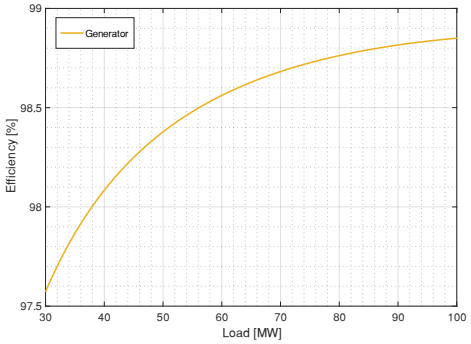

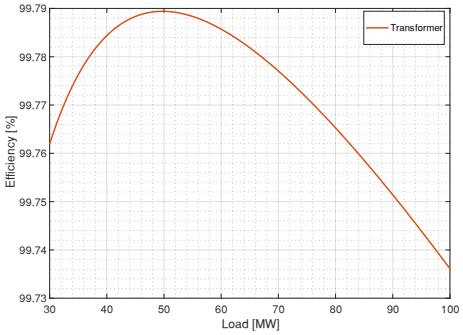

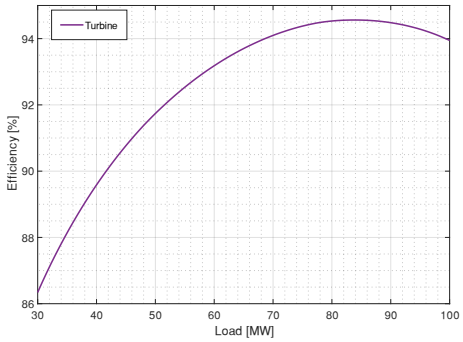

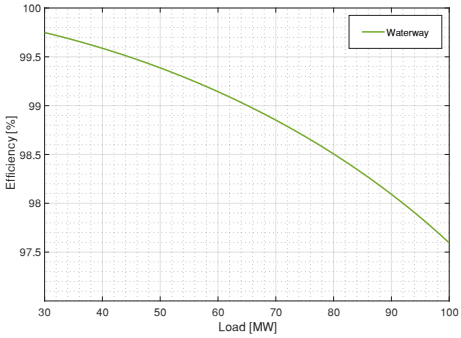

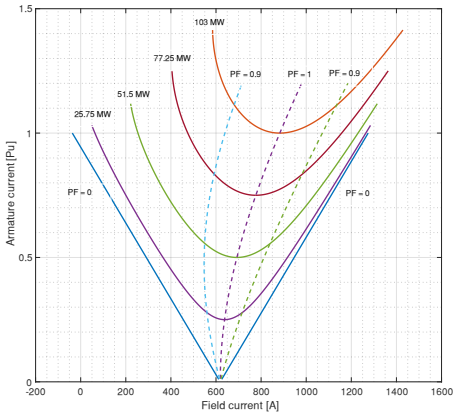

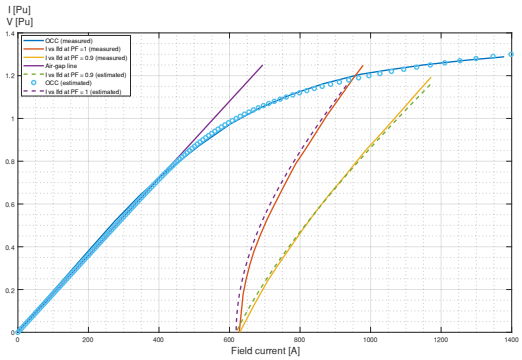

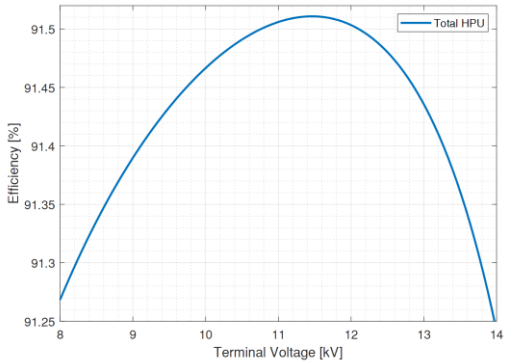
Total HPU
91.5
91.45
91.4
91.35
91.3
91.25
Efficiency [%]
8
9
10
11
12
13
14
Terminal Voltage [kV]

Appendix J

Additional results from Sundsbarm

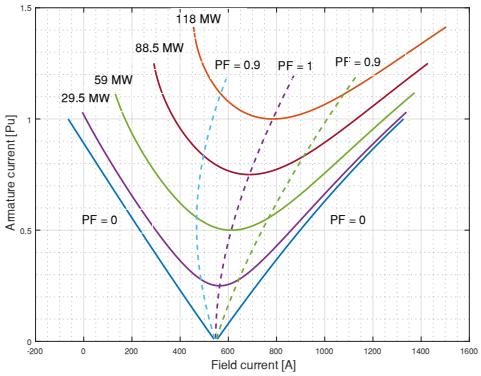

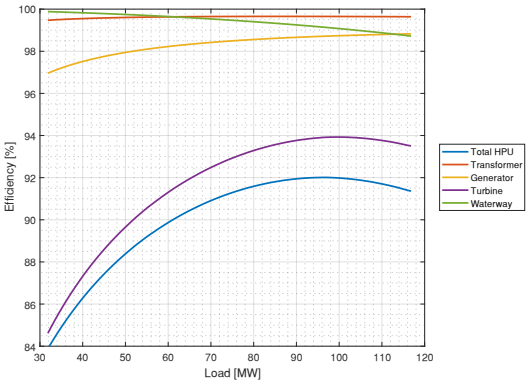

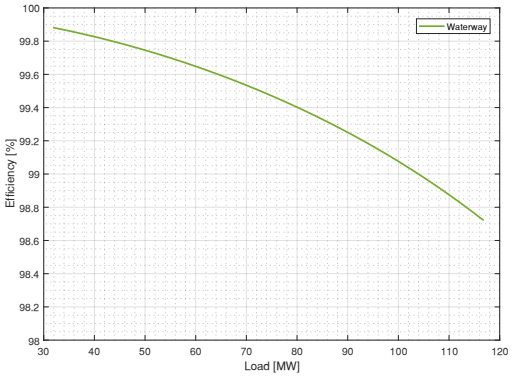

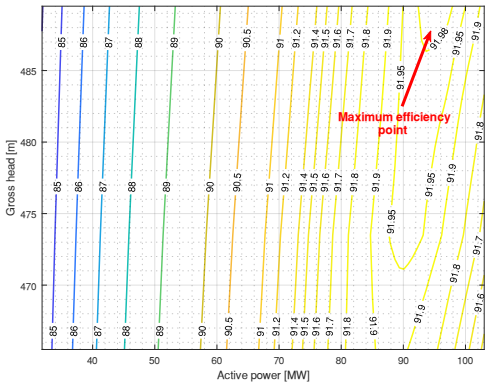

Efficiency mapping of the entire HPU

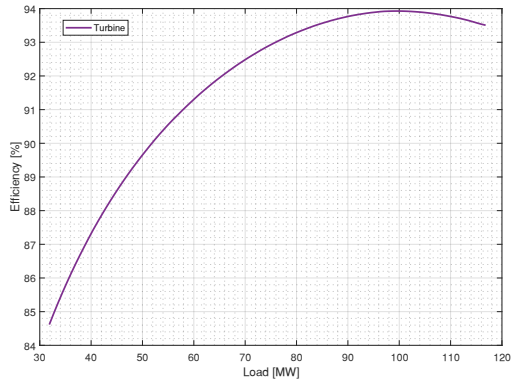

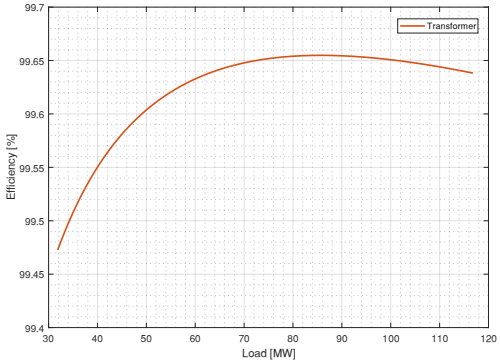

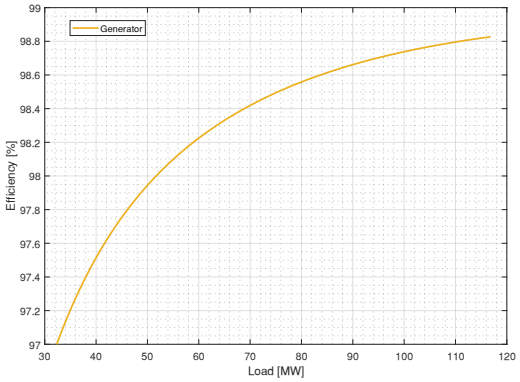

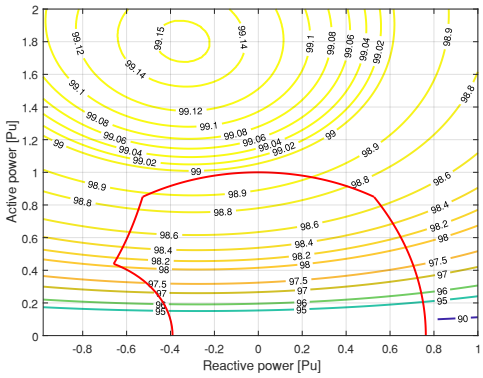

Efficiency mapping of the generator in Sundsbarm

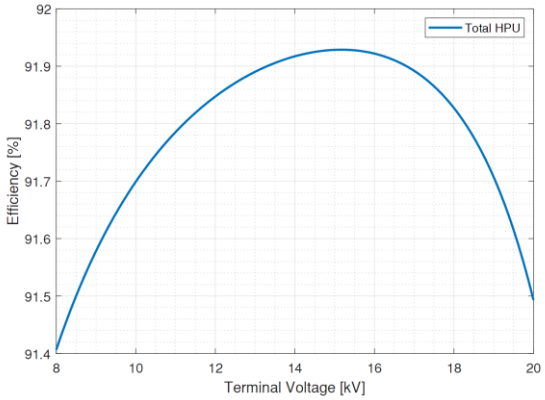

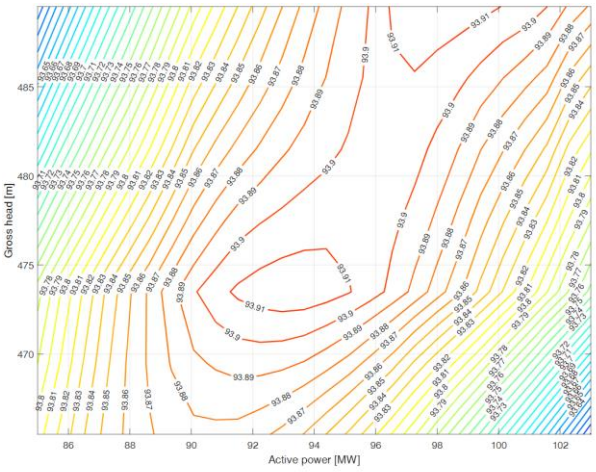

Efficiency mapping of the Francis turbine in Sundsbarm

Appendix K

Function description for the MATLAB program.

PQ_diagram function:	
Description:	This function pots the PQ-diagram with: - Armature current limit - Field current limit - Generator maximum power (active power limit) - Practical stability limit - Minimum field current limit Assumptions: - Practical stability is assumed to start where operational, and armature field current intersects and ends where practical stability limit crosses the minimum field current limit. - The minimum field current is calculated with a minimum excitation voltage assumed to be $E_{min} = k_{min} \cdot E_{max}$, where $k_{min,nom} = 0.3$. (k_{min} is usually between 0-0.3) The variable fig_n is only used to combine the PQ diagram to other figures.
Input parameters	
PF, Xq, Xd, fig_n	

PQ_diagram function:	
Description:	This function pots the PQ-diagram with: - Armature current limit - Field current limit - Turbine maximum operational limit - Practical stability limit - Minimum field current limit Assumptions: - Turbine maximum operational limit = nominal active power of the generator. - Practical stability is assumed to start where operational, and armature field current intersects and ends where practical stability limit crosses the minimum field current limit. - The minimum field current is calculated with a minimum excitation voltage assumed to be $E_{min} = k_{min} \cdot E_{max}$, where $k_{min,nom} = 0.3$. (k_{min} is usually between 0-0.3)
Input parameters	
PF, Xq, Xd	

Data function:			
Description:	Collect data from an excel file, and all input variables must have the same length. There is an additional feature in the function that remove all data points where the active power P is zero. This is done to eliminate zero division and would not influence the program in any practical manner.		
Input variables			
Active power P [MW]	Reactive power Q[MVAr]	Voltage [kV]	System Price [NOK/MWh]
Output variables			
Active power P [MW]	Reactive power Q[MVAr]	Voltage [kV]	System Price [NOK/MWh]

HPU function:	
Description:	The function calulates power losses and efficienies in the HPU, which are determined by the input variables. Input variables could be given as a single value or as a vector. The HPU function uses the "Field current" function to estimate the field current. In addtion, function named "Turbine" which is a 2D interpolation funciton.
Input parameters	
Generator: Sn, Vn, Xq, Xd, Ra, Rf, k_ex, P_FE, P_V, P_F, bv, Xd_tran, X_leak, n_OCC, C_OCC, Ifd_n **Waterway:** k_a **Turbine:** Tur_P0, Tur_N0 **Transformer:** P0_Tran, Pk_Tran, Sn_Tran	
Input variables	
Generator: P [MW], Q [MVAr], V [kV] **Waterway:** Head_gross [m]	
Output variables (Efficiency (N) and Power loss (Ploss [MW])	
Total HPU: Ploss_tot, Total_N **Transformer:** Tran_N, Ploss_Tran **Generator:** Gen_N, Ploss_Gen **Turbine:** Tur_N, Ploss_Tur **Waterway:** Water_N, Ploss_Water	

Field current function:	
Description:	Determines the field current in the generator based on OCC.
Input parameters	
Sn, Vn, Ra, Xq, Xd**,** bv, Xd_tran, X_leak, n_OCC, C_OCC, Ifd_n	
Input variables	
P [MW], Q [MVAr], V [kV]	
Output variables	
Ifd [kA]	

PQ_diagram function:	
Description:	This function pots the PQ-diagram with: - Armature current limit - Field current limit - Generator maximum power (active power limit) - Practical stability limit - Minimum field current limit Assumptions: - Practical stability is assumed to start where operational, and armature field current intersects and ends where practical stability limit crosses the minimum field current limit. - The minimum field current is calculated with a minimum excitation voltage assumed to be $E_{min} = k_{min} \cdot E_{max}$, where $k_{min,nom} = 0.3$. (k_{min} is usually between 0-0.3) The variable fig_n is only used to combine the PQ diagram to other figures.
Input parameters	
PF, Xq, Xd, fig_n	

Symbol	MATLAB	Description
Waterway		
K	k_a	The total head loss coefficient
H_{gross}	Head_gross	Gross head (total water head) [m]
Turbine		
$P_{turbine,i}$	Tur_P0	A vector representing the output power of the turbine [MW]
$\eta_{turbine,i}$	Tur_N0	A vector representing the efficiency to the turbine at a given power [%]
Generator		
S_n	Sn	Nominal apparent power [MVA]
V_n	Vn	Nominal voltage [kV]
$cos\varphi$	PF	Nominal power factor
X_q	Xq	Synchronous reactance q to the machine [Pu]
X_d	Xd	Synchronous reactance d to the machine [Pu]
R_a	Ra	Armature winding resistance per phase [Ω]
R_{fd}	Rf	Field winding resistance [Ω]
X_{ad}	Xad	Equivalent inductance between excitation voltage and field current [Pu]
k_{ex}	k_ex	Additional excitation loss factor, proportional to field winding losses
P_{FE}	P_FE	Magnetization (iron) loss [MW]
P_V	P_V	Ventilation and windage loss [MW]
P_F	P_F	Friction loss in bearing and brushes [MW]
Transformer		
P_0	P0_Tran	Magnetization (iron) loss [MW]
P_k	Pk_Tran	Short circuit loss [MW]
$S_{n,tran}$	Sn_Tran	Nominal apparent power [MVA]

Appendix L

MATLAB codes:

Hydropower (HPU) model:

```
function
[Ploss_tot,Total_N,Tran_N,Ploss_Tran,Gen_N,Ploss_Gen,Tur_N,Ploss_Tur,Water_N,Ploss_Water,Q_flo
w_h] = HPU(P,Q,V,Sn,Vn,Xq,Xd,Ra,Rf,k_ex,P_FE,P_V,P_F,bv, Xd_tran, X_leak, n_OCC, C_OCC, Ifd_n,
Head_gross,k_a, Tur_P0,Tur_N0,Head0, P0_Tran,Pk_Tran,Sn_Tran)
        % Transformer Model:
        P_Tran = P; %Input power
        Ploss_Tran = P0_Tran + Pk_Tran.*(P_Tran./Sn_Tran).^2;
        Tran_N = P./(P + Ploss_Tran);

        % Generator Model:
        P_G = P./Tran_N;
        Q_G = Q;
        % Load dependent losses (ohmic losses)
        Ia = sqrt(P_G.^2+Q.^2)./(sqrt(3).*V);                          %[kA]
        Ifd = Field_current(P, Q, V, Sn, Vn, Ra, Xq, Xd, bv, Xd_tran, X_leak, n_OCC, C_OCC,
Ifd_n);   %[kA]
        P_S = 3*Ia.^2*Ra;                       % Stator loss          %[MW]
        P_R = real(k_ex*Ifd.^2*Rf);             % Rotor loss           %[MW]
        Ploss_Gen = P_S + P_R + P_FE + P_V + P_F;
        Gen_N = P_G./(P_G+Ploss_Gen);


        % Turbine Model:
        P_Tur = P./(Tran_N.*Gen_N);
        if Head0 == 0   %Simplified method (1D interpolation)
            Tur_N = interp1(Tur_P0,Tur_N0,P_Tur, 'spline')/100;
            Ploss_Tur = P.*(1-Tur_N);
        else            %Advanced method (2D interpolation)
            % Sort the given heads, load and efficeincy:
            len_P00 = length(Tur_P0(1,:));
            % Place all data points of power in one vector
            P0_Tur(1,1:len_P00) = Tur_P0(1,:);
            P0_Tur(1,len_P00+1:2*len_P00) = Tur_P0(2,:);
            P0_Tur(1,2*len_P00+1:3*len_P00) = Tur_P0(3,:);
            P0_Tur = P0_Tur.';
            % Create a matrix (3 X length_P00) of all heads
            H0_Tur = ([linspace(Head0(1),Head0(1),len_P00),
linspace(Head0(2),Head0(2),len_P00), linspace(Head0(3),Head0(3),len_P00)]).';

            N0_Tur(1,1:len_P00) = Tur_N0(1,:);
            % Place all data points of efficiency in one vector
            N0_Tur(1,len_P00+1:2*len_P00) = Tur_N0(2,:);
            N0_Tur(1,2*len_P00+1:3*len_P00) = Tur_N0(3,:);
            N0_Tur = N0_Tur.';
            % Collect Turbine efficiency "Tur_N". Hm and Pm represents head and
            % loading matrix (meshgrid) which can be used to plot turbine efficiency
            [Tur_N, Hm, Pm] = Turbine(Head_gross, P_Tur, P0_Tur,H0_Tur,N0_Tur);
            Ploss_Tur = P.*(1-Tur_N);
        end

        % Waterway Model:
        P_W = P./(Tran_N.*Gen_N.*Tur_N);
        Water_N = zeros(length(Head_gross),length(P));

        % Estimate flow rate:
        for i = 1:length(P_W)
            Value = roots([k_a, 0, -Head_gross, (P_W(i)*10^6)/(1000*9.81)]);
            for n = 1:3
                Qest = (Sn*10^6)/(10000*Head_gross);    %Predicting ca. flow rate
                if Value(n)<=2*Qest && Value(n)>=0
                   Qflow(i,1) = Value(n);
```

```
                end
            end
        end
        Q_flow_h = Qflow;
        Ploss_Water = k_a*1000*9.81*Qflow.^3*(1/10^6);
        Water_N = P_W./(P_W+Ploss_Water);

        % Total Plant efficiency and loss:
        Ploss_tot = Ploss_Tran + Ploss_Gen + Ploss_Tur + Ploss_Water;
        Total_N = P./(P+Ploss_tot);
end
```

Field current with saturation:

```
function [Ifd] = Field_current(P, Q, V, Sn, Vn, Ra, Xq, Xd, bv, Xd_tran, X_leak, n_OCC, C_OCC,
Ifd_n)

P = P/Sn;              %Convert to Pu values
Q = Q/Sn;
V = V/Vn;
Zb = Vn^2/Sn;                  %Base impedance
Ra = Ra/Zb;                    %Pu
I = sqrt(P.^2+Q.^2)./V;        %Pu

for n = 1:length(I)
    if Q(n) >= 0
        phi(n,1) = acos(P(n)./(V(n).*I(n)));
    elseif Q(n) < 0
        phi(n,1) = -acos(P(n)./(V(n).*I(n)));
    end
end
% Unsaturation
delta = atan((Xq.*I.*cos(phi)-Ra*I.*sin(phi))./(V+Ra.*I.*cos(phi)+Xq.*I.*sin(phi)));
Eg = V.*cos(delta) + Ra.*I.*cos(phi+delta) + Xd.*I.*sin(phi+delta);
I_FU = Eg/bv;
% Saturation
Xp = X_leak + 0.63*(Xd_tran-X_leak);
delta_p = atan((Xp.*I.*cos(phi)-Ra.*I.*sin(phi))./(V+Ra.*I.*cos(phi)+Xp.*I.*sin(phi)));
Ep = V.*cos(delta_p) + Ra.*I.*cos(phi+delta_p) + Xp.*I.*sin(phi+delta_p);
IF_p = Ifd_n*(Ep+C_OCC.*Ep.^n_OCC);

I_FS = IF_p - Ep/bv;
Ifd = I_FS + I_FU;    %[A]
Ifd = Ifd/1000;       %[kA]
end
```

2D interpolation function for turbine:

```
function [Tur_N, Hm, Pm] = Turbine(Head_gross, P_Tur, P0_Tur,H0_Tur,N0_Tur)
    % A function to ensure no equal numbers due to the function "Griddata"
    for i = 1:length(N0_Tur)-1
        for k = 1:length(N0_Tur)
            if N0_Tur(i) == N0_Tur(k)
                N0_Tur(i) = N0_Tur(i)+k*0.000001;
            end
        end
    end
      [Hm,Pm] = meshgrid(Head_gross, P_Tur);
      Tur_N = griddata(H0_Tur,P0_Tur,N0_Tur,Hm,Pm);
      Tur_N = Tur_N/100;
      % Alternative method (extrapolation included, but not as accurate within measurements)
      %F = scatteredInterpolant(H0_Tur,P0_Tur,N0_Tur,'linear','nearest');
      %Tur_N = F(Hm,Pm);

end
```

Function used to collect data from Excel file:

```
function [P_data, Q_data, V_data, Sys_Price] = Data(data_file)
    Q_data0 = data_file(:,2);
    P_data0 = data_file(:,1);
    P_data = round(P_data0,3);                  %(MW)
    Q_data = round(Q_data0,3);                  %(MVAR)
    Sys_Price = data_file(:,4);                 %(Nok/MWh)
    V_data = data_file(:,3);                    %(kV)

    % In order to eliminate zero-division and unrealistic low average
    % values when HPU is turned off. All data points where P = 0 is neglected
     m = 1;
    for i = 1:length(P_data)
        if P_data(m) <= 10
           P_data(m)    = [];        %Here, all values under 10 MW are neglected
           Q_data(m)    = [];
           V_data(m)    = [];
           Sys_Price(m) = [];
           m = m;
        else
            m = m+1;
        end
    end
end
```

Function for drawing PQ diagram:

```
function [] = PQ_diagram(PF,Xq,Xd,fig_n)
% This function is used to draw the PQ (capability) diagram of the
% generator. The PQ diagram consist of Armature limit, Rotor limit,
% Active power limit, Practical stability limit(PSL) and end region heating
% limit/(minimum field current limit).

% This function assumes PSL to intersect the end of active power limit and
% minimum field current limit.

%Nominal values:
Sn = 1;
I = 1;
V = 1;
phi = acos(PF);
k_min = 0.3;        % E_qmin = k_min*E_qmax, where k_min is usally between 0-0.3


% Armature limit:
delta_arm = linspace(pi-atan((Sn*cos(phi))/(Sn*sin(phi))), atan((Sn*cos(phi))/(Sn*sin(phi))),
100);
Q_a = Sn*cos(delta_arm) + 0;
P_a = Sn*sin(delta_arm) + 0;

% Active power limit:
Max_Q = [-Sn*sin(phi), Sn*sin(phi)];
Max_P = [Sn*cos(phi), Sn*cos(phi)];

% Field current limit:
%   Nominel values
Ax = V^2/Xq;
Bx = V^2/Xd;
delta_n = atan((Sn*cos(phi))/(Sn*sin(phi)+Ax)); % Nominel field limit anlge
En = V*cos(delta_n)+Xd*I.*sin(phi+delta_n);     % Nominel excitation voltage

%   Maximum Field current liimit:
E_qmax = sqrt((V+I*Xd*sin(phi))^2+(I*Xd*cos(phi))^2);
% Finding the the intersection between Field limit and Armature limit:
delta_field_max0 = 0;
for k = 1:10000
    r = E_qmax*V/Xd;
    center = -V^2/Xd;
    % Simplified method:
    Q_fs_max = r*cos(delta_field_max0) + center;
    P_fs_max = r*sin(delta_field_max0) + 0;
    %P_fs_max =((E_qmax*V)./Xd)*sin(delta_field_max0)+V^2/2*(Xd-
Xq)/(Xd*Xq)*sin(2*delta_field_max0);
    %Q_fs_max =((E_qmax*V)./Xd)*cos(delta_field_max0)+V^2*(Xd-
Xq)/(Xd*Xq)*(cos(delta_field_max0)).^2-V^2/Xq;


    if (P_fs_max <= (Sn*cos(phi)+0.001) &&  P_fs_max >= (Sn*cos(phi)-0.001))&& (Q_fs_max <=
(Sn*sin(phi)+0.001) &&  Q_fs_max >= (Sn*sin(phi)-0.001))
        delta_field_max = delta_field_max0;
        break
    end
     delta_field_max0 = k/10000;
end

r = E_qmax*V/Xd;
center = -V^2/Xd;
delta_field_max = linspace(delta_field_max, 0, 100);
Q_fs_max = r*cos(delta_field_max) + center;
P_fs_max = r*sin(delta_field_max) + 0;
%P_fs_max =((E_qmax*V)./Xd)*sin(delta_field_max)+V^2/2*(Xd-Xq)/(Xd*Xq)*sin(2*delta_field_max);
%Q_fs_max =((E_qmax*V)./Xd)*cos(delta_field_max)+V^2*(Xd-
Xq)/(Xd*Xq)*(cos(delta_field_max)).^2-V^2/Xq;

% Finding the practical stability constant "C" and max excitation voltage E
PSL_C = 0;
for C = 0:0.001:1
    for E = 0:0.001:2
        k = (E.*V)./Xd;
```

```
        a = 1/2*(Xd-Xq)./(Xd*Xq)*V^2;    % Constant
        d = 2*a;                         % Constant
        Q0 = -V^2/Xq;                    % Constant
        P_PSL = (sqrt(2)*sqrt(k.*sqrt(k.^2+8*d^2)+4*d^2-
k.^2).*(sqrt(k.^2+8*d^2)+3*k))./(16*d); % Practical stability limit (P)
        Q_PSL = (k.*sqrt(k.^2+8*d^2)+4*d^2+8*d*Q0-k.^2)/(8*d)+C;
% Practical stability limit (Q)
        if round(P_PSL,3) == round(Sn*cos(phi),3) && round(Q_PSL,3) == -(round(Sn*sin(phi),3))
            PSL_C = C;
            E_max = E;
            break
        end
    end
    if PSL_C ~= 0
        break
    end
end

%Finding the minimum excitation voltage
E_min = 0;
for E = 0:0.001:2
    k = (E.*V)./Xd;
    a = 1/2*(Xd-Xq)./(Xd*Xq)*V^2;
    d = 2*a;
    Q0 = -V^2/Xq;
    P_PSL_min = (sqrt(2)*sqrt(k.*sqrt(k.^2+8*d^2)+4*d^2-
k.^2).*(sqrt(k.^2+8*d^2)+3*k))./(16*d);
    Q_PSL_min = (k.*sqrt(k.^2+8*d^2)+4*d^2+8*d*Q0-k.^2)/(8*d)+PSL_C;
    % minimum field current:
    for delta_field_min0 = 0:0.0001:pi
        E_qmin = k_min*E_qmax;            % k_min is usally between 0-0.3
        P_fs_min =((E_qmin*V)./Xd)*sin(delta_field_min0)+V^2/2*(Xd-
Xq)/(Xd*Xq)*sin(2*delta_field_min0);
        Q_fs_min =((E_qmin*V)./Xd)*cos(delta_field_min0)+V^2*(Xd-
Xq)/(Xd*Xq)*(cos(delta_field_min0)).^2-V^2/Xq;

        % Fining when minimum field current is equal to practical stability
        % limit
        if round(P_PSL_min,3) == round(P_fs_min,3) && round(Q_PSL_min,3) ==
(round(Q_fs_min,3))
            E_min = E;
            delta_field_min = delta_field_min0;
            break
        end
    end
    if E_min ~= 0
        break
    end
end
% Recalucate minimum field current (with practical stability limit)
E_qmin = 0.3*E_qmax;
d_min = linspace(delta_field_min,0,20);
P_fs_min =((E_qmin*V)./Xd)*sin(d_min)+V^2/2*(Xd-Xq)/(Xd*Xq)*sin(2*d_min);
Q_fs_min =((E_qmin*V)./Xd)*cos(d_min)+V^2*(Xd-Xq)/(Xd*Xq)*(cos(d_min)).^2-V^2/Xq;
%########   Recalculating Practical limit   ######
m_PSL = 1;
for E_PSL = linspace(E_min,E_max,20)
        k = (E_PSL.*V)./Xd;
        a = 1/2*(Xd-Xq)./(Xd*Xq)*V^2;
        d = 2*a;
        Q0 = -V^2/Xq;
        P_PSL(m_PSL) = (sqrt(2)*sqrt(k.*sqrt(k.^2+8*d^2)+4*d^2-
k.^2).*(sqrt(k.^2+8*d^2)+3*k))./(16*d);
        Q_PSL(m_PSL) = (k.*sqrt(k.^2+8*d^2)+4*d^2+8*d*Q0-k.^2)/(8*d)+PSL_C;
        m_PSL = m_PSL + 1;
end

figure(fig_n)
plot(Q_a,P_a,'Color','r','LineWidth',2.0)
hold('on')
plot(Max_Q,Max_P,'--','Color','r','LineWidth',2.0)
hold('on')
plot(Q_fs_max,P_fs_max,'Color','r','LineWidth',2.0)
hold('on')
```

```
plot(Q_fs_min,P_fs_min,'Color','r','LineWidth',2.0)
hold('on')
plot(Q_PSL,P_PSL,'Color','r','LineWidth',2.0)
hold('on')
xlabel('Reactive power [Pu]');
ylabel('Active power [Pu]');
grid('on')
hold off
end
```

The MATLAB program for Åbjøra HPU:

```
%**********************************************************************
% Author: Sigurd Berg
% Date: 16/05/2021

% This program calculates the efficiency and energy losses
% of a Hydropower unit (HPU), with numerous plots for analysing purposes.

% Credit to "Josè Manuel Amigo" which is the author of the function named:
% densityscatter()
% https://www.mathworks.com/matlabcentral/fileexchange/65024-densityscatter



%**********************************************************************
clear;
clc;

% Read off data points from data file:
data_file = readmatrix('Abjora_OD.xlsx');
[P_data, Q_data, V_data, Sys_Price] = Data(data_file);

% Generator Parapeters:
Sn = 103;           %[MVA]
Vn = 11;            %[kV]
PF = 0.9;           %Power factor
Xq = 0.69;          % [Pu]
Xd = 1.06;          % [Pu]
Ra = 0.003155;      % [ohm] armature winding resistance
Rf = 0.15253;       % [ohm] field winding resistance
k_ex = 1.116;       % excitation constant (typical value around 1.1)
P_FE = 0.21192;     % [MW] Iron loss
P_V = 0.17292;      % [MW] Windage and ventilation loss
P_F = 0.2409;       % [MW] Friciton loss in bearing and brushes
Xd_tran = 0.15;     % Transient D_axis reactance [Pu]
X_leak = 0.11;      % Leakage reactance [Pu]
bv = 1.25/694.2;    % Air-gap line: Voltage/field current
n_OCC = 9;          % Exponent to OCC
C_OCC = 0.12;       % Constant to OCC
Ifd_n = 556;        % Nominal field current

% Waterway Parameters:
k_a = 0.016335;                 % Waterway constant
Head_gross = 442.6;               % Important: must be within what is given for turbine (only
for advanced turbine method)
%Head_gross = [435, 442, 450];

% Turbine Parameters:

% Simplified method: Turbine_method = 1
% Advanced method  : Turbine_method = 2
Turbine_method = 2; %Choose either 1 or 2

if Turbine_method == 1
    % Simplified method (independent of head)
    Tur_P0 = [16.505    17.571  18.635  19.697  20.758  21.816  22.873  23.927  25.002  26.05
27.096  28.136  29.171  30.204  31.235  32.261  33.285  34.309  35.325  36.338  37.347  38.347
```

```
39.348  40.344  41.331  42.315  43.298  44.272  45.246  46.216  47.175  48.135  49.099  50.084
51.069  52.058  53.05   54.019  54.989  55.953  56.911  57.859  58.806  59.742  60.678  61.609
62.521  63.435  64.334  65.235  66.121  67.03   67.904  68.781  69.641  70.505  71.351  72.191
73.036  73.862  74.694  75.507  76.313  77.124  77.917  78.709  79.544  80.378  81.21   82.041
82.869  83.695  84.497  85.281  86.049  86.82   87.574  88.321  89.073  89.806  90.532  91.263
91.975  92.681  93.38   94.084  94.793  95.471  96.142  96.806  97.475  98.125  98.767  99.403
100.03  100.65  101.27  101.87  102.45  103.1];
    Tur_N0 = [77.406    78.418  79.344  80.196  80.982  81.711  82.389  83.022  83.626  84.18
84.701  85.191  85.654  86.092  86.507  86.901  87.276  87.632  87.971  88.295  88.603  88.897
89.178  89.448  89.704  89.95   90.186  90.412  90.629  90.837  91.036  91.227  91.412  91.591
91.764  91.93   92.091  92.244  92.39   92.531  92.665  92.793  92.915  93.032  93.143  93.25
93.351  93.447  93.538  93.625  93.707  93.786  93.859  93.929  93.995  94.056  94.114  94.168
94.218  94.265  94.309  94.349  94.385  94.418  94.448  94.475  94.498  94.516  94.532  94.544
94.553  94.558  94.561  94.561  94.56   94.556  94.55   94.541  94.53   94.516  94.501  94.482
94.462  94.44   94.416  94.389  94.358  94.328  94.295  94.26   94.222  94.183  94.142  94.099
94.054  94.007  93.959  93.908  93.859  93.797];

    Head0 = 0;  % must be zero (is used to verify the method)
elseif Turbine_method == 2
    %### Advanced method (interpolated between different heads) ###############
    %                        IMPORTANT:
    % This method is limited to the active power and head for which are given,
    % meaning heads or loads beyond what is given will have no solution and give "NAN"
    % Can use the alternative method (commented out) given in the function: turbine()

    Head0  = [439,442.6,445.3]; % Vector representing each head (Gross head [m])
    %H = 439.2m
    Tur_P0(1,:) = [0 16.224 17.274  18.323  19.369  20.414  21.457  22.498  23.537  24.596
25.629  26.66   27.685  28.705  29.723  30.739  31.751  32.76   33.768  34.77   35.769  36.763
37.749  38.735  39.718  40.691  41.661  42.63   43.59   44.551  45.507  46.452  47.399  48.35
49.321  50.292  51.268  52.246  53.202  54.158  55.108  56.054  56.988  57.923  58.846  59.769
60.687  61.587  62.488  63.375  64.264  65.138  66.035  66.897  67.762  68.61   69.463  70.298
71.127  71.96   72.776  73.597  74.399  75.194  75.995  76.777  77.559  78.383  79.205  80.027
80.846  81.664  82.479  83.271  84.045  84.802  85.563  86.307  87.044  87.785  88.508  89.224
89.945  90.648  91.344  92.034  92.728  93.429  94.097  94.759  95.414  96.074  96.715  97.349
97.976  98.596  99.209  99.815  100.41  100.98  101.63];
    Tur_N0(1,:) = [0 77.243 78.263  79.197  80.055  80.848  81.582  82.266  82.903  83.513
84.071  84.597  85.091  85.558  85.999  86.418  86.815  87.192  87.552  87.893  88.219  88.53
88.827  89.111  89.382  89.641  89.889  90.127  90.355  90.574  90.784  90.984  91.177  91.364
91.545  91.72   91.888  92.05   92.205  92.353  92.495  92.63   92.76   92.884  93.002  93.115
93.222  93.325  93.422  93.515  93.603  93.686  93.766  93.841  93.912  93.978  94.041  94.1
94.155  94.206  94.254  94.299  94.34   94.377  94.411  94.442  94.47   94.494  94.513  94.53
94.543  94.552  94.559  94.562  94.564  94.563  94.559  94.553  94.545  94.534  94.521  94.506
94.488  94.469  94.447  94.423  94.396  94.366  94.336  94.303  94.269  94.231  94.192  94.152
94.109  94.065  94.018  93.97   93.92   93.87   93.809];
    %H = 442.6m
    Tur_P0(2,:) = [0 16.505 17.571  18.635  19.697  20.758  21.816  22.873  23.927  25.002
26.05   27.096  28.136  29.171  30.204  31.235  32.261  33.285  34.309  35.325  36.338  37.347
38.347  39.348  40.344  41.331  42.315  43.298  44.272  45.246  46.216  47.175  48.135  49.099
50.084  51.069  52.058  53.05   54.019  54.989  55.953  56.911  57.859  58.806  59.742  60.678
61.609  62.521  63.435  64.334  65.235  66.121  67.03   67.904  68.781  69.641  70.505  71.351
72.191  73.036  73.862  74.694  75.507  76.313  77.124  77.917  78.709  79.544  80.378  81.21
82.041  82.869  83.695  84.497  85.281  86.049  86.82   87.574  88.321  89.073  89.806  90.532
91.263  91.975  92.681  93.38   94.084  94.793  95.471  96.142  96.806  97.475  98.125  98.767
99.403  100.03  100.65  101.27  101.87  102.45  103.1];
    Tur_N0(2,:) = [0 77.406 78.418  79.344  80.196  80.982  81.711  82.389  83.022  83.626
84.18   84.701  85.191  85.654  86.092  86.507  86.901  87.276  87.632  87.971  88.295  88.603
88.897  89.178  89.448  89.704  89.95   90.186  90.412  90.629  90.837  91.036  91.227  91.412
91.591  91.764  91.93   92.091  92.244  92.39   92.531  92.665  92.793  92.915  93.032  93.143
93.25   93.351  93.447  93.538  93.625  93.707  93.786  93.859  93.929  93.995  94.056  94.114
94.168  94.218  94.265  94.309  94.349  94.385  94.418  94.448  94.475  94.498  94.516  94.532
94.544  94.553  94.558  94.561  94.561  94.56   94.556  94.55   94.541  94.53   94.516  94.501
94.482  94.462  94.44   94.416  94.389  94.358  94.328  94.295  94.26   94.222  94.183  94.142
94.099  94.054  94.007  93.959  93.908  93.859  93.797];
    %H = 445.3m
    Tur_P0(3,:) = [0 16.722 17.8    18.876  19.951  21.023  22.094  23.162  24.228  25.315
26.375  27.432  28.484  29.531  30.576  31.617  32.656  33.691  34.726  35.753  36.777  37.797
38.808  39.82   40.828  41.825  42.82   43.814  44.798  45.783  46.763  47.732  48.703  49.678
50.673  51.669  52.669  53.671  54.651  55.63   56.605  57.573  58.531  59.488  60.434  61.38
62.321  63.242  64.166  65.074  65.985  66.88   67.799  68.681  69.567  70.436  71.309  72.164
73.013  73.866  74.701  75.541  76.363  77.177  77.997  78.797  79.598  80.441  81.283  82.123
82.962  83.799  84.633  85.443  86.236  87.011  87.791  88.552  89.307  90.067  90.808  91.541
92.28   93  93.713  94.419  95.13   95.847  96.532  97.21   97.881  98.557  99.213  99.862
100.5   101.14  101.77  102.39  103 103.58  104.24];
```

```
    Tur_N0(3,:) = [0 77.525 78.531  79.452  80.298  81.08   81.804  82.478  83.107  83.707
84.258  84.776  85.264  85.724  86.159  86.572  86.963  87.335  87.69   88.027  88.348  88.654
88.946  89.226  89.493  89.749  89.993  90.227  90.452  90.667  90.873  91.071  91.261  91.444
91.622  91.793  91.959  92.118  92.27   92.415  92.554  92.687  92.814  92.935  93.051  93.162
93.267  93.367  93.462  93.552  93.638  93.72   93.797  93.87   93.939  94.003  94.064  94.121
94.174  94.224  94.27   94.313  94.352  94.388  94.42   94.449  94.476  94.497  94.515  94.53
94.542  94.549  94.554  94.556  94.556  94.555  94.55   94.543  94.535  94.523  94.509  94.494
94.475  94.454  94.432  94.408  94.38   94.349  94.318  94.285  94.25   94.212  94.172  94.131
94.088  94.043  93.996  93.947  93.896  93.846  93.785];
end

% Transoformer Parameters:
P0_Tran = 52.5*10^-3;       %(MW)   Transformer No-load constant
Pk_Tran = 225*10^-3;        %(MW)   Transformer loading constant
Sn_Tran = 103;              %(MVA)  Transformer rating

% Plotting variables
n_var = 100;                    % Number of parameter variables
Q_n = 20;                       % Number of Q variables (used in figure 2)

phi0 = acos(0.9);
S = linspace(Sn*0.3,Sn*1.05,n_var);
P = S.*cos(phi0);
Q = S.*sin(phi0);
% P = linspace(Sn*0.3,Sn*0.97,n_var);
% Q = linspace(-20.6,-20.6,n_var);
%Q = linspace(50,50,n_var);
V = linspace(Vn,Vn,n_var);
map_var = [80, 84, 88, 90, 91, 91.5 92, 92.1, 92.185]; % Efficiency lines on efficiency map
%map_var = [0.44, 0.48, 0.5, 0.52, 0.54, 0.56, 0.6, 0.7, 0.8, 0.9, 1]*0.1; % Energy loss
mapping
%map_var = [0.3, 0.4, 0.5, 0.6, 0.7, 0.8, 0.9, 1.0, 1.1, 1.14, 1.16, 1.17, 1.18];

% Data on efficiency
PF_value = 0.9;
phi_value = acos(PF_value);

S_value = 103;
P_value = S_value*cos(phi_value);
Q_value = S_value*sin(phi_value);
% S_value = 103;
% P_value = 0.4*Sn;
% Q_value = -0.21*Sn;
V_value = 11;
Head_gross_value = 442;
[Ploss_Tot,Total_N,Tran_N,Ploss_Tran,Gen_N,Ploss_Gen,Tur_N,Ploss_Tur,Water_N,Ploss_Water] =
HPU(P_value,Q_value,V_value,Sn,Vn,Xq,Xd,Ra,Rf,k_ex,P_FE,P_V,P_F,bv, Xd_tran, X_leak, n_OCC,
C_OCC, Ifd_n, Head_gross_value,k_a, Tur_P0,Tur_N0,Head0, P0_Tran,Pk_Tran,Sn_Tran);

Ploss_Tran
Ploss_Gen
Ploss_Tur
Ploss_Water
Tran_N;
Gen_N
Tur_N;
Water_N;
Total_HPU_losses = Ploss_Tot
Total_efficiency = Total_N*100
Generator_loss = Ploss_Gen;

%**************************************************************************
%                           PLOTS and other calculations
%**************************************************************************

%############################## Efficiency of Components  (Figure 1) #################
P_1 = P.';
Q_1 = Q.';
V_1 = V.';
[Ploss_Tot,Total_N,Tran_N,Ploss_Tran,Gen_N,Ploss_Gen,Tur_N,Ploss_Tur,Water_N,Ploss_Water] =
HPU(P_1,Q_1,V_1,Sn,Vn,Xq,Xd,Ra,Rf,k_ex,P_FE,P_V,P_F,bv, Xd_tran, X_leak, n_OCC, C_OCC, Ifd_n,
Head_gross,k_a, Tur_P0,Tur_N0,Head0, P0_Tran,Pk_Tran,Sn_Tran);

figure(1)
```

```
f1 = plot(P_1,100*Total_N,P_1,100*Tran_N,P_1,100*Gen_N,P_1,100*Tur_N,P_1,100*Water_N);
xlabel("Load [MW]");
ylabel("Efficiency [%]");
legend('Total HPU','Transformer','Generator','Turbine','Waterway','Location','eastoutside');
set(f1(1),'linewidth',2);
set(f1(2),'linewidth',2);
set(f1(3),'linewidth',2);
set(f1(4),'linewidth',2);
set(f1(5),'linewidth',2);
grid('on')

% It is used later for cumulative probability and efficiency comparison:
Total_N_CP = Total_N;
P_1_CP = P_1;

figure(2)
plot(P_1,100*Total_N,P_1,100*Tur_N);
hold on


% Efficiency at different reactive power
P_eff = P.';
V_eff = V.';
Q00 = zeros(n_var,Q_n);

for m = 1:Q_n
    Q00(:,m) = m*(2*Sn)/Q_n-Sn;
    Q_eff = Q00(:,m);
    [Ploss_Tot,Total_N,Tran_N,Ploss_Tran,Gen_N,Ploss_Gen,Tur_N,Ploss_Tur,Water_N,Ploss_Water]
= HPU(P_eff,Q_eff,V_eff,Sn,Vn,Xq,Xd,Ra,Rf,k_ex,P_FE,P_V,P_F,bv, Xd_tran, X_leak, n_OCC, C_OCC,
Ifd_n, Head_gross,k_a, Tur_P0,Tur_N0,Head0,P0_Tran,Pk_Tran,Sn_Tran);
    Total_N0(:,m) = 100*Total_N;
end

Q_s = round(Q00(1,:),1);
figure(3)
for m = 1:Q_n
    plot(P_eff ,Total_N0(:,m),'--')
    Q_string(m) = sprintf("Q = %3.1f MVAr", Q_s(m));
    hold 'on'
end
legend(Q_string)
hold 'off'
xlabel('Active power [MW]')
ylabel('Efficiency [%]')
grid('on')


% % Efficiency vs voltage
% P_volt = P.';
% V_volt = V.';
% Q_volt = Q.';
% [Ploss_Tot,Total_N,Tran_N,Ploss_Tran,Gen_N,Ploss_Gen,Tur_N,Ploss_Tur,Water_N,Ploss_Water] =
HPU(P_volt,Q_volt,V_volt,Sn,Vn,Xq,Xd,Ra,Rf,k_ex,P_FE,P_V,P_F,Bv, Xd_tran, X_leak, n0, C, kk,
Head_gross,k_a, Tur_P0,Tur_N0,Head0, P0_Tran,Pk_Tran,Sn_Tran);
%
% figure(4)
% plot(V_volt,Total_N)


% Efficiency VS Head:
P_head = P.';
V_head = V.';
Q_head = Q.';
Head = 439:0.01:445;
%Head = 300:5:500;
for k = 1:length(Head)
    [Ploss_Tot,Total_N,Tran_N,Ploss_Tran,Gen_N,Ploss_Gen,Tur_N,Ploss_Tur,Water_N,Ploss_Water,
Q_flow_h] = HPU(P_head,Q_head,V_head,Sn,Vn,Xq,Xd,Ra,Rf,k_ex,P_FE,P_V,P_F,bv, Xd_tran, X_leak,
n_OCC, C_OCC, Ifd_n, Head(k),k_a, Tur_P0,Tur_N0,Head0, P0_Tran,Pk_Tran,Sn_Tran);
    Total_N_head(:,k) = 100*Total_N;
    Turbine_N_head(:,k) = 100*Tur_N;
    Waterway_loss_head(:,k) = Ploss_Water;
    Q_flow_head(:,k) = Q_flow_h;
```

```
    Turbine_loss_head(:,k) = 100*Tur_N;
end


figure(5)
yyaxis left
plot(Head,Waterway_loss_head(length(P_head),:))
hold on
yyaxis right
plot(Head,Q_flow_head(length(P_head),:))
hold off

figure(6)
plot(Head,Turbine_loss_head(length(P_head),:))

%############### Total HPU efficiency mapping ####################
figure(7)
for h = 1:length(Head)
    plot(P_head,Total_N_head(:,h))
    B(h) = sprintf("Head %0.1fm", Head(h));
    hold 'on'
end
legend(B)
hold 'off'
xlabel 'Active Power [MW]'
ylabel 'Efficiency [%]'
grid 'on'

figure(8)
[Px,Hy] = meshgrid(P_head, Head.');
surf(Px,Hy,Total_N_head.')
xlabel 'Active power [MW]'
ylabel 'Gross head [m]'
zlabel 'Efficiency [%]'
grid 'on'

figure(9)
Nz = round(Total_N_head.',4);
map_var2 = [86:0.5:91, 91:0.4:92, 92.1, 92.1:0.002:93];
[Hc,Hh]=contour(P_head,Head.',Nz,map_var2);
clabel(Hc,Hh)
xlabel 'Active power [MW]'
ylabel 'Gross head [m]'

% Turbine efficiency mapping:

figure(10)
Nz = round(Turbine_N_head.',4);
map_var2 = [94.5:0.01:95];
[Hc,Hh]=contour(P_head,Head.',Nz,map_var2);
clabel(Hc,Hh)
xlabel 'Active power [MW]'
ylabel 'Gross head [m]'


fig_n11 = 11;
Q_n2 = Q_n*5;                       % Number of Q variables
n_var2 = n_var*5;
P3 = (linspace(Sn*0.1,Sn*0.95,n_var2)).';
V3 = (linspace(Vn,Vn,n_var2)).';
eta_res = 4;                         % Decimal numbers of rounding of efficiency (should be
equal lim_1 and lim_2)

Q00 = zeros(n_var2,Q_n2);
for m = 1:Q_n2
    Q00(:,m) = m*(2*Sn)/Q_n2-Sn;
    Q3 = Q00(:,m);
    [Ploss_Tot,Total_N,Tran_N,Ploss_Tran,Gen_N,Ploss_Gen,Tur_N,Ploss_Tur,Water_N,Ploss_Water]
= HPU(P3,Q3,V3,Sn,Vn,Xq,Xd,Ra,Rf,k_ex,P_FE,P_V,P_F,bv, Xd_tran, X_leak, n_OCC, C_OCC, Ifd_n,
Head_gross,k_a, Tur_P0,Tur_N0,Head0, P0_Tran,Pk_Tran,Sn_Tran);
    Total_N02(:,m) = 100*Total_N;
    %Total_N02(:,m) = Ploss_Tot/Sn   %Energy loss mapping
    %Total_N02(:,m) = 0.1.*(P3./Ploss_Tot);
end
```

```
z = Total_N02;
z = round(z,eta_res);
zz = zeros(n_var2,Q_n2);

figure(fig_n11)
[X,Y] = meshgrid(Q00(1,:)/Sn,P3/Sn);
Z = round(z,eta_res);
map_var3 = [88 90 91 91.5 92 92.1 92.2 92.25 92.25:0.05:99];
[c,h]= contour(X,Y,Z,map_var3);
clabel(c,h)
axis([-0.7 0.8 0.3 1])
hold('on')
x1 = [2.5/Sn 2.5/Sn]
y1 = [0 1]
x2 = [-0.6 0.6]
y2 = [81/Sn,81/Sn]
plot(x1,y1,x2,y2)
hold on

%Data point plotting
bins = 30;
Msize = 6;
figure(fig_n11)
densityscatter(Q_data/Sn,P_data/Sn,bins,Msize)      % Function created by "Josè Manuel Amigo"
hold ('on')
%#################### PQ diagram plotting ###################################
PQ_diagram(PF,Xq,Xd,fig_n11)    %Plots PQ diagram
PQ_diagram(PF,Xq,Xd,21)         %Plots PQ diagram



% Effieicncy and Power loss of data points
[Ploss_tot,Total_N,Tran_N,Ploss_Tran,Gen_N,Ploss_Gen,Tur_N,Ploss_Tur,Water_N,Ploss_Water] =
HPU(P_data,Q_data,V_data,Sn,Vn,Xq,Xd,Ra,Rf,k_ex,P_FE,P_V,P_F,bv, Xd_tran, X_leak, n_OCC,
C_OCC, Ifd_n, Head_gross,k_a, Tur_P0,Tur_N0,Head0, P0_Tran,Pk_Tran,Sn_Tran);

Annual_loss = sum(Ploss_tot,'all')
Total_Prod = sum(P_data,'all')
Production_time = Total_Prod/Sn
Average_efficiency = mean(Total_N,'all')



%Efficiency mapping Generator:
fig_n12 = 12;
Q_n2 = Q_n*5;                       % Number of Q variables
n_var2 = n_var*5;
P3 = (linspace(Sn*0.1,Sn*0.95,n_var2)).';
V3 = (linspace(Vn,Vn,n_var2)).';
eta_res = 4;                         % Decimal numbers of rounding of efficiency (should be
equal lim_1 and lim_2)

Q00 = zeros(n_var2,Q_n2);
for m = 1:Q_n2
    Q00(:,m) = m*(2*Sn)/Q_n2-Sn;
    Q3 = Q00(:,m);
    [Ploss_Tot,Total_N,Tran_N,Ploss_Tran,Gen_N,Ploss_Gen,Tur_N,Ploss_Tur,Water_N,Ploss_Water]
= HPU(P3,Q3,V3,Sn,Vn,Xq,Xd,Ra,Rf,k_ex,P_FE,P_V,P_F,bv, Xd_tran, X_leak, n_OCC, C_OCC, Ifd_n,
Head_gross,k_a, Tur_P0,Tur_N0,Head0, P0_Tran,Pk_Tran,Sn_Tran);
    Gen_N02(:,m) = 100*Gen_N;
    %Total_N02(:,m) = Ploss_Tot/Sn   %Energy loss mapping
    %Total_N02(:,m) = 0.1.*(P3./Ploss_Tot);
end
z = Gen_N02;
z = round(z,eta_res);
zz = zeros(n_var2,Q_n2);
figure(fig_n12)
[X,Y] = meshgrid(Q00(1,:)/Sn,P3/Sn);
Z = round(z,eta_res);
map_var_gen = [92 93 94 95 96 97 97.5 98 98.2 98.4 98.6 98.8 98.86  98.92 98.96  99 99.1];
[c,h]= contour(X,Y,Z,map_var_gen);
clabel(c,h)
hold('on')
```

```
PQ_diagram(PF,Xq,Xd,fig_n12)    %Plots PQ diagram


% Energy loss mapping HPU:
fig_n13 = 13;
Q_n2 = Q_n*5;                       % Number of Q variables
n_var2 = n_var*5;
P3 = (linspace(Sn*0.1,Sn*0.95,n_var2)).';
V3 = (linspace(Vn,Vn,n_var2)).';
eta_res = 4;                         % Decimal numbers of rounding of efficiency (should be
equal lim_1 and lim_2)

Q00 = zeros(n_var2,Q_n2);
for m = 1:Q_n2
    Q00(:,m) = m*(2*Sn)/Q_n2-Sn;
    Q3 = Q00(:,m);
    [Ploss_Tot,Total_N,Tran_N,Ploss_Tran,Gen_N,Ploss_Gen,Tur_N,Ploss_Tur,Water_N,Ploss_Water]
= HPU(P3,Q3,V3,Sn,Vn,Xq,Xd,Ra,Rf,k_ex,P_FE,P_V,P_F,bv, Xd_tran, X_leak, n_OCC, C_OCC, Ifd_n,
Head_gross,k_a, Tur_P0,Tur_N0,Head0, P0_Tran,Pk_Tran,Sn_Tran);
    Ploss_Tot2(:,m) = Ploss_Tot/Sn;   %Energy loss mapping

    %Total_N02(:,m) = 0.1.*(P3./Ploss_Tot);
end
z = Ploss_Tot2;
z = round(z,eta_res);
zz = zeros(n_var2,Q_n2);

figure(fig_n13)
[X,Y] = meshgrid(Q00(1,:)/Sn,P3/Sn);
Z = round(z,eta_res);
map_var_gen = [0.040:0.002:0.055 0.059, 0.063,0.063:0.008:0.1];
[c,h]= contour(X,Y,Z,map_var_gen);
clabel(c,h)
axis([-0.8 0.8 0.3 1])
hold('on')

PQ_diagram(PF,Xq,Xd,fig_n13)    %Plots PQ diagram

% Efficiency VS Voltage:
phi_0V = acos(0.9);
S_0V = (linspace(Sn,Sn,100)).';
P_0V = S_0V*cos(phi_0V);
Q_0V = S_0V*sin(phi_0V);
V_0V = linspace(8,14,100).';
[Ploss_Tot,Total_N_V,Tran_N,Ploss_Tran,Gen_N,Ploss_Gen] =
HPU(P_0V,Q_0V,V_0V,Sn,Vn,Xq,Xd,Ra,Rf,k_ex,P_FE,P_V,P_F,bv, Xd_tran, X_leak, n_OCC, C_OCC,
Ifd_n, Head_gross,k_a, Tur_P0,Tur_N0,Head0, P0_Tran,Pk_Tran,Sn_Tran);

figure(14)
plot(V_0V,100*Total_N_V)
xlabel 'Terminal Voltage [kV]'
ylabel 'Efficiency [%]'




% Simulaitng with operation data:

% Operation data with zero operation:
data_file2 = readmatrix('Abjora_OD.xlsx');
Q_data2 = data_file2(:,2);
P_data2 = data_file2(:,1);
P_data2 = round(P_data2,3);                 %(MW)
Q_data2 = round(Q_data2,3);                 %(MVAR)
Sys_Price2 = data_file2(:,4);                %(Nok/MWh)
V_data2 = data_file2(:,3);                   %(kV)

P_data2(P_data2 < 10) = 0;
P_data_CP = 1*sort(P_data2);
```

```
P_CP = round(P_data_CP,3)/Sn;
numbers_CP =unique(P_CP);
count_CP=hist(P_CP,numbers_CP);

for i=1:length(count_CP)
     if i == 1
        prob_CP(i) =  count_CP(i)/sum(count_CP);
    else
        prob_CP(i) =  count_CP(i)/sum(count_CP)+ prob_CP(i-1);
    end
end
figure(15)
plot(P_1_CP/Sn,100*Total_N_CP) %results from the first figure
hold on
plot(numbers_CP,100*prob_CP)
axis([0.3 1 0 100])
hold on

days = length(P_data2)/(24*4);
t = minutes(0:15:24*4*15*days-15);
[h,m,s] = hms(t);

figure(16)
%yyaxis left
ylabel 'Active power [MW]'
plot(hms(t),P_data2,'R','linewidth',2)
hold on
plot(([1680, 2400]),([72.2, 72.2])) % Average efficiency line
hold on
plot(([1680, 2400]),([77.3, 77.3])) % BEP
xlabel 'Hours [h]'

 %#########################################################################

t1 = datetime(2020,1,6,15,0,0);
time = t1 + hours(0:length(P_data)-1);

figure(17)
plot(time,P_data, time,Sys_Price)
xlabel('Date')
ylabel('Power loss [MW]')

P_opt = linspace(76,76,length(P_data)).';
Ploss_opt = P_opt*(1-0.9218);

figure(18)
plot(time, P_data,  time, P_opt)

figure(19)
plot(time, Ploss_tot,time, Ploss_opt)
sum(P_data,'all')
sum(P_opt,'all')
%#########################################################################

[Ploss_tot,Total_N,Tran_N,Ploss_Tran,Gen_N,Ploss_Gen,Tur_N,Ploss_Tur,Water_N,Ploss_Water] =
HPU(P_data,Q_data,V_data,Sn,Vn,Xq,Xd,Ra,Rf,k_ex,P_FE,P_V,P_F,bv, Xd_tran, X_leak, n_OCC,
C_OCC, Ifd_n, Head_gross,k_a, Tur_P0,Tur_N0,Head0, P0_Tran,Pk_Tran,Sn_Tran);

average_efficiency = mean(Total_N.','all')*100
average_produciton = mean(P_data.','all')
average_production_r = mean(Q_data.','all')
sum1_prod = (sum(P_data.','all')/4)/10^3
sum1_loss = (sum(Ploss_tot.','all')/4)/10^3



% Dividing the data set into months (manually)
date_name = ['Jan','Feb', 'Mar','Apr','May','Jun','Jul','Aug','Sep','Oct','Nov','Des'];
data_length = [1, 572, 1267, 2011, 2731, 3475, 4195, 4939, 5683, 6402, 7146, 7866, 8610];
for d = 1:12
    average_prod(d) = sum(P_data(data_length(d):data_length(d+1)));
    average_loss(d) = sum(Ploss_tot(data_length(d):data_length(d+1)));
    average_efficiency(d) = 100*mean(Total_N(data_length(d):data_length(d+1)));
end
```

```
Average_production = average_prod.';
Average_loss = average_loss.';
Average_efficiency = average_efficiency.';

% WAE and EAE calcualtion

Deg = 2;    %Number of decimals rounding
des = 100*10^Deg;
P_WAE = P_data;
V_WAE = V_data;
Q_WAE = Q_data;
%################## Collecting and sorting of list ###############
[Ploss_tot,Total_N_WAE] =
HPU(P_WAE,Q_WAE,V_WAE,Sn,Vn,Xq,Xd,Ra,Rf,k_ex,P_FE,P_V,P_F,bv,Xd_tran, X_leak, n_OCC, C_OCC,
Ifd_n, Head_gross,k_a, Tur_P0,Tur_N0,Head0, P0_Tran,Pk_Tran,Sn_Tran);
Total_N_WAE = 100*sort(Total_N_WAE);
N = round(Total_N_WAE,Deg);

N_max = max(N);
size = (100/des):(100/des):N_max;
len = length(size);
val = zeros(1,len);             % VALUE of how often each efficiency value
prob = zeros(1,len);

for i = 1:len
    m = i/10^Deg;
    val(1,i) = sum(N == m, 'all');
    if m == 1/10^Deg
        prob(1,i) =  val(1,i)/length(N);
    else
        prob(1,i) =  (val(1,i)/length(N))+ prob(1,i-1);
    end
    Ak(1,i) = val(1,i)/length(N);
    eta_sum(1,i) = m * Ak(1,i);
end

% Comparion between WAE method and standard average calculation
eta= sum(eta_sum);      % WAE
avg = mean(N,'all');    % Standard Average

%line representing average efficiency
x_avg = [avg,avg];
y_avg = [0,100];


val_sum = val(1,len);    % initiation (representing maximum efficiency)
for m = (len-1):-1:1 % 1 - 922 or 0%-92.2%
    EAE(m) = mean(N((length(N)- val_sum):length(N)));      % Expected average efficiency (EAE)
    EAE_X(m) = 100 * (val_sum/length(N));
    val_sum = val(1,m) + val_sum;
    if val_sum >= length(N)
        break
    end
end
EAE;
EAE(EAE==0)=[];
EAE_X(EAE_X==0)=[];
EAE = flipud(EAE);

figure(20)
h1 =
plot(size(floor(0.01*length(size)):length(size)),100*prob(1,floor(0.01*length(size)):length(si
ze)));             % 0.8, means 80% of maximum efficeicny
hold 'on'
h2 = plot(x_avg, y_avg);
hold 'on'
plot(EAE,EAE_X);
xlabel('Efficiency [%]');
ylabel('Percentage [%]');
legend('Cumulative probability', sprintf("Average efficiency = %3.1f", avg));
set(h1(1),'linewidth',2);
axis([91.6 92.23 0 100])
grid('on')
hold on
```